THE SCAFFOLDING PROTEIN EBP50 REGULATES MITOCHONDRIAL DYNAMICS AND REDOX BALANCE IN VASCULAR SMOOTH MUSCLE CELLS

by

Vera Procaccia

B.S. The Hebrew University of Jerusalem, Israel, 2007

M.S. The Hebrew University of Jerusalem, Israel, 2009

Submitted to the Graduate Faculty of

School of Medicine in partial fulfillment

of the requirements for the degree of

Doctor of Philosophy

University of Pittsburgh

2018

UNIVERSITY OF PITTSBURGH

SCHOOL OF MEDICINE

This dissertation was presented

by

Vera Procaccia

It was defended on

April 6, 2018

and approved by

Thomas W. Kensler, Professor of Pharmacology and Chemical Biology

Sruti Shiva, Associate Professor of Pharmacology and Chemical Biology

Donna Beer Stolz, Associate Professor of Cell Biology

Fransicso J. Schopfer, Associate Professor of Pharmacology and Chemical Biology

Dissertation Advisor: Alessandro Bisello, Associate Professor of Pharmacology and Chemical Biology

THE SCAFFOLDING PROTEIN EBP50 REGULATES MITOCHONDRIAL DYNAMICS AND REDOX BALANCE IN VASCULAR SMOOTH MUSCLE CELLS

Vera Procaccia, M.S.

University of Pittsburgh, 2018

Cardiovascular disease is the leading cause of death worldwide. Vascular smooth muscle cells (VSMC) have a critical role in vascular pathologies such as restenosis, atherosclerosis and pulmonary arterial hypertension. Following injury or inflammation VSMC switch from a quiescent state to proliferative, migratory and secretory phenotype. These changes contribute to the progression of vascular disease and are regulated by various cellular factors including mitochondria.

Mitochondria are a central source of reactive oxygen species (ROS) in the cell and are undergoing constant morphological changes (fusion and fission) that allow a proper response to changes in the cellular environment. A family of large GTPases that include mitofusin-2 (Mfn2) and dynamin related protein 1 (Drp1) regulates mitochondrial shape. The activity and expression of these shaping proteins are regulated by multiple mechanisms including post translational modifications, degradation and transcription. The scaffolding protein Ezrin Radixin Moesin binding phosphoprotein-50 (EBP50) plays an important role in vascular remodeling. EBP50 regulates numerous cellular processes by controlling localization and function of proteins it interacts with. Among EBP50 partners are the S-phase kinase associated protein 2 (Skp2) that ubiquitinates and targets for degradation Forkhead box protein O1 (FoxO1) and Protein Kinase Cζ (PKCζ) that is activated by Tumor Necrosis Factor α (TNFα) in VSMC.

In my thesis work I found that EBP50 regulates mitochondrial morphology and fragmentation by affecting Mfn2 levels, through regulation of FoxO1 stability, and Drp1

phosphorylation through activation of PKCζ. In addition, I demonstrated that EBP50 regulates the expression of two important enzymes, MnSOD and catalase and affects mitochondrial superoxide levels. Cellular bioenergetics analysis revealed that EBP50$^{-/-}$ VSMC have lower glycolytic metabolism consistent with the lower proliferative response of EBP50 depleted VSMC to TNFα. In addition, increased levels of MnSOD in EBP50$^{-/-}$ VSMC reduced cell migration and conversely, MnSOD knock down, increased VSMC migration.

Taken together, my data shows that the effects of EBP50 on mitochondrial morphology and redox balance have significant impacts on VSMC metabolism, proliferation and migration and could contribute to the progression of vascular diseases. Therefore, EBP50 should be considered as a central regulator of vascular remodeling and a potential therapeutic target for vascular disorders.

TABLE OF CONTENTS

LIST OF TABLES

LIST OF FIGURES

PREFACE

Finding the ideal lab for yourself is not a trivial thing, and I believe that I was lucky enough to find my "home" in Dr. Alessandro Bisello's lab. So, first of all, I would like to thank Sandro for taking me as his graduate student, as I transitioned from another graduate program, and for making my four years in his lab and in the graduate school so enjoyable. Dr. Bisello has an amazing quality – optimism. He is able to see the good side in almost everything and the positive energy that is reflected from his optimism encouraged me every time I was unsure or doubting myself. Dr. Bisello's mentoring approach stimulated the development of my independent scientific thinking which is extremely important in order to become a scientist. He gave me a lot of freedom in developing my thesis project and let me follow my scientific curiosity and interests that motivated me during my research work. Dr. Bisello sent me to numerous conferences, where I developed new connections and advanced my scientific career and I am very grateful for that. The last two years were very difficult for Sandro on a personal level, and I want to express my admiration for his emotional strength – I do not take that for granted.

The next person to whom I want to express my gratitude is Dr. Michael Klagsbrun. Dr. Klagsbrun had a big part in my decision to do a Ph.D. While working in his lab, at the Vascular Biology Program at Children's Hospital Boston, I realized that I want to continue my education and get a doctorate. He told me so many times "You should really do a Ph.D!" that eventually made me realize that if he thinks that, then I really have to, at least, try. Obviously, I did try, and

I am so happy that I took that path. I have heard many times from students that “graduate school is hard”, but I can say from my experience, that if you find the right lab, like I did in Dr. Bisello’s lab, graduate school is actually fun!

A big part of my experience in a graduate school is attributed to our graduate program. So, I would like to thank the director of the Molecular Pharmacology graduate program, Dr. Patrick Pagano, for his commitment to the program and the investment in us, the students. I spent quite a bit of time in other graduate programs and I can tell that the Molecular Pharmacology graduate program is excellent in training students and I will always appreciate the respect and the mentoring that I got. A special thanks goes to our department chair Dr. Bruce Freeman that besides being the head of the Department of Pharmacology and Chemical Biology is also very involved in the graduate program and supports students scientifically and financially. In my opinion, that contributes greatly to the success of the program. Additionally, I would like to express my gratitude to Dr. John Horn, an associate dean for graduate studies that helped and advised me during the complex situation of transition between two graduate programs, his input made it possible for me to get to where I am today.

I am very thankful for my thesis committee members, Dr. Thomas Kensler, Dr. Sruti Shiva, Dr. Donna Beer Stolz and Dr. Francisco Schopfer for their advice and scientific input during our meetings. I also want to thank our graduate program coordinator, Shannon Granahan that was always available to help, advice and sometimes just to discuss various matters related to graduate school. I also want to thank the GPCR group members, particularly Dr. Peter Friedman, Dr. Frederic Jean Alphonse and Dr. Guillermo Romero for their input during lab meetings. These meetings provided me with a unique opportunity to regularly present my research and get a

feedback from a diverse group of people that could evaluate my work from a different perspective.

Finally, I would like to thank my family for their continuous support during my studies. My mom and dad that, despite the fact of living so far away, were always able to express their unconditional love and how proud they are of what I do. My little sister, Taly Ganzburg, that told me so many times that she looks up to me and made me think that it is all worth it. My beautiful children, Ethan and Maya, for forcing me to keep the "family-work" balance that allowed me to take a brake and think of things other than research and to come back with a fresh mind and ideas. Last but not the least, I would like to thank my dear husband, Ariel Procaccia that gave me an example of how to be a good scientist and supported me and our family throughout my journey in the graduate school. You gave me countless advices and encouragements that helped me to get to through challenging situations. I am absolutely sure that I could not have done it without you!

ABBREVIATIONS

AngII	Angiotensin II
Ant A	Antimycin A
β2-AR	β2 Adrenergic Receptor
CamK	Calcium-calmodulin-dependent Kinase
C/EBP-β	CCAT-enhancer-binding protein β
CDK1	Cyclin Dependent Kinase 1
CHX	Cycloheximide
COX	Cyclooxygenase
CVD	Cardiovascular Disease
DCA	Dichloroacetate
DES	Drug Eluting Stent
Drp1	Dynamin Related Protein 1
EBP50	Ezrin radixin moesin binding phosphoprotein of 50 kDa
EBD	Ezrin Binding Domain
ECSOD	Extracellular Superoxide Dismutase
E2F	E2 Factor
EGF	Epidermal Growth Factor
EGFR	Epidermal Growth Factor Receptor

ER	Estrogen Receptor
ER	Endoplasmic Reticulum
ERE	Estrogen Responsive Elements
ERK1/2	Extracellular Signal Regulated Kinase 1/2
ERM	Ezrin Radixin Moesin
ECAR	Extracellular Acidification Rate
eNOS	Endothelial Nitric Oxide Synthase
Gcn5	General Control Nonderepressible 5
GFP	Green Fluorescence Protein
GPCR	G protein-coupled Receptor
IKK	IκB Kinase
FAD	Flavin Adenine Dinucleotide
FAK	Focal Adhesion Kinase
FGF	Fibroblast Growth Factor
FoxO1	Forkhead box protein O1
FoxO3A	Forkhead box protein O 3A
FoxM1	Forkhead box protein M1
GPx	Glutathione Peroxidase
GRK6A	G-protein-coupled Receptor Kinase 6A
HIF-1α	Hypoxia Inducible Factor α
ICAM	Intercellular Adhesion Molecule 1
INFγ	Interferon γ
KD	Kinase Dead

LDHA	Lactate Dehydrogenase A
MAPK	Mitogen Activated Protein Kinase
Mdivi-1	Mitochondria Division Inhibitor 1
MET	Mitochondrial Electron Transport
Mfn1	Mitofusin 1
Mfn2	Mitofusin 2
MI	Myocardial Infarction
MIF	Macrophage Migration Inhibitory Factor
MitoRFP	Mitochondrial Red Fluorescent Protein
MMP	Matrix Metalloproteinase
MnSOD	Manganese Superoxide Dismutase
NAD	Nicotinamide Adenine Dinucleotide
NF-2	Neurofibromatosis Type 2
NF-κB	Nuclear Factor κ-light-chain-enhancer of activated B cells
NHERF1	$Na^{2+/}H^{+}$ Exchanger Regulatory Factor 1
NO	Nitric Oxide
NOS	Nitric Oxide Synthase
Nox	NADPH Oxidase
OCR	Oxygen Consumption Rate
OPA-1	Optic Atrophy 1
oxLDL	Oxidized Low Density Lipoprotein
PAH	Pulmonary Arterial Hypertension
PASMC	Pulmonary Arterial Smooth Muscle Cells

PCNA	Proliferating Cell Nuclear Antigen
PDGF	Platelet Derived Growth Factor
PDGFR	Platelet Derived Growth Factor Receptor
PDH	Pyruvate Dehydrogenase
PDK	Pyruvate Dehydrogenase Kinase
PDZ	PSD95/Disc large/ZO-1
PGC-1α	Peroxisome Proliferator-activated Receptor γ Coactivator 1-α
PKA	Protein kinase A
PKCζ	Protein kinase C ζ
PLC-β2	Phospholipase β2
POU2F1	POU Domain Class 2 Transcription Factor
PP2A	Protein Phosphatase 2
PTEN	Phosphate and Tensin Homolog
PTH	Parathyroid Hormone
PTH1R	Parathyroid Hormone Receptor 1
PTHrP	Parathyroid Hormone Related Protein
PKCζ	Protein Kinase C ζ
Rb	Retinoblastoma
ROS	Reactive Oxygen Species
RNS	Reactive Nitrogen Species
RSC	Respiratory Super Complexes
RTK	Receptor Tyrosin Kinase
RSK	Ribosomal S6 Kinase

SOD	Superoxide Dismutase
Sp1	Specificity Protein
Skp2	S phase Kinase-associated Protein 2
TGF-β	Transforming Growth Factor β
TNFα	Tumor Necrosis Factor α
VCAM	Vascular Cell Adhesion Molecule 1
VSMC	Vascular Smooth Muscle Cells
XO	Xanthine Oxidase

1.0 INTRODUCTION

1.1 HYPERPROLIFERATIVE VASCULAR DISEASES

Vascular disease is a sub group in the cardiovascular diseases (CVD) class that involves the heart or blood vessels. CVD are the leading cause of deaths worldwide accounting for 32.1% of all deaths in 2015 [1]. Surgical, biochemical or immunological stresses, that are characteristic of vascular disease, trigger cellular proliferation that leads to vessel obstruction – a condition called vascular proliferative disease.

Blood vessels consist of three layers (Figure 1). The **intima** is a single layer of endothelial cells that serve as a protective barrier between the lumen and the blood vessel and regulate multiple processes including, neutrophil recruitment, angiogenesis and vascular tone. After the intima there is an elastic lamina that separates intima from the media and is comprised of connective tissue and elastin. The **media** is the middle layer that consists of vascular smooth muscle cells (VSMC) and is the thickest part of an arterial blood vessel. The main role of the media layer is to maintain vascular tone through contractions and relaxations and by that to regulate blood pressure and vessel diameter. The last, outermost layer is the **adventitia** that is

comprised of fibroblasts and connective tissue. The adventitia is separated from the media by the external elastic lamina [2].

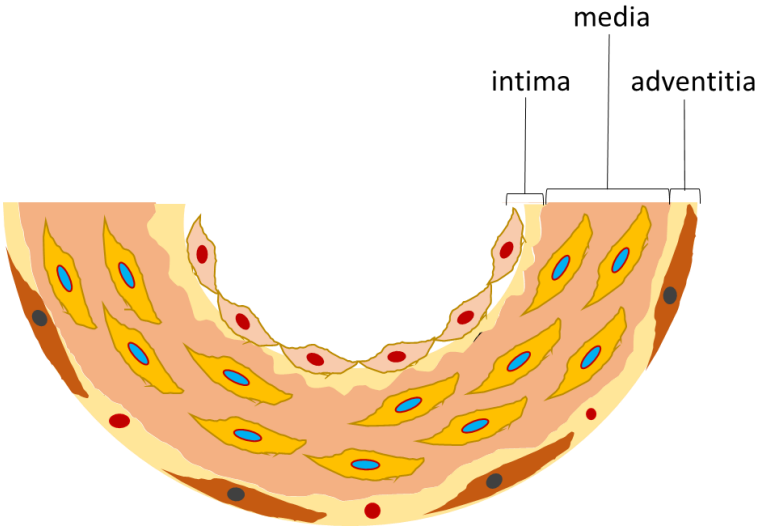

Figure 1: Arterial vessel wall structure

Tunica intima is the thinnest layer in the blood vessel that is comprised of a single layer of endothelial cells (and VSMC in humans). Tunica media is the thickest layer in the arterial vessel wall and is comprised from vascular smooth muscle cells supported by connective tissue that is mostly made of elastic fibers. Tunica adventitia is comprised of fibroblasts, connective tissue, small blood vessels and nerves.

Vascular injury triggers a series of events that includes endothelial denudation or dysfunction, inflammation and VSMC activation and proliferation. Multiple growth factors and cytokines are present in human vascular lesions. These mediators may be released by dysfunctional endothelial cells, inflammatory cells, platelets and VSMC, affecting chemo-attraction, cell migration, proliferation, apoptosis and matrix modulation [3].

Hyper-proliferation is considered a pathological event that is present in cancer and vascular diseases. In the vascular system VSMC are the main cell type responsible for the

progression of the proliferative disease. Under normal physiological state, VSMC are quiescent and maintain vascular tone through contraction and relaxation. However, following inflammation or injury to the vessel VSMC undergo a phenotypic switch characterized by de-differentiation and increased protein secretion, proliferation and motility. During these processes VSMC migrate from the media layer where they are normally localized to the intima layer. As a result, the vessel narrows, interfering with blood flow and further damaging to the organism [4]. Numerous extracellular and intracellular factors regulate these changes in VSMC. Platelet derived growth factor (PDGF), tumor necrosis factor α (TNFα), epidermal growth factor (EGF) and mitochondria are among them [5-10]. Signaling cascades that are activated by these factors impact the cell cycle and promote proliferation and migration.

1.1.1 Restenosis

Arterial bypass and angioplasty have been the main treatment for arterial disease for several decades [11]. While arterial bypass is a complicated surgical procedure, angioplasty is less invasive. However, several studies show that angioplasty leads to higher re-intervention compared to coronary arterial bypass [12]. During angioplasty a balloon is inflated at the site of atherosclerotic blockage in order to widen the vessel. As a result, the artery undergoes superficial and deep injuries. These injuries lead to sequential response of vascular cells that eventually result in narrowing and occlusion of the vessel [13].

Restenosis can be defined as a re-narrowing of the vessel by more than 50% and its incidence after balloon angioplasty is 25-50% [13, 14]. Three processes lead to development of restenosis: elastic recoil, neointimal proliferation and negative remodeling. Elastic recoil is a passive process that occurs immediately after the mechanical stretch by the balloon and causes

40% reduction of the lumen [15, 16]. Inflammation plays an important role in neointimal proliferation. The inflammatory response can be divided into several phases. First, the early thrombotic phase occurs, when the endothelial cells are removed due to the mechanical forces and the sub-intima layer is exposed. The exposed layer contains collagen, Von Willebrand factor, fibronectin, and laminin that stimulate platelet adherence and aggregation [16]. Later on, platelets begin to release mitogenic factors (such as PDGF), that in combination with circulating angiotensin II (AngII) and plasmin induce proliferation and migration of VSMC to the intima [16, 17]. Late neo-intimal proliferation phase occurs when new extracellular matrix forms providing a scaffold for new VSMC in the intima [17]. Negative remodeling is the third phase that happens in restenosis. Negative remodeling is defined as a local shrinkage of vessel size. Intravascular ultrasound studies show that negative remodeling accounts for two thirds of lumen loss in restenosis following angioplasty [18].

Intravascular stenting was introduced in order to overcome some of these limitations. It was found that stents mainly prevent the elastic recoil thus supporting a larger initial gain in lumen size compared to angioplasty alone [19, 20]. The stent is inserted into the lumen of the vessel and prevents its closure. Stents improved the outcome of coronary angioplasty by reducing restenosis rates by 10% [17]. However, restenosis may still occur in the presence of a stent. In fact, it was shown that stenting causes greater neointimal growth, a process called in-stent restenosis [16]. To prevent in-stent restenosis a new methodology has emerged in the form of drug eluting stents (DES). These devices considerably improved the outcome of angioplasty by reducing restenosis to 5% [21]. DES inhibit multiple biological processes involved in restenosis and allow local drug delivery of higher doses without systemic effects. Among the drugs that are used in DES are Rapamycin, that inhibits inflammatory responses and VSMC

proliferation, and taxenes, that inhibit tubulin polymerization and consequently proliferation [11]. Despite numerous advantages of DES there are several limitations to this method. One of them is late in stent thrombosis that necessitates life-long treatment with anti-platelet therapies. In stent thrombosis is seen at higher rates in patients with diabetes treated with DES and is accompanies with an increased risk of death [22]. In order to overcome these limitations new strategies are being developed. Biodegradable stents are one of the approaches that have been studied in multiple trials [23, 24]. Biodegradable stents allow temporal mechanical support for the vessel but eventually will fully degrade, preventing the inflammatory response to foreign material.

1.1.2 Atherosclerosis

Atherosclerosis is a chronic inflammatory condition of the vessels that cause, lipid accumulation and plaque formation in vessel wall. During atherogenesis, monocytes and lymphocytes adhere to the endothelial cell surface and migrate into the sub-endothelial space. There, monocytes differentiate into macrophages that ingest low density lipoproteins (LDL) and modified or oxidised low density lipoproteins (oxLDL). These events lead to accumulation of cholesterol esters and formation of "foam cells". Foam cells and VSMC migrate from the media into the intima and proliferate with the formation of atherosclerotic plaques. These processes which involve cell adhesion, migration, differentiation, proliferation and cell interaction with the extracellular matrix are regulated by a complex network of cytokines and growth regulatory peptides [25, 26].

Endothelial dysfunction, inflammation, vascular proliferation and matrix alterations are some of the processes that contribute to the progression of atherosclerosis [27]. VSMC are the

main cellular component in the arterial wall and their role in atherosclerosis includes extracellular matrix deposition, monocyte retention, thickening of the arterial wall through increased proliferation and migration, expression of inflammatory mediators and production of ROS. In the media VSMC have a contractile phenotype and they are able to maintain vascular tone. But, in response to inflammation and growth factors VSMC start to proliferate, migrate and acquire a synthetic phenotype [28]. The synthetic phenotype is instrumental for the remodeling and repair of the injured vessel and in the same time contributes to the pathogenicity of the disease.

In order to support VSMC migration the extracellular matrix has to be degraded. Many proteases including matrix metalloproteinases (MMPs) contribute to extracellular matrix proteolysis and VSMC migration [29] and have been implicated in plaque formation. Factors that promote atherosclerosis such as PDGF, transforming growth factor β (TGF-β) and ROS increase MMPs expression [30, 31] and indeed, MMPs expression is increased in atherosclerotic lesions [32]. Furthermore, knock out of MMP-9 leads to reduced VSMC hyperplasia and reduced lumen loss [33]. Despite these evidence the exact mechanism of MMPs effects on atherosclerotic lesions remains unknown.

Vascular proliferation is linked to inflammation, apoptosis and matrix alterations. Growth promoting actions usually inhibit apoptosis, and inflammatory responses induce proliferation. Therefore, inhibiting cellular proliferation through cell cycle regulators has arisen as a promising strategy to treat atherosclerosis. VSMC proliferation is regulated through several mechanisms. Cyclin-dependent kinases (CDKs) that form holoenzymes with their regulatory subunits, the cyclins [34] are major regulators of cell cycle. Initially, increasing accumulation of cyclin D/CDK4 and cyclin E/CDK2 complexes, in cooperation with proliferating cell nuclear antigen

(PCNA), coordinate DNA replication by regulating the transition through the G1 and S phases [35]. Then, G2/M transition is regulated by cyclin A/CDK2 and cyclin B/CDK1 complexes. Furthermore, cell cycle progression is regulated by cyclin-dependent kinase inhibitors (CKIs) such as $p27^{KIP1}$ and $p21^{CIP1}$, which bind to CDK and prevent their activation. Cell cycle progression is also modulated by transcription factors that trans-activate CDKs and CKIs. Transcription factor p53 induces expression of $p21^{CIP1}$ and consequently inhibits the activity of the G1 cyclin/CDK complexes, resulting in G1-phase arrest [36]. Conversely, the E2 factor (E2F) family of transcription factors control the expression of genes in S-phase. In quiescent conditions, E2F members exist in inactive complexes with retinoblastoma (Rb) protein. Cyclin D/CDK4 and cyclin E/CDK2 complexes hyper-phosphorylate Rb, leading to dissociation of E2F, which in turn activates the expression of genes such as those encoding cyclin E and A and CDK1[36]. Growth arrest homeobox transcription factor (GAX) and GATA-binding factor 6 (GATA-6) transcription factors are also relevant cell cycle regulators in VSMC. GAX is a homeobox transcription factor that regulates cell differentiation, proliferation and migration, and is expressed in quiescent VSMC [37]. GATA-6 is a transcription factor involved in tissue-specific gene expression in VSMC [38]. Both GAX and GATA-6 stimulate the expression of $p21^{CIP1}$ and induce subsequent cell cycle arrest [37, 39]. Furthermore, GAX and GATA-6 are down-regulated by mitogen stimulation *in vitro* and in response to vascular injury *in vivo.*

In addition to transcription factors, nitric oxide (NO) is able to suppress cyclin A promoter activity and upregulate $p21^{CIP1}$ [40]. *In vivo* overexpression of nitric oxide synthase resulted in reduction of atherosclerotic or restenotic lesion formation through both inhibition of VSMC proliferation and inhibition of adhesion molecule expression with subsequent reduction of vascular mononuclear cell infiltration [41]. In contrast, impaired NO bioactivity in vascular

disease is associated with VSMC proliferation and inflammation [27]. These effects of NO on cell cycle directly link inflammation and proliferation processes. Additional evidence in support of the connection between proliferation and inflammation comes from the observation that cell cycle arrest preserves a non-activated cellular phenotype through prevention of adhesion molecule expression *in vivo*, thereby reducing the susceptibility to atherosclerosis or vasculopathy [42]. Moreover, CDKs regulate transcriptional gene activation by nuclear factor κ-light-chain-enhancer of activated B cells (NF-κB) [43], providing another mechanism for coordination between inflammation, adhesion molecule expression and cell cycle progression. Conversely, cytokines can influence cell cycle progression. For example, macrophage migration inhibitory factor (MIF) is a pleiotropic cytokine with chemokine-like functions that is studied in different aspects of cardiovascular disease. MIF stabilizes the cell cycle–inhibitory protein $p27^{KIP1}$ and blocks proliferation [44]. Contrarily, MIF has been shown to functionally inactivate p53 and by that promotes proliferation [45]. Cyclooxygenase 2, essential in inflammation, is also expressed in a cell cycle–dependent way [46].

Due to the broad impact of proliferation on various processes in the vascular cells, anti-proliferative drugs have been tested as means to prevent vascular proliferative diseases in humans. These agents include heparins, angiotensin-converting enzyme inhibitors and antagonists to growth factors such as terbinafine or trapidil (inhibitory to PDGF and more). However, in clinical trials these treatments failed to replicate the effect that were seen in animal models [47]. These failures could be explained by species differences in the response to vascular injury or limitations on matching experimental dosing regimens in humans. Moreover, they could emphasize the improbability that a multifactorial disease, such as atherosclerosis, can be treated successfully by targeting a single mitogenic factor. So far, anti-proliferative therapies are

mainly used to treat disorders such as in-stent restenosis and by-pass graft failure in which excessive proliferation is the basis of the disorder.

1.1.3 Pulmonary arterial hypertension

Pulmonary arterial hypertension (PAH) is a fatal disease caused by small pulmonary artery obstruction due to vascular proliferation and remodeling. PAH is characterized by elevated pulmonary arterial pressure and increased pulmonary vascular resistance, frequently leading to right heart failure and death [48]. The two main components thought to be responsible for PAH include structural changes within the pulmonary vasculature and increased vasoconstriction of the pulmonary vasculature [48]. The structural changes include smooth muscle cell proliferation and hypertrophy, and the deposition of matrix proteins within the media of the pulmonary arterial vessels, which will influence the properties of the pulmonary arteries. In addition, histologic findings of PAH indicate intimal hyperplasia, adventitial proliferation, thrombosis in situ, infiltration of inflammatory cells, and the presence of angio-proliferative "plexiform lesions", which are complex vascular formations originating from remodeled pulmonary arteries [48].

At the level of the media, pulmonary artery smooth muscle cells exhibit an increase in proliferation and suppression of apoptosis. This suggests that the pathogenesis of PAH is similar to that underlying cancer, since both diseases show excessive proliferation and impaired apoptosis. In both PAH and cancer, pyruvate dehydrogenase kinase (PDK) is elevated, and this enzyme is responsible for phosphorylation and inhibition of pyruvate dehydrogenase (PDH), a vital enzyme regulating the rate of oxidative metabolism. PDK activation results in a metabolic shift to glucose metabolism, and these metabolic abnormalities enhance cell proliferation and

impair apoptosis [48]. In addition, pathologic specimens from patients with PAH reveal an increase in the number of macrophages, T and B lymphocytes, and mast cells, suggestive of an underlying inflammatory process. Another component contributing to the pathogenesis of PAH is abnormal smooth muscle cell contractility. This hyper-contractility can be caused by exacerbated mechanisms that lead to smooth muscle cell contraction, but also by blunting mechanisms that would normally produce relaxation of the smooth muscle. For instance, PAH is associated with alterations in nitric oxide (NO) mediated vaso-relaxation due to reduced activity of endothelial nitric oxide synthase (eNOS) [49].

It has been well-established that VSMCs can modulate their phenotype from a contractile to a non-contractile-proliferative phenotype in many settings, including atherosclerosis, restenosis and PAH. In PAH, pulmonary vascular cells have increased aerobic glycolysis as a result of normoxic upregulation of hypoxia-inducible factor 1α (HIF-1α) and inhibition of pyruvate dehydrogenase. The pseudo-hypoxic state that leads to normoxic activation of HIF-1α occurs due to changes in the cellular redox state [50], which in turn is affected by a decrease in the levels of mitochondrial reactive oxygen species generation. Activation of HIF-1α in PAH upregulates pyruvate dehydrogenase kinase isoforms 1 and 2 (PDK1 and PDK2), leading to phosphorylation and inhibition of pyruvate dehydrogenase, and switch to aerobic glycolysis. The small molecule dichloroacetate (DCA), which is a PDK inhibitor, has shown promise as a potential therapy in experimental pulmonary hypertension. DCA improves mitochondrial structural integrity and function, decreases pulmonary artery smooth muscle cell proliferation, and regresses established pulmonary hypertension [51]. This suggests that cellular metabolism and mitochondria have critical role in proliferative vascular diseases such as PAH.

1.2 MITOCHONDRIA

Mitochondria are double membrane organelles with their own DNA. Mitochondria are thought to have evolved from bacteria that developed a symbiotic relationship with larger cells (endosymbiosis). This theory is supported by the striking similarities between the genomes of mitochondria and of the bacterium *Rickettsia prowazekii* [52]. Mitochondrion size ranges from 0.5 μm to 10 μm and the number of mitochondria per cell varies greatly depending on cell type. For example, red blood cells do not contain any mitochondria, while liver cells and muscle cells may have hundreds or thousands of mitochondria.

The inner mitochondrial membrane forms numerous folds (cristae) that extend into the mitochondrial matrix and increase the surface area of the membrane. The composition of the inner membrane consists of 70% proteins that are involved in oxidative phosphorylation and transport of metabolites between the cytoplasm and the mitochondrion (such as pyruvate and fatty acids). Otherwise, the inner membrane is impermeable to ions and small molecules. This is crucial to the maintenance of the proton gradient that drives ATP synthesis. In contrast, the outer membrane is freely permeable to small molecules and the composition of the inter-membrane space is very similar to the cytoplasm. This is due to proteins called porins that form channels through which molecule smaller than 6000 daltons can defuse freely.

The mitochondrial matrix contains the genetic material and the enzymes that are needed for the reactions of oxidative metabolism. Mitochondrial genome is usually a circular DNA, like in bacteria, which is present in multiple copies per organelle. The mitochondrial 16 kb genome encodes 13 polypeptides of the respiratory chain, which is essential for oxidative

phosphorylation and ATP generation, while the remaining 79 polypeptides are nuclear-encoded [53] .

Glucose and fatty acids oxidative breakdown is the main mechanism of energy generation in mammalian cells. The initial stage of glucose metabolism (glycolysis) occurs in the cytoplasm. During this stage glucose is converted to pyruvate which is then imported to mitochondria. Here pyruvate is oxidized to acetyl CoA which in turn is broken to CO_2 in the citric acid cycle. Oxidation of fatty acids also results in acetyl CoA that is metabolized in the citric acid cycle in mitochondria. Therefore, mitochondrial metabolism is responsible for both glucose and fatty acid breakdown. The oxidation of acetyl CoA to CO_2 is coupled to the reduction of flavin adenine dinucleotide (FAD) and nicotinamide adenine dinucleotide (NAD) to $FADH_2$ and NADH during which high energy electrons are transferred through series of carriers in the inner membrane of the mitochondrion to molecular oxygen. The reactions in the electron transport chain create a proton gradient that is used by ATP synthase to generate ATP (Figure 2). Therefore, the inner membrane is an extremely important compartment for ATP synthesis. In addition, mitochondria are a major site for the production of ROS due to the high predisposition for aberrant release of free electrons. While several different antioxidant proteins within mitochondria scavenge and neutralize these molecules, some ROS may inflict damage to mtDNA.

1.2.1 Mitochondrial reactive oxygen species production

ROS are by-products of aerobic metabolism. ROS include the superoxide anion ($O_2^{\bullet -}$), hydrogen peroxide (H_2O_2), and hydroxyl radicals (•OH), all of which have inherent chemical properties that confer reactivity to different biological targets [54]. In mitochondria, electrons that leak

from the electron transport chain react with molecular oxygen and superoxide anion is formed [55]. The electrons can be supplied by either NADH at complex I or by succinate at complex II. Ubiquinone (QH2) mediates electron transfer to complex III, which in turn reduces complex IV. Complex IV couples oxygen reduction to water and the proton pump, transporting protons (H^+) from the matrix to the inter-membrane space. The resultant proton motive force across the inner mitochondrial membrane is used by complex V for ATP synthesis (Figure 2). It has been shown that the main superoxide sources in mitochondria are complex I and complex III [56]. Complex I can produce superoxide both in the forward and reverse electron transfer in the mitochondrial matrix. Complex III produces superoxide both in the mitochondrial matrix and in the inter-membrane space under conditions of hypoxia and complex IV inhibition [57].

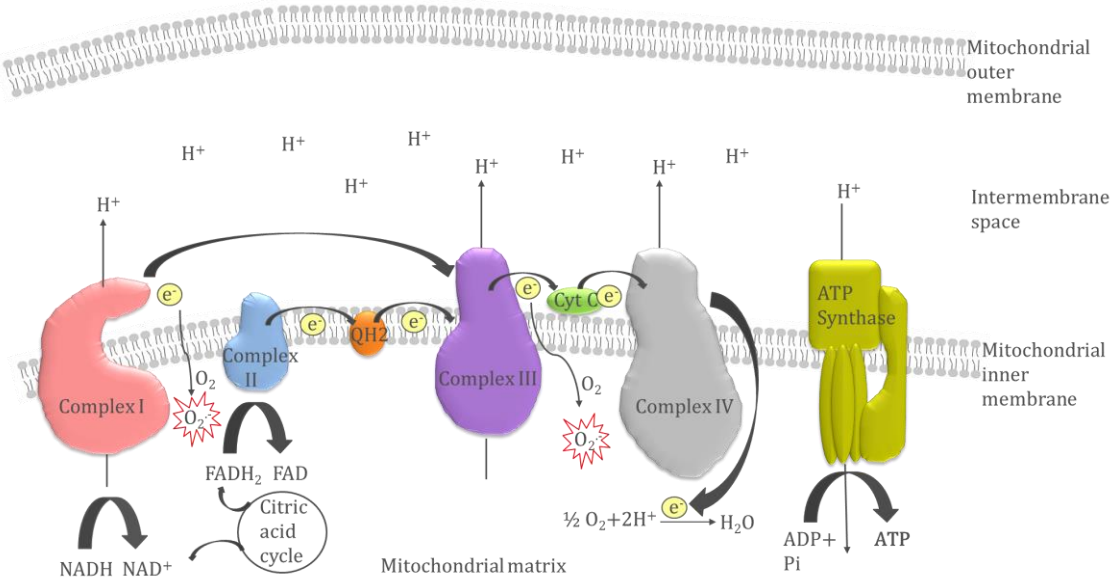

Figure 2: Schematic representation of the electron transport chain.

The electrons are supplied by either NADH at complex I or by $FADH_2$ at complex II. Ubiquinone (QH2) mediates electron transfer to complex III, which in turn reduces complex IV. Complex IV couples oxygen reduction to water and the proton pump. Complexes I, III and IV transport protons (H^+) from the matrix to the inter-membrane space. The resultant proton motive force across the inner mitochondrial membrane is used by complex V for ATP synthesis. Complexes I and III can produce superoxide due to electron leak.

Mitochondria are not only a major ROS generation site but also can be a target of these species. Superoxide can react and inactivate proteins containing sulfur iron clusters, including complex I and complex II. It has been shown that damage to complex I and complex II by oxidizing iron sulfur clusters lead to increased ROS from mitochondria [58]. In addition, oxidative damage to mitochondrial DNA can lead to defects in the synthesis of the components of electron transfer chain, which are encoded by mitochondrial DNA and eventually to mitochondrial dysfunction. Usually, superoxide in mitochondria is rapidly converted to H_2O_2 by manganese superoxide dismutase (MnSOD). Therefore, MnSOD prevents the accumulation of superoxide in mitochondria and protects them from oxidative damage. Following the reaction with MnSOD superoxide is converted to H_2O_2 and can diffuse out of the mitochondria and react with cysteine residues on various proteins. Cysteine residues exist as a thiolate anion (Cys–S) at physiological pH and are more susceptible to oxidation compared to the protonated cysteine thiol (Cys–SH). When oxidized by H_2O_2 the thiolate anion is converted to a sulfenic form (Cys-SOH) leading to allosteric change in the protein that alters its function. The sulfenic form of proteins is reversible by thioredoxin and glutaredoxin. However, higher levels of H_2O_2 lead to irreversible oxidation to sulfinic and sulfonic species [59].

1.2.2 Mitochondrial dynamics

Mitochondria may attain a diverse range of shapes depending on cell type and tissue. This heterogeneous morphology was observed back in 1898 by Carl Benda that noted that the organelle can have a ball shape and sometimes a linear shape. This observation inspired the name mitochondrion that originates from Greek and means: mitos = thread and chondrion = granule. In

1914 the field of mitochondrial dynamics was established when it was noted that "Any one type of mitochondria such as a granule, rod or thread may at times change into any other type or may fuse with another mitochondrion, or it may divide into one or several mitochondria." [60]. Alterations in mitochondria shape occur as a result of fusion and fission events.

Fission and fusion are regulated by a number of proteins that are localized in mitochondria and the cytosol. Key fusion regulators are mitofusin-1 (Mfn1) and mitofusin-2 (Mfn2) that are located on the outer mitochondrial membrane and optic atrophy 1 (OPA1) that is located on the inner mitochondrial membrane. Mfn1 and Mfn2 govern the fusion of the outer mitochondrial membrane and OPA1 governs the fusion of the inner mitochondrial membrane. During mitochondrial fusion two adjacent mitochondria are fused and their contents are mixed. Mitochondrial fusion proteins contain a GTPase domain, a trans-membrane domain and a coiled coil domain. Fusion proteins are anchored to mitochondria through a trans-membrane domain and the coiled coil domain that faces the cytosol and mediates homotypic (Mfn1-Mfn1, Mfn2-Mfn2 or OPA1-OPA1) and heterotypic (Mfn1-Mfn2) physical connections. Mutations in OPA1 cause an autosomal dominant inherited neuropathy [61, 62]. The loss of OPA1 mediated fusion causes unopposed fission that ultimately leads to optic nerve degeneration because of increased apoptosis in retinal ganglia [63]. Mutations in fusion mediating, coiled coil and GTPase domains of Mfn2, cause Charcot-Marie-Tooth disease type 2A, a neurologic disorder that is characterized by distal muscle weakness and sensory loss [64].

Pro-fusion activity of Mfn1 is facilitated through binding to guanine nucleotide binding protein-β subunit 2 (Gβ2) [65] that facilitates Mfn1 clustering on the outer mitochondrial membrane. In contrast, Mfn2 is mainly regulated through expression levels. Peroxisome proliferator-activated receptor γ coactivator 1-α (PGC-1α) and peroxisome proliferator-activated

receptor γ coactivator 1-β (PGC-1β) have been shown to up-regulate Mfn2 in order to promote fusion [66, 67]. Forkhead box protein O1 (FoxO1) has been shown to act together with PGC-1α [68] to induce the expression of Mfn2 [69]. Mfn1 and Mfn2 are also regulated by the ubiquitin proteasome pathway and participate in mitochondrial quality control. Upon the induction of mitochondrial stress Mfn1 and Mfn2 are ubiquitinated by PINK1/Parkin and targeted for degradation. The reduction of Mfn1 and Mfn2 levels promotes fission and allows selective removal of damaged mitochondria through a process called, mitophagy [70, 71]. OPA1 function is determined by alternative splicing and post-translational modifications [72]. Proteolytic cleavage of OPA1 at two discovered sites add further complexity to its regulation, with longer isoforms in general mediating fusion, and small, soluble isoforms that are located in the intermembrane space, responsible for keeping cytochrome c contained within cristae, thereby preventing apoptosis [73, 74].

Mitofusins exhibit other roles that are not fusion dependent. Mfn2 dysfunction has been associated with several pathological conditions such as Charcot-Marie-Tooth (CMT) disease type 2A, diabetes mellitus type 2, obesity, hypertension and atherosclerosis, which points to its diverse regulatory effects. On a molecular level, Mfn2 over-expression inhibits cell proliferation by interacting with Ras and Raf and inhibiting the Ras-Raf–extracellular signal-regulated kinase 1/2 (ERK1/2) signaling pathway [75, 76]. In addition, Mfn2 has been shown to tether the endoplasmic reticulum to the mitochondria thus regulating calcium transport to the mitochondria [77]. This function is particularly important in cardiac muscle that relays on calcium for proper muscle contraction [78]. Disruption of Mfn2 in the heart leads to impaired tethering of sarcoplasmic reticulum to the mitochondrial that ultimately leads to impaired calcium signaling and deterioration of left ventricular systolic function [79]. Similarly to mitofusins, OPA1 also

exhibits non fusion regulatory roles. OPA1 regulates cristae remodeling by maintaining the cristae junctions closed. This prevents the redistribution and the release of cytochrome C that leads to apoptosis [73]. In addition, OPA1 plays a role in mitochondrial respiration. Complexes in the electron transport chain can form respiratory super complexes (RSC) to facilitate the electron transfer and improve respiratory efficiency [80]. It has been shown that the stability of RSC is critically dependent on cristae morphology, thus puts OPA1 functions as an important regulator of mitochondrial respiratory efficiency.

The key component of mitochondrial fission is dynamin related protein 1 (Drp1). Fission results in smaller, more discrete, mitochondria that can be engulfed by autophagosomes and to be eliminated through the mitophagy pathway. In addition, mitochondrial fission facilitates the redistribution of mitochondria between daughter cells during mitosis and by that promotes proliferation. Drp1 is a cytosolic GTPase that is recruited to the mitochondria to promote fission. On mitochondria, Drp1 multimerizes and forms ring-like structures that constrict and divide the organelle. Drp1 activity is regulated by multiple post-translational modifications that include phosphorylation, ubiquitination and sumoylation [81-83]. Interestingly, phosphorylation of Drp1 has opposite effects depending on the phosphorylation site. Phosphorylation on Ser616 increases Drp1 activity while phosphorylation on Ser637 decreases it. Different kinases can phosphorylate these sites. Cyclin B1/CDK1 and calcium-calmodulin-dependent kinase (CamK) phosphorylate Drp1 on Ser616 providing a link from cell cycle and calcium homeostasis to mitochondrial fission [84-86]. PKCδ also phosphorylates Drp1 on Ser616 and links mitochondrial fission to oxidative stress and hypertension [87]. Phosphorylation of Drp1 on Ser637 by PKA inactivates it [88] and de-phosphorylation by calcineurin activates Drp1 [89].

1.2.3 Mitochondrial alterations in hyper-proliferative vascular disorders

Cellular hyper proliferation has been long considered an important etiological factor in CVD. Although VSMC are localized in the tunica media layer in the artery and are quiescent, in pathological states they proliferate and migrate towards the intimal layer. VSMC proliferation is stimulated by various extracellular mitogenic stimuli that include growth factors and cytokines. Specifically PDGF, EGF and TNFα have all been implicated in VSMC proliferation [5, 90, 91]. Proliferating VSMC decrease glucose oxidation and increase fatty acid oxidation. In this way, VSMC redirect glucose to bio-synthetic pathways that support DNA and protein synthesis. This process is similar to the Warburg effect that was described in cancer cells. These changes in metabolic pathways underlie the importance of mitochondria in proliferation. Indeed, mitochondrial dynamics has been recognized as a critical regulator of VSMC proliferation [8] and several growth factors have been shown to induce mitochondrial fission. For instance, in PAH, mitochondria in VSMC appear fragmented and is associated with increased VSMC proliferation [92]. Inhibition of Drp1 with a small molecule mitochondria division inhibitor 1 (Mdivi-1) induces mitochondrial fusion and suppresses PDGF induced proliferation [8]. VSMC proliferation is also controlled by Mfn2. In spontaneous hypertensive and atherosclerotic prone rats Mfn2 levels are diminished whereas over-expression of Mfn2 reduces VSMC proliferation [67].

PAH is an obstructive pulmonary vasculopathy. A new “oncologic view” is emerging that increased proliferation and decreased apoptosis of pulmonary arterial smooth muscle cells (PASMC) mediates the progression of PAH. Similar to cancer, PASMC in PAH upregulate HIF-1α under normoxic conditions that lead to Drp1 mediated mitochondrial fission [93]. In addition,

down-regulation of PGC-1α and consequently Mfn2 further contribute to the unopposed fission. Administration of Mdivi-1 restores mitochondrial fusion and diminishes PAH [94].

In atherosclerosis there is also evidence for mitochondrial dysfunction. There are multiple mtDNA anomalies such as deletions and oxidative damage in addition to reduced mitochondrial protein and ATP production [95-99]. Respiratory chain dysfunction has been also associated with atherosclerosis although the causality between the two has not been shown yet [100]. Mitochondrial dysfunction in cardiovascular diseases could arise because of risk factors such as smoking, ROS, diabetes and hyperlipidemia. For example, smoking can induce DNA damage and inhibit DNA repair [101]. Diabetes has been associated with failed DNA repair and excess of ROS [102]. Mitochondrial DNA is particularly susceptible to oxidative damage because of the proximity to the site of ROS generation and because of the limited mtDNA repair machinery. Altered mitochondrial dynamics can also lead to mitochondrial dysfunction. For example, inhibition of fusion does not allow content mixing from healthy mitochondria thus promoting accumulation of damaged and impaired mitochondria. Whether this contributes to vascular disease remains to be determined.

1.3 REACTIVE NITROGEN AND OXYGEN SPECIES IN THE CARDIOVASCULAR SYSTEM

The roles of ROS and reactive nitrogen species (RNS) in the normal vasculature and disease states have been the subject of intense investigation and continue to engender considerable debate. A disturbance in the oxidation–reduction state of the cell, in which ROS production exceeds antioxidant defenses, is called oxidative stress. By analogy, nitrosative stress is an

impairment in nitric oxide (NO) signaling caused by increased amounts of RNS, which may be caused by or associated with a disturbance in the redox state. The forms of ROS that are most relevant in biological systems include the superoxide radical ($O_2\bullet^-$), hydrogen peroxide (H_2O_2), and hydroxyl radical (•OH). RNS of biological importance include NO, low and high-molecular-weight S-nitrosothiols, and peroxynitrite ($ONOO^-$) (Figure 3). In the next section I will describe the main sources of ROS and RNS and the importance and regulation of the anti-oxidants to cellular health.

1.3.1 Sources of ROS and RNS

Traditionally macrophages were thought to be the main source of ROS in blood vessels [103], but it became clear that all cells in the vessel wall (endothelial cells, VSMC and adventitial cells) can produce ROS in various amount and in response to different stimuli. In the cardiovascular system, the majority of enzymatic sources of ROS include NADPH oxidases (Nox), lipooxygenase, cyclooxygenase (COX), xanthine oxidase (XO), uncoupled nitric oxide synthases (NOS), cytochrome P450, and mitochondrial respiration. The major ROS in the vasculature is $O_2\bullet^-$. $O_2\bullet^-$ is generated through one electron reduction of molecular oxygen and results in a free radical. $O_2\bullet^-$ can react with nitric oxide (NO) that is produced in endothelial cells and inactivate it. This reaction affects vascular relaxation and generates peroxynitrite anion ($ONOO^-$) that at high concentrations can react with and modify DNA, lipids and proteins which can lead to cytotoxicity [104]. After its generation superoxide is dismutated by SODs and converted to hydrogen peroxide that is more stable and in turn is converted to water by catalase and glutathione peroxidase (Figure 3). Hydroxyl radicals (•OH) are generated from H_2O_2 reaction with ferrous ions and they are extremely reactive with lipids, proteins and DNA (Figure 3).

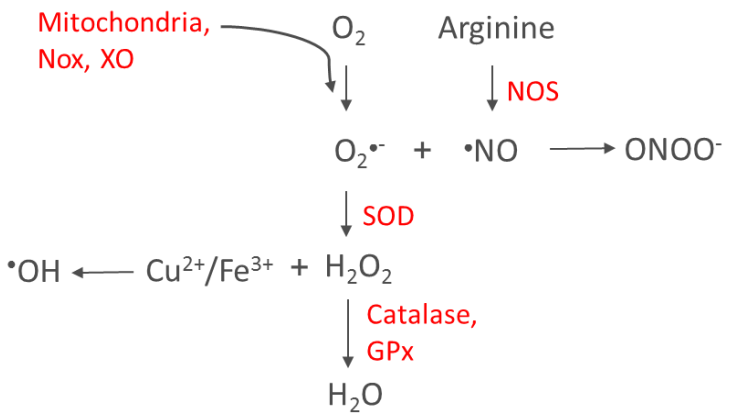

Figure 3: Reactive oxygen and nitrogen derived species and the anti-oxidants network

A simplified schematics of reactive oxygen species (ROS), reactive nitrogen species (RNS) and the anti-oxidants reactions. Mitochondria, NAPDH oxidases (Nox), Xanthine oxidases (XO) and uncoupled nitric oxide synthase (NOS) are some of the main enzymatic sources of ROS and RNS in the cardiovascular system. Mitochondria, Nox and XO lead to generation of superoxide ($O_2^{\bullet-}$). NOS generate nitric oxide (NO). $O_2^{\bullet-}$ reacts with NO to form peroxinitrite that can react and modify DNA, lipids and proteins. H_2O_2 can also react with ferrous ions (Cu^{2+}/Fe^{3+}) and generate hydroxyl radical (•OH). SODs react with $O_2^{\bullet-}$ and convert it to hydrogen peroxide (H_2O_2) and catalase and glutathione peroxidase (GPx) react with H_2O_2 and convert it to water.

H_2O_2 and other peroxidases have important signaling activities that are involved in VSMC and endothelial cells growth, differentiation, migration, vascular tone and inflammatory responses in vascular lesions. ROS can activate the MAPK/ERK pathway [105] and promote cell growth and differentiation as well as NFκB [106] and activator protein 1 (AP-1) [107] that regulate inflammatory responses that have a critical role in CVD.

In mitochondria, oxygen is utilized for energy production and oxidative phosphorylation. During mitochondrial electron transport (MET) reactions, electrons leak and react with oxygen to form superoxide. Because of the presence of MnSOD in mitochondria, superoxide is rapidly

converted to H_2O_2. However, in conditions of hypoxia and or ischemia the amount of ROS exceeds MnSOD capacity, which leads to high levels of ROS, resulting in mitochondrial dysfunction that can lead to cell death [108, 109].

NADPH oxidases (Nox) are found in cellular membranes and are activated in phagocytic cells which leads cells to generate superoxide, that is essential for neutrophils function and protection from pathogens [110]. Overexpression of Nox2 [111] and Nox4 [112] causes an increase in oxidative stress in CVD. In cardiac cells Nox4 knockdown results in low levels of superoxide, pointing to the significance of Nox4 the heart tissue [113]. On the other hand, Nox4 overexpression worsens cardiac function under pressure overload [114].

ROS are neutralized by intracellular antioxidants (such as glutathione peroxidase (GPx), SODs and catalase) and consumption of other non-enzyme antioxidants like β-carotene, ascorbic acid, and tocopherols. However, overproduction of ROS that exceeds that ability of antioxidants defense can cause significant damage to the cells and lead to apoptosis. In the next section I will describe in detail the function and the regulation the two major anti-oxidant enzymes – MnSOD and catalase.

1.3.2 The anti-oxidant enzymes

To ameliorate the injury from oxidative damage aerobic organisms developed a defense system of enzymatic and non-enzymatic anti-oxidants. Primary enzymatic anti-oxidants in eukaryotic cells are SODs, catalase and several peroxidases. In addition, there are secondary enzymes that act together with small molecular weight non-enzymatic anti-oxidants to form redox cycles that provide the primary anti-oxidants with the necessary co-factors. Among these glutathione, thioredoxin, NADPH, vitamin C and vitamin E that directly scavenge ROS.

1.3.2.1 MnSOD

The superoxide dismutase family is specialized in eliminating $O_2^{\bullet-}$ radicals generated from extracellular as well as intracellular stimuli. There are three distinct SOD isoforms: copper-zinc superoxide dismutase (Cu/ZnSOD, encoded by *sod1*), manganese superoxide dismutase (MnSOD, encoded by *sod2*) and extracellular superoxide dismutase (ECSOD, encoded by *sod3*). These forms of SOD have similar enzymatic functions, but differ in their protein structures, chromosome localizations, metal cofactor requirements, gene distributions and cellular compartmentalization. The compartmentalization and control of SOD expression and activity determine localized ROS level. Among the three SOD isoforms only MnSOD has been proven to be essential to the survival of aerobic organisms [115].

Human MnSOD is a tetrameric enzyme with four identical subunits each harboring a Mn^{+3} atom. *Sod2* gene is located on the 6th chromosome, 6q25.3 region encoding a ~223 amino acids/26 kD precursor monomer containing a mitochondria targeting sequence of 26 amino acids that is required for mitochondrial localization. MnSOD is highly conserved with 40% sequence homology among yeast, human and *E.coli*. The importance of MnSOD was demonstrated in knock out mice that died shortly after birth due to dilated cardiomyopathy and neurodegeneration [116, 117]. A number of studies have identified polymorphisms in *sod2* in cancer, type II diabetes and hypertension [118-120]. Since MnSOD is localized in the mitochondrial matrix, it has to be transported across two mitochondrial membranes and to be activated in mitochondria. This transport requires a targeting-sequence in the N-terminal of the polypeptide. As MnSOD is taken up by mitochondria, the targeting sequence is cleaved, leaving a 22 kD monomer, which later incorporates an Mn^{+3} ion and assembles into the mature 88 kD homotetramer in the

mitochondrion. Cytosine to thymine (C to T) single nucleotide polymorphism in the MnSOD mitochondrial targeting sequence, which causes the substitution of alanine (GCT) with valine (GTT) can disrupt the secondary α-helix structure of MnSOD and affect the localization and efficiency of mitochondrial transport of MnSOD enzyme [121].

In contrast to SOD1 that is constitutively expressed in cells, MnSOD is easily inducible under stress conditions. Stimuli such as ionizing radiation [122], interferon γ (INF-γ) and pro-inflammatory cytokines have been shown to induce MnSOD expression [123]. NF-κB has been identified as the most crucial factor that regulates MnSOD transcription [124] and is required for cytokine mediated induction of MnSOD [125]. In addition, *sod2* contains a p53 binding region [126]. p53 has both suppressive and inducing effects on MnSOD transcription that are dependent on cell type and p53 levels. At low concentrations, p53 induce MnSOD expression together with NF-κB, whereas at high levels it suppresses MnSOD transcription [127]. FoxO1 and Forkhead box O3 (FoxO3A) transcription factors can bind to *sod2* promoter and induce its transcription to protect quiescent cells from oxidative stress [128]. Specificity protein 1 (Sp1) is a zinc-finger protein that acts as a transcription factor by binding directly to DNA through three consecutive zinc-finger domains in the C-terminus and enhances gene transcription with one of the two glutamine-rich domains. Sp1 is essential for both constitutive and inducible expression of MnSOD [129].

In addition to transcriptional regulation, various post-translational modifications including phosphorylation, nitration, acetylation, gluthationylation and metal incorporation regulate MnSOD activity. $ONOO^-$ that is generated from NO and $O_2^{\cdot -}$ is a potent nitrating agent and can inactivate MnSOD through nitration of Tyr34 [130]. NAD+ dependent protein de-acetylase SIRT3 can remove acetyl groups from Lys53 and Lys89 on MnSOD and increase

MnSOD activity under conditions of ionizing radiation and oxidative stress [131, 132]. Therefore, both transcriptional and post-translational regulations of MnSOD expression and activity are sensitive to redox balance and allow immediate adaptive responses to protect the cells from excess of ROS. The fact that MnSOD is a primary defense mechanism of mitochondria form oxidative stress and that its dysfunction is detected in many pathological conditions, places it at a critical position of protecting mitochondrial and cellular faith.

1.3.2.2 Catalase

The human catalase gene (*Cat*) is located on the short arm of chromosome 11 and has all the characteristics of a housekeeping gene, with no TATA box, no initiator element sequence, and high GC content in the promoter. The enzyme, first described by Loew more than 100 years ago, is a homotetramer in which each monomer (62.5 kD) contains a heme b group responsible for the enzymatic activity. The human catalase belongs to the family of typical catalases, which predominantly catalyze the dismutation of H_2O_2 into water and molecular oxygen. In addition to its dominant "catalytic" activity, catalase can also decompose $ONOO^-$, oxidize NO to nitrogen dioxide, and exhibit marginal peroxidase (i.e., oxidation of organic substrates with concomitant reduction of a peroxide) as well as low oxidase activity (O_2-dependent oxidation of organic substrates).

Decreased catalase expression and/or activity has been associated with diseases such as diabetes, hypertension, vitiligo, Alzheimer disease, and acatalasemia [133]. Diseases that are associated with mutations of catalase gene illustrate the importance of this anti-oxidant enzyme

for human life. For example, acatalasemia is an autosomal inherited deficiency of erythrocyte catalase due to guanine-to-adenine substitution (Japanese type A), threonine deletion (Japanese type B), or guanine– adenine insertion (Hungarian type) [134]. Catalase-deficient mice are viable and fertile and develop normally with a normal hematological profile. However, after trauma mitochondria show defects in oxidative phosphorylation [135]. This phenotype could be explained by the presence of other H_2O_2-degrading enzymes such as glutathione peroxidases and peroxiredoxins. Mitochondrial catalase overexpression in mice increases life-span by 20% [136]. In addition, expression and activity of catalase in the aortic wall closely correlate with the formation of abdominal aortic aneurysms (AAA) in mice. Administration of PEG-catalase prevents the loss of tunica media and the formation of AAA induced by calcium chloride on mouse infrarenal aortas [137]. Similarly, catalase over-expression in VSMC results in enhanced VSMC survival and reduced AAA formation [137]. Over-expression of human catalase in $ApoE^{-/-}$ mice delays atherosclerotic development correlated with reduced F2-isoprostanes in plasma and aortas [138]. Increasing evidence suggest that catalase is also involved in other processes. ROS are able to activate various signaling pathways that increase the capacity for proliferation, migration, and invasion. Catalase can modulate these cellular responses by various mechanisms, the first obviously being its ability to directly reduce H_2O_2 levels. The second is its ability to bind and protect certain proteins from potential oxidative damage, such as growth factor receptor-bound protein 2 (Grb2) [139] and Src homology region 2-containing protein tyrosine phosphatase 2 (SHP2) [140], that are involved in the processes of proliferation and migration.

Catalase expression is predominantly regulated at the level of transcription. Catalase transcriptional regulators include Sp1 [141], nuclear factor Y (NF-Y) [142], FoxO [143]and

other transcription factors such CCAAT-enhancer-binding protein β (C/EBP-β) [144], peroxisome proliferator-activated receptor γ (PPARγ) [145], and POU Domain Class 2 Transcription Factor (POU2F1) [146]. The FoxO family consists of four proteins (FoxO1, 3A, 4, and 6) that regulate hormonal, nutrient, and stress responses [147]. Regulation of the FoxO protein family is post-translationally controlled by the Akt/Protein kinase B (PKB) signaling pathway [148]. The serine/threonine kinase, Akt, phosphorylates FoxO, which is consequently excluded from the nucleus by 14-3-3 protein and degraded by the ubiquitin proteasome system [148]. FoxO3A [149], FoxO1 [143, 150] and Forkhead box protein M1 (FoxM1) [151] have been mentioned as positive regulators of catalase expression. FoxO1, cooperates with PGC-1α to bind the *Cat* promoter at the consensus sequence TTATTTAC. The suppression of PGC-1α activity due to phosphorylation by Akt or the acetylation by histone acetyltransferase general control nonderepressible 5 (Gcn5), prevents DNA binding of FoxO1 to the *Cat* promoter and represses the expression of the enzyme [152]. Moreover, overexpressing an active form of FoxO1 stimulates catalase expression [153]. Therefore, FoxO1 can regulate the expression of both catalase and MnSOD. This places FoxO1 in a critical locus for redox control.

1.4 THE SCAFFOLDING PROTEIN EBP50/NHERF-1

1.4.1 Structure and function

Mammalian Na^+/H^+ exchange regulatory factor 1 (NHERF-1) is a member of a scaffolding proteins family that creates macromolecular complexes with trans-membrane or intracellular proteins to regulate their localization, function and signaling. NHERF-1 contains two PSD95-

/Disc large/ZO-1) (PDZ) domains (PDZ1 and PDZ2) protein-protein interaction domains that can bind to PDZ binding motifs, if present on other proteins. PDZ domains consist of 80-90 amino acids structure that is comprised of six β-sheets and two α-helixes. PDZ domains bind to specific motifs present on carboxy-terminus of binding protein partners. The carboxylate binding loop in PDZ domains contains a core motif (G-φ-G-φ, where φ is aromatic amino acid) which is G-Y-G-F in EBP50. There are three classes of PDZ proteins that are divided according to the binding motif of the ligand they interact with. NHERF-1 belongs to class I PDZ proteins that interact with ligands having [S/T]-X-φ in their C-terminus where X is any amino acid and φ is a hydrophobic residue. NHERF-1 interacts with GPCRs, receptor tyrosine kinases (RTK), ion channels and other signaling molecules (Figure 4 and Table 1). NHERF-1 also contains a carboxy-terminal domain to the membrane cytoskeleton linker, ezrin (EBD). Due to the interaction with ezrin NHERF-1 has another name – ezrin binding protein 50 (EBP50). Both terms, NHERF-1 and EBP50 are used interchangeably in the literature. In my thesis I will refer to the protein as EBP50.

Table 1: Some of the EBP50 binding partners with relevance to vascular biology.

Ligand	Binding domain	Reference
G Protein Coupled Receptors:		
β2-Adrenergic Receptor	PDZ1	Hall et al., 1998
Parathyroid Hormone Receptor 1	PDZ1, PDZ2	Wang et al., 2007, Weinmann et al., 2010
κ-Opioid Receptor	PDZ1	Huang et al., 2004
Ion transporters:		
Cystic Fibrosis Transmembrane Regulator	PDZ1	Wang et al., 1998, Short et al., 1998
Sodium Hydrogen antiporter 3	PDZ2	Weinmann et al., 2003
Sodium Phosphate co-transporter type IIa	PDZ1	Gisler et al., 2001
Receptor Tyrosine Kinases:		
Epidermal Growth Factor Receptor	PDZ1	Lazar et al., 2004
Platelet Derived Growth Factor Receptor	PDZ1	Maudsley et al., 2000
Others:		
S-phase Kinase-associated Protein 2	PDZ1	Song et al., 2015
Focal Adhesion Kinase	EBD	Song et al., 2012
Phospholipase lipase C β1/2	PDZ1	Tang et al., 2000
β-catenin	PDZ2	Shibara et al., 2003
AKT		Song et al., 2015

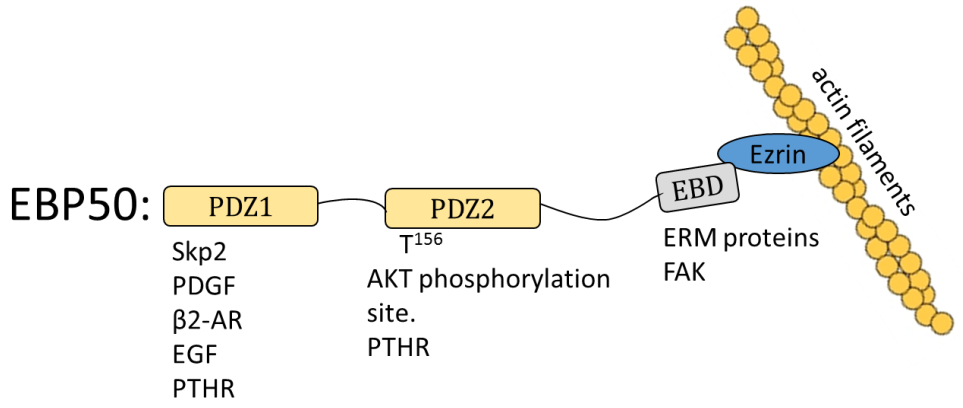

Figure 4: EBP50/NHERF-1 structure and binding partners.

EBP50 is a 358 amino acids protein that contains two PDZ domains (PDZ1 and PDZ2) and a C-terminal ezrin binding domain (EBD) through which it binds the cytoskeleton. Some of EBP50 binding partners are indicated under each domain.

EBP50 expression is particularly high in tissue with polarized epithelium such as kidney, placenta and liver. EBP50 is primarily localized near actin cytoskeleton. That is due to the cholesterol binding domain in PDZ1 [154] and the C-terminal EBD [155] that tethers EBP50 to the cytoskeleton through secondary protein interactions with ERM proteins (Figure 4). The interaction with ERM proteins is critical for EBP50 localization and affects the organization of cellular compartments. Depletion of EBP50 results in loss of microvilli in vitro [156] and $EBP50^{-/-}$ mice exhibit disorganized microvilli in the intestine [157-159]. Moreover, loss of EBP50 expression in the apical membrane of intestinal cells leads to a loss of epithelial polarity [160]. Overall, the localization of EBP50 to the apical membrane is critical to maintain epithelial polarity, an effect that is important in various cancers. Studies revealed that EBP50 contains numerous estrogen response elements (ERE) half sites that are sufficient for estrogen binding [161]. Consistently, there is a correlation between EBP50 and estrogen levels during the reproductive cycle. In addition, ER+ positive breast cancer tissue show increased EBP50 expression compared to ER- negative or normal tissues [162]. Interestingly, the mouse promoter does not contain ERE sites which suggests the presence of other mechanisms of regulation of EBP50. Indeed, Leslie et. al., demonstrated that NFκB transcriptionally regulates EBP50 expression in mouse vascular cells [163].

EBP50 contains multiple Ser/Thr residues that comprise 12% of the molecule and, not surprisingly, its activities are regulated by phosphorylation. EBP50 is phosphorylated by PKC [164], CDK1 [165], G-protein-coupled receptor kinase 6A GRK6A [166], AKT [167] and p90 ribosomal S6 kinase (RSK1) [168] (Figure 5). EBP50 phosphorylation plays a critical role in its activity and provides allosteric regulation of the PDZ domains. For example, phosphorylation of EBP50 by PKC on human Ser339/340, two sites within the EB domain,

increases the accessibility of PDZ2 domain to its targets [169]. Similarly, EBP50 phosphorylation by AKT on Thr156, in PDZ2, promotes the binding to S-phase kinase-associated protein 2 (Skp2) to PDZ1, which leads to stabilization of Skp2 in the cytoplasm and promotes cellular proliferation [167]. An additional phosphorylation site of EBP50 is Ser290 that is constitutively phosphorylated by GRK6A. Interestingly, GRK6A contains PDZ1 binding motif that is required for phosphorylation [166]. Moreover, Ser77 that is located in PDZ1, is phosphorylated in response to parathyroid hormone (PTH) stimulation and is critical for supporting Na^{2+}/H^{+} exchange and Na-Pi co-transport. Additional phosphorylation sites on EBP50 by PKC are residues Thr71, Ser77, Ser277, Ser287, Ser288, Ser299, Ser337, and Ser338; Ser339, Ser340. [164, 170].

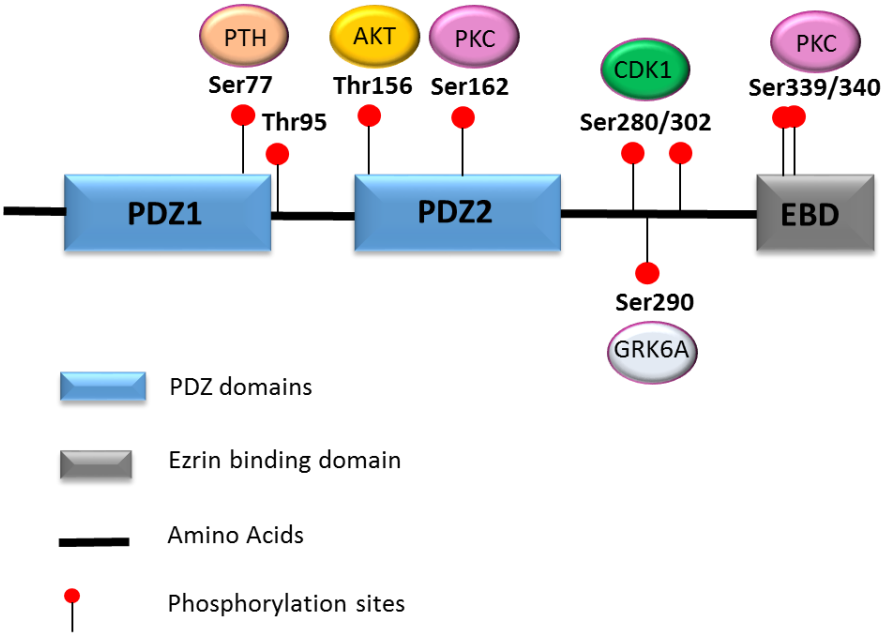

Figure 5: EBP50 phosphorylation sites

EBP50 is phosphorylated on multiple sites by various kinases such as AKT, PKC, CDK1 and GRK6A. EBP50 phosphorylation affects its activity, localization and oligomerization.

1.4.1.1 Roles of EBP50 in ion homeostasis

EBP50 binds to the renal sodium phosphate co-transporter 2a (Npt2a) and is critical to its function by controlling its localization. In the absence of EBP50 or in individuals with specific mutations in EBP50, Npt2a is not able to tether to the brush border of the apical membrane of the proximal nephron resulting in reduced phosphate reabsorption [171]. Npt2a, and consequently phosphate reabsorption, is regulated by PTH [172]. People with mutations or polymorphism in EBP50 also exhibit similar symptoms. Patients with EBP50 mutations also exhibit osteopenia that was initially thought to be a secondary event to hypophosphatemia [173]. However, later on it was found that EBP50 has a direct effect on bone mineralization and osteoblast differentiation that affect bone strength [174].

1.4.1.2 EBP50 effects in cancer

Many proteins that are involved in cancer interact with EBP50. This includes phosphate and tensin homolog (PTEN), PDGF, EGF, Neurofibromatosis type 2 (NF-2) and β-catenin. However the effects of EBP50 depend on the type of cancer. Some studies show that EBP50 act as tumor suppressor [175-177] while other show that EBP50 promotes tumor invasiveness and is associated with poor prognosis [162, 178, 179]. EBP50 contains ERE elements and it is therefore expected to exhibit correlation with estrogen receptor expression in breast cancer. Indeed, EBP50 is present in most ER-positive breast cancer tumors and is completely absent in the majority of ER-negative tumors [178, 180]. However, there is a controversy whether the correlation is positive or negative. Analysis of EBP50 expression in a large number of breast tumor samples, in two independent studies, revealed that EBP50 overexpression is significantly associated with

tumor stage, invasiveness, poor prognosis and ER status [162, 178]. These results position EBP50 as an oncogenic protein. In the contrary, other studies found that in breast and ovarian tumors EBP50 gene on locus 17q25.1 undergoes allelic loss [181, 182]. Clinically, EBP50 mutations are present in 3% of breast cancers and loss of heterozygosity occurs in nearly 50% of breast cancers. Both are associated with poor prognosis and survival [175]. In addition, missense mutation in PDZ2 domain of EBP50 was found in DNA extracted from breast tumor tissues but not in the adjacent tissue [175]. These results indicate a tumor suppressor role of EBP50. One explanation to these contradictory observations is that when EBP50 is localized at the cell membrane it acts as tumor suppressor, but when EBP50 is cytoplasmic it has oncogenic actions [183]. In support of this, a progressive shift from membranous to cytoplasmic localization is noted in breast tumors. Cytoplasmic localization is increased in advanced stages of cancer and is associated with more aggressive tumor characteristics [162, 178, 184, 185]. In contrast, invasive breast tumors that retain membranous localization of EBP50 have favorable prognosis [185]. In addition to membranous and cytoplasmic localization EBP50 is also found in the nucleus. Nuclear localization of EBP50 is seen in invasive breast tumors and metastases [179, 186]. Similar observations were made in glioblastoma and non-small cell lung carcinoma. In these tumors EBP50 is mainly localized in the cytoplasm and the nucleus and not at the membrane [187].

1.4.1.3 EBP50 roles in inflammation

Work from our lab indicates that under inflammatory conditions EBP50 expression is increased in NF-κB dependent manner. On the other hand, VSMC, endothelial cells and macrophages lacking EBP50 exhibit reduced NFκB activation. Following inflammatory stimuli EBP50

assembles a complex with PKCζ that in turn propagates NF-κB signaling cascade. ICAM and VCAM expression was reduced in EBP50 depleted cells and *in vivo* there was a reduction in macrophage recruitment after endoluminal denudation in the femoral arteries [163]. In addition, macrophage activation and expression of inflammatory cytokines was reduced in EBP50$^{-/-}$ mice.

ERM proteins have been shown to interact with Intercellular Adhesion Molecule 1 (ICAM1) and Vascular Cell Adhesion protein 1 (VCAM1) and promote leucocyte trans-endothelial migration [188]. ERM are activated by phosphatidylinositol 4,5-bisphosphate and bind to membrane proteins through EBP50. EBP50 assembles a macromolecular complex with ERM proteins, ICAM and f-actin to promote neutrophils infiltration in the liver [189]. EBP50 null mice exhibit reduced ERM and ICAM expression, attenuation in neutrophils accumulation in the liver and are protected from liver injury following bile duct ligation [189]. In addition, EBP50 mediates the physical coupling between phospholipase C β2 (PLC-β2) and C-X-C chemokine receptor type 2 (CXCR2) in neutrophils and disturbing CXCR2-EBP50-PLC-β2 complex significantly suppress intracellular calcium signaling, chemotaxis and trans-epithelial migration of neutrophils [190]. Collectively, EBP50 promotes inflammation in immune cells, VSMC and endothelial cells and therefore is a strong candidate to regulate inflammatory diseases such as atherosclerosis, inflammatory bowel disease and more.

1.4.1.4 Actions of EBP50 in the vasculature

Studies over the past decade highlight the important actions of EBP50 in the vasculature. In normal vessels, EBP50 is primarily expressed in the endothelial cells and at low levels in VSMC. However, under inflammatory conditions or following injury EBP50 expression in VSMC is markedly increased. Our lab demonstrated EBP50 null mice exhibit significant differences in

neointima formation after vascular injury [191]. EBP50 regulates VSMC migration and proliferation – processes that have a crucial role in vascular diseases (Figure 6). EBP50 promotes degradation of the cell cycle regulator $p21^{CIP}$ by potentiating the activity of Skp2 that degrades $p21^{CIP}$. Skp2 is the substrate recognition unit of Skp1/Cullin-1/F-box E3-ligase complex that promotes cell cycle and is upregulated in proliferative diseases [192]. Skp2 binds to EBP50 and this interaction localizes Skp2 in the cytoplasm. This prevents Skp2 degradation that happens in the nucleus and increases Skp2 stability. Phosphorylation of EBP50 by Akt promotes the interaction between EBP50 and Skp2 and results in increased expression and stability of Skp2 [167]. Overall our studies indicate that EBP50 promotes VSMC proliferation through stabilization of Skp2 (Figure 6).

Parathyroid hormone related protein (PTHrP) is elevated in proliferating VSMC especially after angioplasty [193]. Secretion of the 1-36 amino acid fragment of PTHrP typically inhibits VSMC proliferation in a PTH1R-cAMP dependent pathway [194]. However, EBP50 overexpression increases PTH1R at the membrane and restores its ability to signal through calcium. As a result, there is attenuation of the anti-proliferative effects of PTHrP fragments and induction of proliferation [195] (Figure 6).

EBP50 also regulates VSMC migration. VSMC migration is markedly increased in CVD. Focal adhesion kinase (FAK) is a central regulator of focal adhesion turnover and cell migration. EBP50 facilitates the formation of a complex between EGFR and FAK thus increases the phosphorylation of FAK and induces cell migration [196] (Figure 6). These observations are consistent with reduced neointima formation in $EBP50^{-/-}$ mice. However, Morel group described EBP50 functions in rat vasculature that are different. They propose that EBP50 inhibits VSMC migration. EBP50 knock down in rat VSMC resulted in an increase of the number and the size of

focal adhesions and induction of migration [197]. In addition, the group shows that depletion of EBP50 drastically changed VSMC morphology by decreasing actin bundles and increasing microtubules localized at the membrane lamellae. This species-specific difference in how EBP50 affects VSMC migration is still unresolved.

Even though EBP50 is highly expressed in endothelial cells there is a very limited understanding of EBP50 role in these cells. In bovine pulmonary artery endothelial cells EBP50 is expressed in the nucleus and translocates to the cytoplasm after phosphorylation during mitosis [198]. Cell cycle dependent specific interactions between EBP50 and protein phosphatase 2 (PP2A) suggest that PP2A can be responsible for the de-phosphorylation of EBP50 during cytokinesis [198]. In addition, it was shown that EBP50 is required for nuclear localization of merlin in endothelial cells and is needed to maintain merlin in non-phosphorylated (Ser518) form. When EBP50 is depleted merlin translocates to the cytoplasm, becomes phosphorylated and promotes endothelial migration [199].

ROS play a critical role in the progression of CVD. A recent study demonstrated that EBP50 facilitates agonist induced Nox1 superoxide production in VSMC, via binding to Nox organizing subunit - $p47^{phox}$. Depletion of EBP50 abrogates AngII induced cellular hypertrophy and resistance artery vasoconstriction [200].

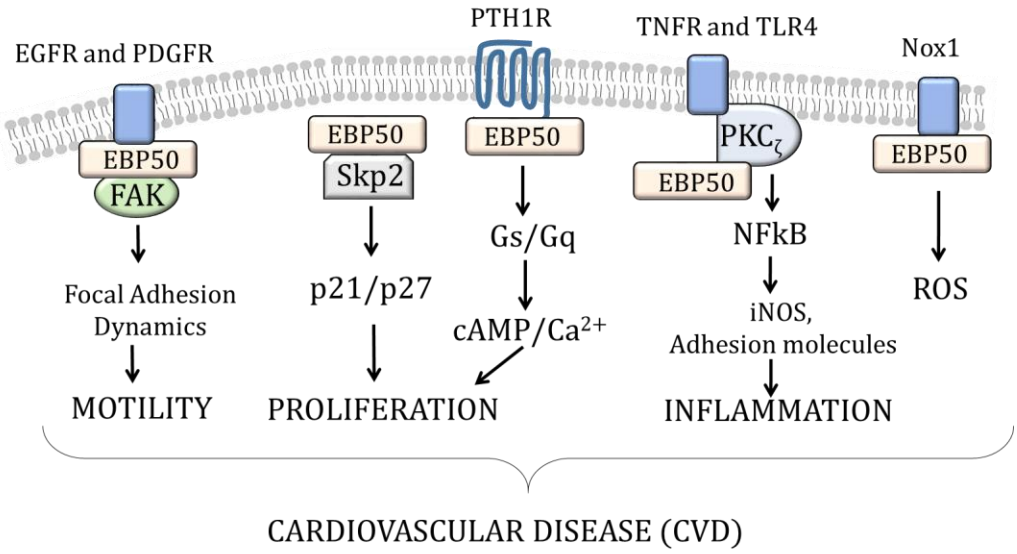

Figure 6: EBP50 effects in VSMC

Summary of EBP50 effects in VSMC. EBP50 interacts with multiple binding partners in VSMC and through those interactions promotes migration, proliferation, inflammation and ROS production.

1.5 RATIONALE, HYPOTHESIS AND SPECIFIC AIMS

1.5.1 Rational and hypothesis

CVD is the leading cause of death worldwide. Hyper-proliferation of VSMC, inflammation and oxidative stress play a central role in CVD. Inhibition of these processes is an important target for pharmaceutical interventions to treat CVD. Mitochondria are dynamic organelles that undergo continuous fusion and fission in order to support proper cell function. Alterations in mitochondria dynamics have been associated with CVD such as pulmonary hypertension and

restenosis. EBP50 is a scaffolding PDZ-domain phospho-protein, which is also known as NHERF-1. In a murine model of arterial injury we showed that EBP50$^{-/-}$ mice exhibit significant (80%) reduction in neointima formation. Mechanistically, we showed that EBP50 promotes PKCζ activity that is critical for inflammatory response in VSMC, and increases Skp2 stability which causes VSMC proliferation [163, 191]. My preliminary studies suggest that depletion of EBP50 increases the stability of FoxO1 due to reduced Skp2 levels. FoxO1 has been shown to transcriptionally co-regulate the mitochondrial fusion protein, Mfn2, and the anti-oxidant enzymes MnSOD and catalase. On the other hand, PKC phosphorylates and activates a key fission protein, Drp1 in neuronal cells. Based in these observations, I hypothesize that EBP50 regulates mitochondrial dynamics and redox balance in VSMC. To test this hypothesis I designed 2 aims:

1.5.2 Aim 1: To determine the effect of EBP50 on mitochondrial fission and fusion in VSMC

In this aim I will explore the mechanism by which EBP50 regulates mitochondrial dynamics. Inflammation is associated with increased mitochondrial fission, a process that is regulated by post-translational modifications of Drp1. TNFα is a central inflammatory cytokine, but surprisingly the mechanism of its effect on mitochondrial fission has not been described in VSMC. EBP50 promotes PKCζ activation in response to TNFα. Therefore, I will determine the role of TNFα and PKCζ on Drp1 activation. In addition, I will determine whether Mfn2 is regulated by EBP50 through the Skp2-FoxO1 axis. I will use confocal and transmission electron microscopy to characterize mitochondrial connectivity and morphology in WT and EBP50$^{-/-}$ VSMC and to determine the role of TNFα on mitochondrial dynamics.

1.5.3 Aim 2: To determine the effect of EBP50 on mitochondrial function, metabolism and ROS production

Alterations in mitochondrial morphology and dynamics can lead to mitochondrial dysfunction, defects in oxidative phosphorylation, further increase in ROS and cellular damage. In addition, anti-oxidants are critical regulators of redox balance in cells. In this aim I will explore the effects of EBP50 on mitochondrial function and on MnSOD and catalase. I will perform cellular bioenergetics analysis (oxygen consumption rate and extracellular acidification rate) and examine mitochondrial ultrastructure. To assess the effects of EBP50 on ROS levels, I will determine MnSOD and catalase levels in VSMC and in mice vessels. In addition, I will use TNFα and antimycin A (Ant A) to induce mitochondria derived ROS and will measure mitochondrial superoxide in WT and EBP50$^{-/-}$ VMSC. Due to the important role of ROS in the regulation of VSMC migration, I will measure WT and EBP50$^{-/-}$ VMSC migration in response to TNFα.

2.0 EBP50 REGULATES BASAL AND TNF-ALPHA-INDUCED MITOCHONDRIAL DYNAMICS AND VASCULAR SMOOTH MUSCLE CELLS PROLIFERATION

Mitochondrial dysfunction and changes in mitochondrial dynamics (fission and fusion) are associated with phenotypic switch of vascular smooth muscle cells (VSMC) and vascular diseases. Mitochondrial dynamics is regulated by several key molecules, including dynamin-related protein 1 (Drp1) and mitofusin-2 (Mfn2). We previously showed that scaffolding ezrin-radixin-moesin binding phosphoprotein of 50 kD (EBP50) increases proliferation and inflammatory responses in VSMC. These actions are mediated by the activation of PKCζ under inflammatory stimuli and the stabilization of the S-phase kinase associated protein 2 (Skp2), a component of an E3 ligase that promotes proliferation. Thus, EBP50 knockout ($EBP50^{-/-}$) mice are protected from neointimal hyperplasia following arterial injury. Here we report that EBP50 knockdown, by decreasing Skp2 levels, increases FoxO1 stability and nuclear localization and leads to higher Mfn2 expression. In contrast, inhibition of FoxO1 reduces Mfn2 levels. High resolution morphological analysis with both TEM and confocal microscopy revealed that mitochondria are more elongated in $EBP50^{-/-}$ VSMC than in WT VSMC. We also show that PKCζ mediates phosphorylation of Drp1 following TNFα and $EBP50^{-/-}$ VSMC exhibit significantly reduced Drp1 phosphorylation following TNFα treatment. Consistently, live-cell 3D imaging demonstrate that TNFα elicits rapid mitochondrial fragmentation in WT, but not in $EBP50^{-/-}$ VSMC. Finally, $EBP50^{-/-}$ VSMC exhibit lower extracellular acidification rate (ECAR)

and lower TNFα- induced proliferation than WT VSMC. Collectively, these findings delineate a new mechanism of regulation of mitochondrial dynamics by the scaffolding protein EBP50 in response to inflammatory stimuli. Therefore, EBP50 can be viewed as a potential therapeutic target for vascular proliferative diseases.

2.1 INTRODUCTION

Vascular smooth muscle cells (VSMC) play an essential role in the regulation of vascular tone. Normally, VSMC have a very low proliferation rate, however during cardiovascular disease VSMC begin to proliferate as the disease progresses. Proliferation of VSMC is affected by various growth factors and cytokines and limits the success of treatments such as coronary bypass vein grafts and angioplasty [201].

Mitochondrial dysfunction has been associated with VSMC proliferation and multiple vascular diseases such as atherosclerosis, pulmonary hypertension and restenosis. Mitochondrial dynamics have a crucial role in mitochondrial function and alterations in fission and fusion have been associated with numerous cardiovascular pathologies [7, 76, 202, 203]. Mitochondrial fission and fusion events are regulated by number of GTPase proteins, including mitofusin-2 (Mfn2) and dynamin related protein 1 (Drp1). Mfn2 is localized on the outer mitochondrial membrane and promotes fusion. The expression of Mfn2 is mainly regulated transcriptionally and through ubiquitination [66, 67, 69, 204-206]. Previous studies showed that activation of FoxO1/PGC-1α induces Mfn2 transcription [69]. Drp1 is a cytoplasmic protein that is recruited to mitochondria upon activation and promotes fission. Its activity is tightly regulated though

phosphorylation by several kinases, including PKCδ [87]. Ultimately, the balance of fusion and fission is a critical determinant of mitochondrial function, and dysregulation of Mfn2 and Drp1 can lead to alterations in cellular metabolism and proliferation [6, 67, 207].

Ezrin radixin moesin (ERM) binding phosphoprotein of 50 KDa (EBP50), also known as Na/H exchange regulatory factor 1 (NHERF1), is a PDZ-domain scaffolding protein that plays a critical role in vascular inflammation and remodeling. EBP50 directs the cellular localization of its partners, the assembly and regulation of signaling complexes and the function of various proteins [163, 191, 196]. EBP50 interacts with Skp2 (the substrate recognition unit of the Skp1/Cul-1/Rbx-1/Skp2 E3-ligase) and promotes its cytoplasmic localization and stability [167]. Thus, the interaction between EBP50 and Skp2 leads to more effective ubiquitination and degradation of Skp2 target proteins such as $p21^{CIP}$ resulting in VSMC proliferation [191]. Moreover, in TNFα- and LPS-stimulated VSMC EBP50 facilitates the recruitment and activation of PKCζ thereby promoting inflammatory responses [163].

Because of these significant effects on VSMC proliferation and inflammation and its ability to regulate multiple signaling pathways we hypothesize that EBP50 regulates mitochondrial dynamics. Here we characterize two mechanisms by which EBP50 regulates Mfn2 expression and Drp1 activation, leading to alterations in mitochondrial dynamics, VSMC metabolism and proliferation both in basal conditions and under inflammatory stimuli. Our results provide further insight into the mechanisms impacting VSMC phenotype in pathological conditions.

2.2 MATERIALS AND METHODS

2.2.1 Cell culture and transfections

Primary VSMC were isolated from mouse aortic explants and grown in DMEM containing 10% FBS in 5% CO_2 at 37^0 C as described previously [196]. Various constructs including pcDNA, Flag-Skp2 (a generous gift from Dr. Michele Pagano, New York University School of Medicine), Flag-FoxO1 (pCMV5) a gift from Domenico Accili (Addgene plasmid #12148) [208], mitoRFP (a generous gift from Dr. Lippincott-Schwartz, NICHD NIH) and siSkp2 (0.1μM) were introduced to VSMC by electroporation with AMAXA electroporator and the basic Nucleofector kit for primary vascular smooth muscle cells (Lonza) as described previously [196] and the siSkp2 transfected cells were used 72h after transfection. Small molecule FoxO1 inhibitor (AS1842856) from Calbiochem was used at 0.5 μM concentration for 24 hours. For expression of PKCζ-kinase dead (KD) (K281W), a generous gift from Dr. Adolfo Garcia-Ocaña (Mount Sinai Medical Center) and shFoxO1 (kindly provided by Dr. Adam Straub, University of Pittsburgh) constructs, VSMC were seeded on 6-well plate at 50-70% confluency and incubated with adenovirus in serum free media for 1 hour and following that in DMEM with 2% FBS overnight. Then media was changed to DMEM with 10% FBS. 48 hours post infection cells were starved in 0.1% FBS overnight (for Drp1 activation) and experiments were performed 72 hours post infection.

Lentiviral shRNA vector specific to mouse EBP50 and GFP-expression control were prepared by the Lentiviral Facility at the University of Pittsburgh Cancer Institute. The target sequence of the EBP50 shRNA is GAGTTCTTCAAGAAGTGCAAA. WT VSMCs were

infected at 4 MOI with 8 μg/mL polybrene in the media. Media was changed 24 hours post infection and the cells were used 7 days post infection.

2.2.2 Real time PCR

RNA was isolated from cells using Quick-RNA MiniPrep kit (Zymo Research) and cDNA was generated using SuperScript III First-Strand Synthesis system kit (Thermo Fisher). TaqMan mouse primers for Mfn2, 18S and β-actin were purchased from Applied Biosystems. PCR reactions were run using Taqman Fast Universal Master Mix (Applied Biosystems) reagent. FoxO1 inhibitor AS1842856 (Calbiochem) was used at 0.5 μM concentration for 24 hours.

2.2.3 Western blot

For pDrp1 detection cells were starved in 0.1% FBS overnight. Cells were lysed in urea lysis buffer (4 M urea, 62.5 mM Tris, 2% SDS, 1 mM EDTA) containing protease and phosphatase inhibitors (Roche). Cell lysates were resolved by SDS-PAGE. Proteins were transferred onto nitrocellulose membrane and incubated with primary antibodies (1:1000 dilution for Tom20 (Santa Cruz), 1:500 dilution for IKK (Cell Signaling), 1:500 dilution for EBP50 and PKCζ (Santa Cruz Biotechnology), 1:200 for Skp2 (Santa Cruz Biotechnology); 1:1000 dilution for pDrp1, Drp1, pIKK (Cell Signaling), 1:1000 for Mfn2 (Abcam); 1:5000 dilution for β-actin (Sigma) and 1:2000 dilution for horseradish peroxidase-conjugated anti-rabbit and anti-mouse IgG antibody (Cell Signaling). Immunoreactivity was detected by incubation with WesternBright ECL HRP substrate (Advansta). Quantification of band intensity was performed with ImageJ (National Institute of Health).

SKP2 E3 Ligase Inhibitor III (Calbiochem) was used at 20 μM concentration for 24 hours. Recombinant mouse TNFα (R&D Systems) was used at 10 ng/mL concentration. VSMC were serum starved in 0.1% FBS DMEM overnight and pre-incubated with 9-10 μM PKCζ presudosubstrate (Calbiochem) for 1 hour prior to TNFα treatment.

2.2.4 Immunofluorescence

For TNFα induced fragmentation experiments, primary mouse WT and EBP50$^{-/-}$ VSMC were seeded on coverslips and serum starved in 0.1% FBS DMEM overnight. Then, VSMC were treated with 10 ng/mL TNFα for 5-6 hours. Following TNFα treatment or under basal conditions without serum starvation, cells were fixed with 4% paraformaldehyde and permeabelized in 0.1% SDS, 0.2% Triton X-100, 4% FBS in PBS for 30 minutes and incubated with Tom20 antibody (Santa Cruz, 1:500) overnight at 4 degrees Celsius. As a secondary antibody anti-rabbit Alexa-Flour 546 (Invitrogen, 1:1000) was used together with α-smooth muscle actin (FITC-conjugated, Sigma, 1:1000) for 1.5 hours at room temperature prior to DAPI staining. For imaging cells were visualized using Olympus Fluoview 1000 confocal laser scanning microscope with a 60X oil immersion objective.

For FoxO1 localization primary mouse WT and EBP50$^{-/-}$ VSMC were seeded on coverslips and treated with Akt inhibitor (Akt I) (5 μM) or EGF (10 ng/mL) for 2.5 hours. Then, cells were fixed in 4% paraformaldehyde (PFA) and permeabelized in 0.1% SDS, 0.2% Triton X-100, 4% FBS in PBS for 30 minutes and incubated with FoxO1 (Cell Signaling, 1:100) primary antibody overnight at 4 degrees celsius. As a secondary antibody anti-rabbit Alexa-Flour 546 (Invitrogen, 1:1000) was used together with α-smooth muscle actin (FITC-conjugated, Sigma, 1:1000) for 1.5 hours at room temperature prior to DAPI staining. Cells were visualized

using Olympus Fluoview 1000 confocal laser scanning microscope with a 60X oil immersion objective. Number of cells that contained nuclear FoxO1 was quantified and transposed to percentage.

2.2.5 Live cell imaging

Cells were transfected with mitoRFP using Amaxa electroporation and seeded in a glass bottom 30 mm tissue culture dish (MatTek). On the next day media was changed and 5 randomly chosen cells were imaged every 2 minutes for 30 minutes per dish. Then TNFα 10 ng/mL was added and the cells were imaged for additional 30 minutes. Images were acquired with a Nikon Ti inverted microscope equipped with a 1.40 N.A. 60x objective. Confocal images were captured using a Swept Field confocal scan head from Prairie Technologies equipped with a Photometrics Evolve camera. Image acquisition was performed with Nikon NIS Elements software equipped with a National Instruments Data Acquisition Card (NI DAQ) which controlled system triggering for high speed image acquisition and Piezo Z stage control (Mad City Labs Piezo Z stage insert). Following acquisition images were processed with Imaris software for mitochondria detection. Fragmentation was calculated as an increasing number of mitochondria per field and plotted on a graph. Slopes were calculated using linear regression for WT and EBP50$^{-/-}$ to determine differences between slopes and in fragmentation.

2.2.6 Sphericity calculation

In order to develop an unbiased method to quantify mitochondrial morphology we implemented the Imaris software (Bitplane) that automatically detects 3D mitochondrial Tom20 staining and

can apply numerous algorithms to it. Following image acquisition we used “surfaces” function (in Imaris) - a computer based representation of the region of interest, in our case Tom20 mitochondrial staining (Figure 7F). Analyzed images contained 3-7 confocal images per condition, with approximately 5 cells in each field and >1000 mitochondria (surfaces particles) per cell, that were analyzed with sphericity Imaris packet. Sphericity is defined as the ratio of the surface area of a sphere (with the same volume as the given particle) to the surface area of the particle. Sphericity values range from 0 to 1 when 1 is a perfect sphere and low ratios indicate less spheric morphology. Our assumption was that single non-fused mitochondrion will have more spheric morphology (values closer to 1) and fused mitochondria will have less spheric morphology (values closer to 0). After measuring the sphericity of mitochondrial particles we plotted the values on a frequency distribution graph to compare between WT and EBP50$^{-/-}$ distributions. On the graph the vertical columns represent how many time each sphericity value occurs in the population. To compare between WT and EBP50$^{-/-}$ populations we used Kolmogorov-Smirnov statistical test.

2.2.7 Measurement of cellular bioenergetics using XFe96 extracellular flux analyzer

Cellular bioenergetics was measured in intact VSMC using a Seahorse Bioscience XFe96 extracellular flux analyzer (Agilent Seahorse Technologies, Santa Clara, CA). Twenty thousand cells per well were seeded and subsequently were treated with TNFα 10 ng/mL for 24 or 2 hours prior to measurements. After equilibration in non-buffered DMEM, baseline oxygen

consumption rates (OCR) and extracellular acidification rate (ECAR) were recorded. Then oligomycin A 1 μM, carbonyl cyanide p-(trifluoro-methoxy) phenyl-hydrazone (FCCP) 2.5 μM and rotenone 2 μM were consecutively injected and changes in OCR were measured after each injection. Upon completion of the assay, cells were stained with crystal violet and the data was normalized to cell number.

2.2.8 Transmission electron microscopy

Primary WT and EBP50$^{-/-}$ VSMC were grown in 6-well plate to at least 80% confluency. Then, cells were washed once with 1x PBS and fixed with 2.5% EM Grade Glutaraldehyde for 1 hour, washed 3x in PBS, and postfixed in aqueous 1% OsO4 and 1% Potassium Ferricyanide for 1 hour. After 3x PBS washes, cells were dehydrated through a graded series of 30% to 100% ethanol. The final 100% was removed and immediately replaced with EPON for 1 hour. After 3 additional 1 hour changes of EPON, Epon was removed and BEAM capsules filled with EPON were inverted into the dish and allowed to harden in a 37C oven for one day and a 60C oven for two days. Hardened blocks were then popped off of the dish and 70nm sections of the monolayer were taken using a Leica EM UC7 ultramicrotome. Sections were placed on 200 mesh copper grids, counterstained with lead citrate and uranyl acetate and then imaged on a JEOL JEM- 1011 TEM (Peabody, MA) at 80 kV with an AMT camera system.

2.2.9 Proliferation assay

For BrdU incorporation experiments, cells were grown on coverslips. Cells were starved in 0.1% FBS DMEM for 24 hours. TNFα (100 ng/mL) and Mdivi-1 (10 μM) were added to the cells and

6 hours after, BrdU (0.1 mM) was added for total 18 hours. Following fixation with 4% parafolmadehyde, cells were permiabilized with 0.5% Triton X-100/PBS for 10 minutes, rinsed with PBS and permiabilized again with 0.05% Tween 20/PBS for 5 minutes. Then, the cells were incubated with anti-BrdU (1:100, Capralogics) in buffer that contained RQ1 DNase I (Promega), 1 M $MgCl_2$, 1 M $CaCl_2$, 1% BSA and 1% FBS in PBS for 30 minutes at 37^0C. Cells were rinsed with PBS and incubated with secondary anti-sheep Alexa 594 (1:750, Molecular Probes) in 1% BSA, 1% FBS containing PBS for 30 minutes at 37^0C. When finished coverslips were rinsed in PBS/0.05% Tween 20 for 30 minutes (wash changes 4 times). Coverslips were mounted in Fluorogel (Electron Microscopy Sciences) contacting DAPI. Cells were visualized using Olympus Flouview 1000 confocal laser scanning microscope with a 20X oil immersion objective.

2.2.10 Statistical analysis

Data are presented as mean +/-SEM. Sphericity data are plotted on a Frequency distribution graph. Sphericity distributions of WT and $EBP50^{-/-}$ VSMC were compared using Kolmogorov-Smirnov Test. For live cell fragmentation slopes were compared using linear regression analysis. Two groups were compared using student t-test and multiple groups were compared with One-way or Two-way Anova tests. Statistical analyses were done using GraphPad Prism 7.03 and p values < 0.05 were considered significant.

2.3 RESULTS

2.3.1 EBP50 depletion increases FoxO1 stability

FoxO1 is a transcription factor that regulates genes involved in stress resistance, longevity, cell cycle and metabolism [209]. FoxO1 protein levels are regulated post-translationally by the ubiquitin proteasome system. FoxO1 is phosphorylated by Akt. Upon phosphorylation, FoxO1 translocates from the nucleus to the cytosol where it is ubiquitylated by the Skp2-containing E3 ligase and targeted for proteasomal degradation [147]. We have shown that EBP50 interacts with Skp2 and increases its cytoplasmic localization and stability, and EBP50$^{-/-}$ cells have reduced levels of Skp2 [167]. In addition, EBP50 increases the activity of Akt in VSMC [167]. Therefore we hypothesized that reduced Skp2 levels in EBP50 depleted VSMC will result in more stable FoxO1. Using immunofluorescence, we found a greater fraction of FoxO1 in the nucleus of EBP50$^{-/-}$ VSMC compared to WT cells (Figure 7A-B). To ensure that FoxO1 ability to translocate form the nucleus to the cytoplasm was not impaired in EBP50$^{-/-}$ VSMC, we treated the cells with Akt inhibitor (Akt I), to promote nuclear localization, or with EGF to promote cytoplasmic localization. Under these conditions WT and EBP50$^{-/-}$ VSMC had similar translocation of FoxO1 between nucleus and cytoplasm (Figure 7A-B), indicating that FoxO1 ability to shuttle between nucleus and cytoplasm is not affected by EBP50 depletion. Next, we monitored FoxO1 stability in primary VSMC in which EBP50 expression was reduced with a lentiviral construct expressing shEBP50. Seven days post infection, shEBP50 cells exhibited reduced Skp2 levels compared to GFP control cells (Figure 7C). EBP50 knock-down increased

FoxO1 stability determined in the presence of cycloheximide (CHX) (Figure 7D), whereas the level of FoxO1 increased in both WT and shEBP50 cells upon treatment with the proteasome inhibitor MG132 (Figure 7D). To further characterize the direct involvement of Skp2 in FoxO1 degradation we overexpressed Skp2 in primary VSMC. In these cells we observed reduced expression of FoxO1 (Figure 7E). In contrast, depletion of Skp2 by siRNA increased FoxO1 levels (Figure 7E). Collectively, these results indicate that EBP50 regulates FoxO1 stability and localization through Skp2.

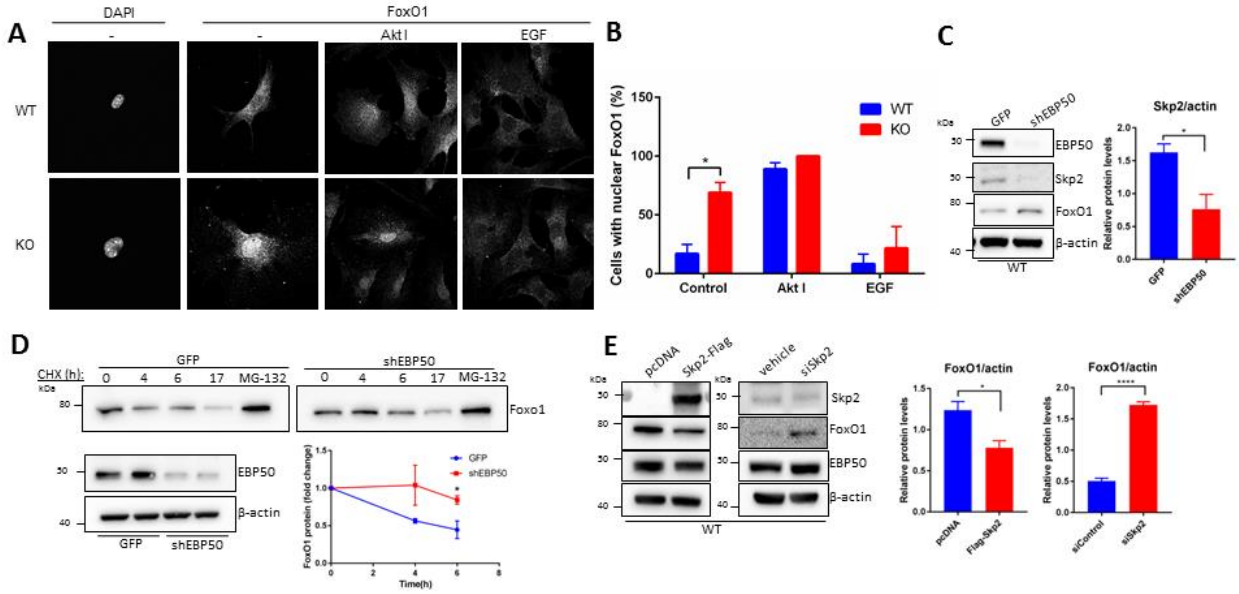

Figure 7: FoxO1 is more stable and nuclear in EBP50 depleted VSMC.

A, Primary mouse WT and EBP50$^{-/-}$ VSMC were seeded on coverslips and treated with Akt inhibitor (Akt I) (5 μM) or EGF (10 ng/mL) for 2.5 hours. Then, cells were fixed in 4% paraformaldehyde (PFA) and stained with FoxO1 antibody. **B**, Number of cells that contained nuclear FoxO1 was quantified and transposed to percentage (n=3, $p < 0.05$). **C**, Primary mouse WT VSMC were infected with lentivirus expressing shEBP50 or GFP. 7 days post infection cells were lysed in urea lysis buffer (see Materials and Methods) and Western blot was performed. Graphs represent means +/-SEM of three independent experiments ($p<0.05$). **D**, Primary mouse WT VSMC were infected with lentivirus expressing shEBP50 or GFP. 7 days post infection cells were treated with cycloheximide (10 μg/mL) for the indicated times and MG-132 (2 μM) for 17 hours. Proteins were extracted and subjected to Western blot. Data presented as mean +/- SEM. ($p < 0.05$, n=3).

E, Primary mouse WT VSMC were transfected with Skp2-Flag plasmid for 24 hours or with siSkp2 for 72 hours. Cells were lysed in urea lysis buffer and western blot was performed. Graphs represent means +/-SEM of three independent experiments ($p<0.05$).

2.3.2 EBP50 regulates Mfn2 levels and mitochondrial fusion

FoxO1 is a transcriptional co-regulator of mitofusin-2 (Mfn2) expression [69]. Because EBP50$^{-/-}$ VSMC have more stable and nuclear FoxO1, we expected that EBP50$^{-/-}$ VSMC will have increased Mfn2 expression. Indeed, compared to WT, EBP50$^{-/-}$ VSMC have higher mRNA and Mfn2 protein levels (Figure 8A-B). Furthermore, the small molecule FoxO1 inhibitor (AS1842856) reduced Mfn2 mRNA (Figure 8C). Conversely, over-expression of FoxO1 resulted in an increase of Mfn2 mRNA (Figure 8C). Finally, down regulation of FoxO1 with an adenovirus expressing shFoxO1 resulted in decreased protein levels of Mfn2 (Figure 8D). These results indicate that FoxO1 regulates transcription and protein levels of Mfn2 in VSMC.

Mfn2 promotes mitochondrial fusion and increased Mfn2 expression leads to more fused mitochondrial network [76, 205, 210] . Therefore, we wanted to examine whether the increased Mfn2 levels in EBP50$^{-/-}$ VSMC impact mitochondrial morphology. To this end, we visualized mitochondria by immunostaining fixed VSMC with a Tom20 antibody. Z-stack confocal images (Figure 8E) were analyzed with Imaris software package (Figure 8F) using sphericity as the parameter of mitochondria morphology (see Experimental Procedures section) and plotted on a "Frequency distribution" graph (Figure 8G). We found that the percentage of mitochondria in EBP50$^{-/-}$ VSMC that is represented by red bars on a graph (Figure 8G) is consistently higher at

lower sphericity values (0-0.65) compared to WT mitochondria, which indicates that the percentage of more fused mitochondria in higher in EBP50$^{-/-}$ VMSC compared to WT VSMC. On the other hand, the percentage of mitochondria with higher sphericity values (0.65-1) is consistently higher in WT VSMC that are represented with blue bars on a graph (Figure 8G), which indicates that the percentage of fragmented mitochondria is higher in WT VSMC compared to EBP50$^{-/-}$ VSMC. Overall, the distributions of mitochondrial sphericity of WT and EBP50$^{-/-}$ VSMC are significantly different when distribution of mitochondria from EBP50$^{-/-}$ VSMC is shifted towards lower sphericity (i.e. more fused) compared to WT cells. Thus, the increased levels of Mfn2 in EBP50$^{-/-}$ VSMC lead to more fused and elongated mitochondria.

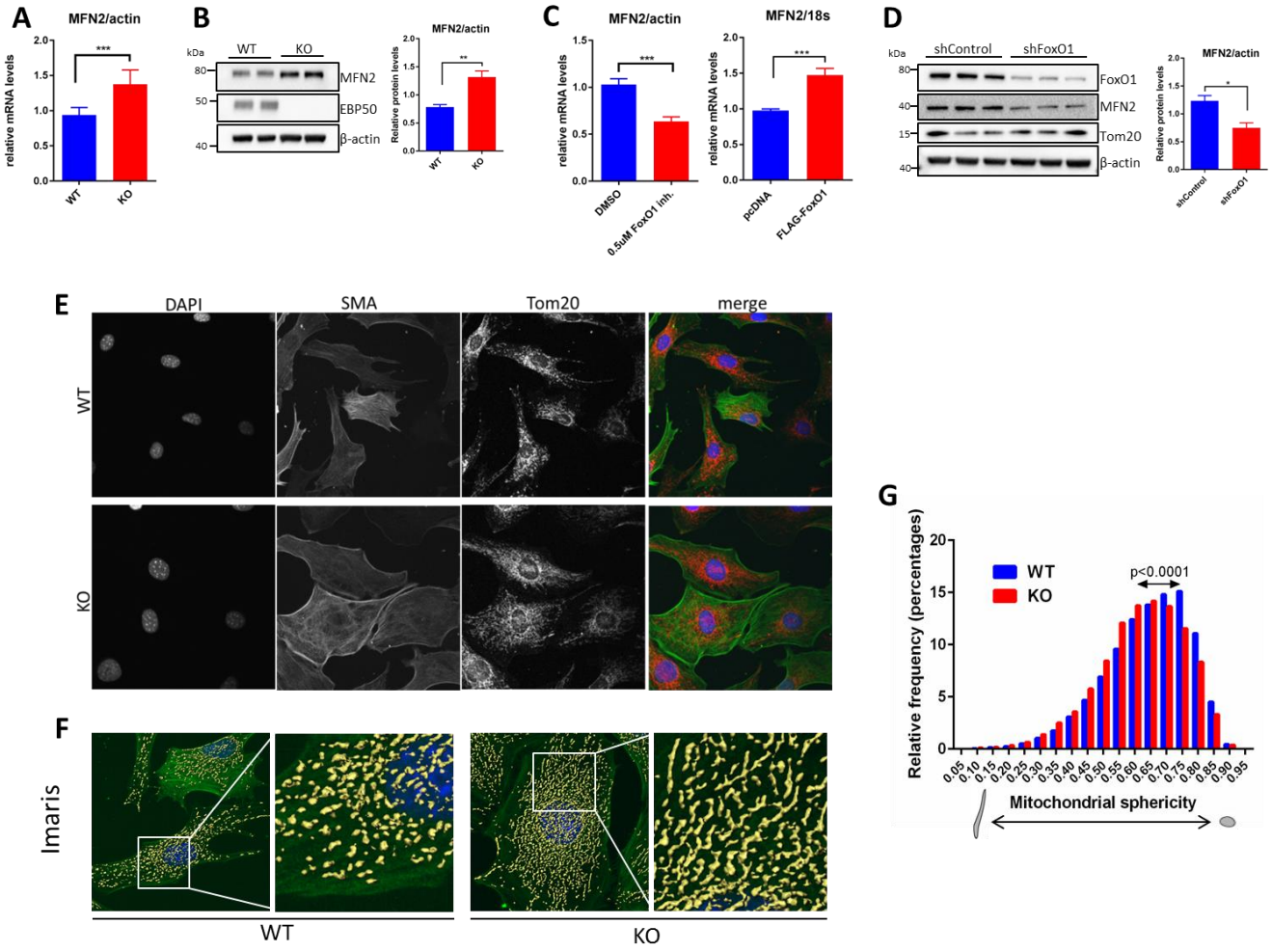

Figure 8: EBP50$^{-/-}$ VSMC express more Mfn2 and have more fused mitochondria compared to WT VSMC. **A**, RNA from primary mouse WT and EBP50$^{-/-}$ VSMC was isolated and analyzed by quantitative RT-PCR with actin as normalizing gene. **B**, Representative western blot with Mfn2 protein levels in WT and EBP50$^{-/-}$ VSMC. Tom20 was used as mitochondrial control and actin as loading control. Graph represents means +/- SEM of at least 3 independent experiments ($p<0.05$). **C**, Primary mouse WT VSMC were treated with DMSO and FoxO1 inhibitor (AS1842856) (0.5 μM) or transfected with FLAG-FoxO1 plasmid for 24 hours. RNA was isolated and analyzed by quantitative RT-PCR with actin and 18s as normalizing genes (n=3, $p< 0.001$). **D**, Primary mouse WT VSMC were infected with adenovirus expressing non targeting shRNA or shFoxO1 constructs. 72 hours following infection cells were lysed and FoxO1 and Mfn2 protein levels were analyzed with western blot (n=4, $p<0.05$).

E, Primary mouse WT and EBP50$^{-/-}$ VSMC were seeded on coverslips, fixed in 4% paraformaldehyde (PFA) and stained with Tom20 (red), α-smooth muscle actin (green) antibodies and DAPI (blue). Confocal images of 3-7 different fields per condition were taken with 60X oil immersion objective. **F**, Imaris detection (yellow particles) of Tom20 mitochondrial stain from a representative experiment. **G**, Sphericity ratio was calculated with Imaris software. Calculations were made for 3-7 different field per coverslip that contained approximately 5 cells each, from three independent experiments and plotted as frequency distribution (n=3, $p<0.0001$).

2.3.3 EBP50 promotes TNFα – stimulated Drp1 phosphorylation through PKCζ and regulates mitochondrial fragmentation

In order to maintain proper function, mitochondria have to maintain a balance between fusion and fission [203]. Mitochondrial fission is primarily induced by the dynamin-related protein 1 (Drp1). Drp1 is activated upon phosphorylation on Ser616 and is then recruited to mitochondria to promote fission. One of the kinases that have been reported to phosphorylate and activate Drp1 is PKCδ [87], a member of the novel class of PKCs. On the other hand, we previously reported that under inflammatory stimuli EBP50 promotes the activation of PKCζ that belongs to the atypical PKC subfamily [163]. Because of structural similarity of the catalytic domain between PKC isoforms we wanted to determine whether PKCζ induces Drp1 phosphorylation in VSMC and whether EBP50 is involved in this pathway. Therefore, we determined pDrp1 levels by immunoblotting in VSMC treated with or without TNFα or PDGF. We found that Drp1 phosphorylation in response to TNFα was significantly lower in EBP50 depleted VSMC (Figure

9A). Similar results were obtained in WT and EBP50$^{-/-}$ primary VSMC (Figure 9B). To determine if Drp1 phosphorylation is mediated, at least in part, by PKCζ we used two approaches. First, we treated VSMC with pseudo-substrate of PKCζ (ζ-PS) to inhibit PKCζ activity (Figure 9C). Drp1 phosphorylation following TNFα treatment was significantly reduced in ζ-PS -treated cells. In the second approach, we infected primary VSMC with a virus expressing a kinase-dead form of PKCζ ([K281W] PKCζ, KD-PKCζ). To validate the reduced activity of KD-PKCζ we checked IKK activation that is downstream of PKCζ with immublotting the phosphorylated IKK (pIKK). Our results indicate that KD-PKCζ construct has reduced ability to induce phosphorylation of IKK (Figure 9D), meaning that PKCζ activation is indeed inhibited with KD-PKCζ construct. Consistent with the previous results, both basal and TNFα-stimulated Drp1 phosphorylation were significantly reduced in cells expressing KD-PKCζ compared to control GFP-expressing cells (Figure 9D). Importantly, the effect of PDGF also known to induce Drp1 phosphorylation [211], was similar in VSMC expressing KD-PKCζ and the control (GFP) VSMC (Figure 9E). Taken together, these results point out that EBP50 promotes TNFα induced phosphorylation of Drp1 on Ser616 via a PKCζ-mediated mechanism.

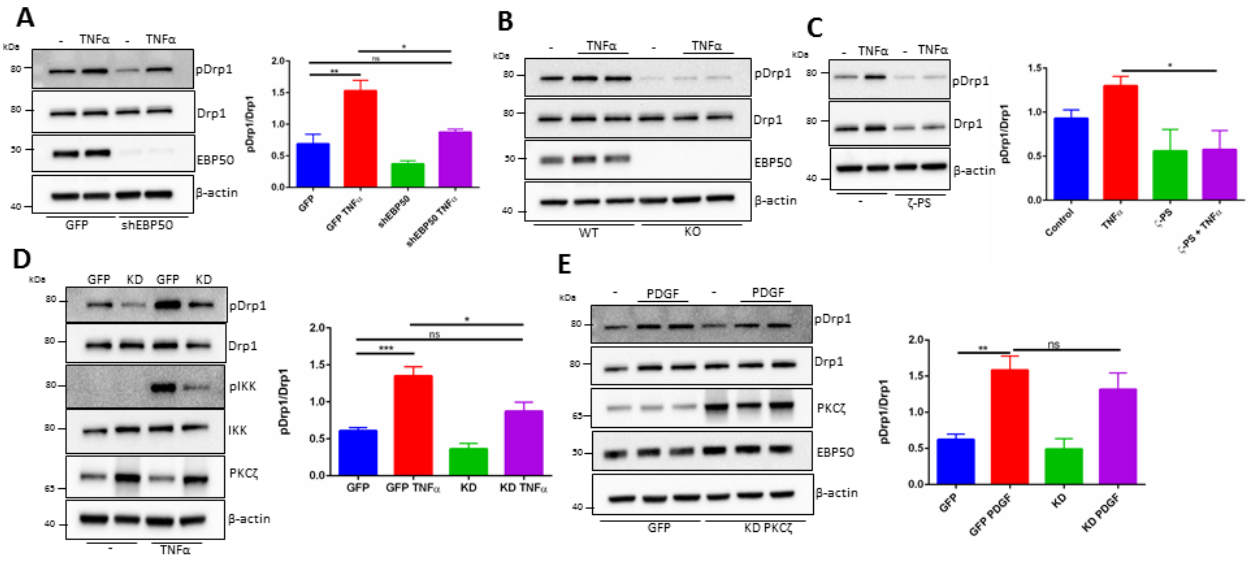

Figure 9: EBP50 promotes TNFα induced Drp1 phosphorylation in VSMC that is mediated through PKCζ.

A, Primary mouse WT VSMC were infected with lenti-virus expressing shEBP50 or GFP. 7 days post infection cells were starved in 0.1% FBS DMEM overnight and treated with 10 ng/mL TNFα for 15 minutes. pDrp1 levels were detected with anti-pDrp1 (Ser616) antibody and normalized to total Drp1 levels. Graph represents means +/- SEM of at least 3 independent experiments ($p<0.05$). **B**, A representative graph of primary mouse WT and EBP50$^{-/-}$ VSMC were starved overnight in 0.1% FBS DMEM and treated with 10 ng/mL TNFα for 15 minutes. Proteins expression was determined with western blot using anti-pDrp1 (Ser 616) antibody (n=3). **C**, Primary mouse WT VSMC were starved in 0.1% FBS DMEM overnight and treated with 10 μM PKCζ pseudo-substrate (Calbiochem) for 1.5 hours. Then 10 ng/mL TNFα was added for 15 minutes and cells were lysed in urea lysis buffer for protein expression determination by western blot. Graph represents means +/- SEM of 3 independent experiments ($p<0.05$). **D**, Primary mouse WT VSMC were infected with adenovirus expressing kinase-dead (KD) PKCζ construct or GFP. 2 days post infection cells were starved in 0.1% FBS DMEM overnight and treated with 10 ng/mL TNFα for 15 minutes. Proteins expression was determined with western blot. Graph represents means +/- SEM of six independent experiments ($p<0.05$). **E**, Primary mouse WT VSMC were infected with adenovirus expressing kinase-dead (KD) PKCζ construct or GFP. 2 days post infection cells were starved in 0.1% FBS DMEM overnight and treated with 10 ng/mL PDGF for 15 minutes. Proteins expression was determined with western blot. Graph represents means +/- SEM of at four independent experiments ($p<0.05$).

To examine the functional consequence of EBP50 deletion on mitochondrial fragmentation, we quantified mitochondrial fission in WT and EBP50$^{-/-}$ VMSC in response to TNFα in two ways. First, using Tom20 immuno-staining, we quantified mitochondrial morphology following 6 hours of TNFα treatment (Figure 10A). We found that in the presence of TNFα, WT mitochondria exhibit significantly more spheric morphology compared to EBP50$^{-/-}$ mitochondria (Figure 10A), indicating more fission in WT VSMC in response to TNFα. Then, we transfected VSMC with mitoRFP construct to enable visualization of mitochondria in live cells, and performed real-time confocal 3D imaging during 30 minutes following TNFα addition (Figure 10C). To quantify fission, we counted the number of mitochondria in each cell during the time lapse imaging relative to time zero, using Imaris software, and performed a linear regression analysis (Figure 10D). Increase in mitochondria number in the same cell over time, indicates fission. After quantifying mitochondria number we found that EBP50$^{-/-}$ VSMC exhibited significantly smaller increase in the number of mitochondria compared to WT (Figure 10D). This reduced mitochondrial fission in EBP50$^{-/-}$ VSMC is consistent with lower phosphorylation of Drp1 in response to TNFα.

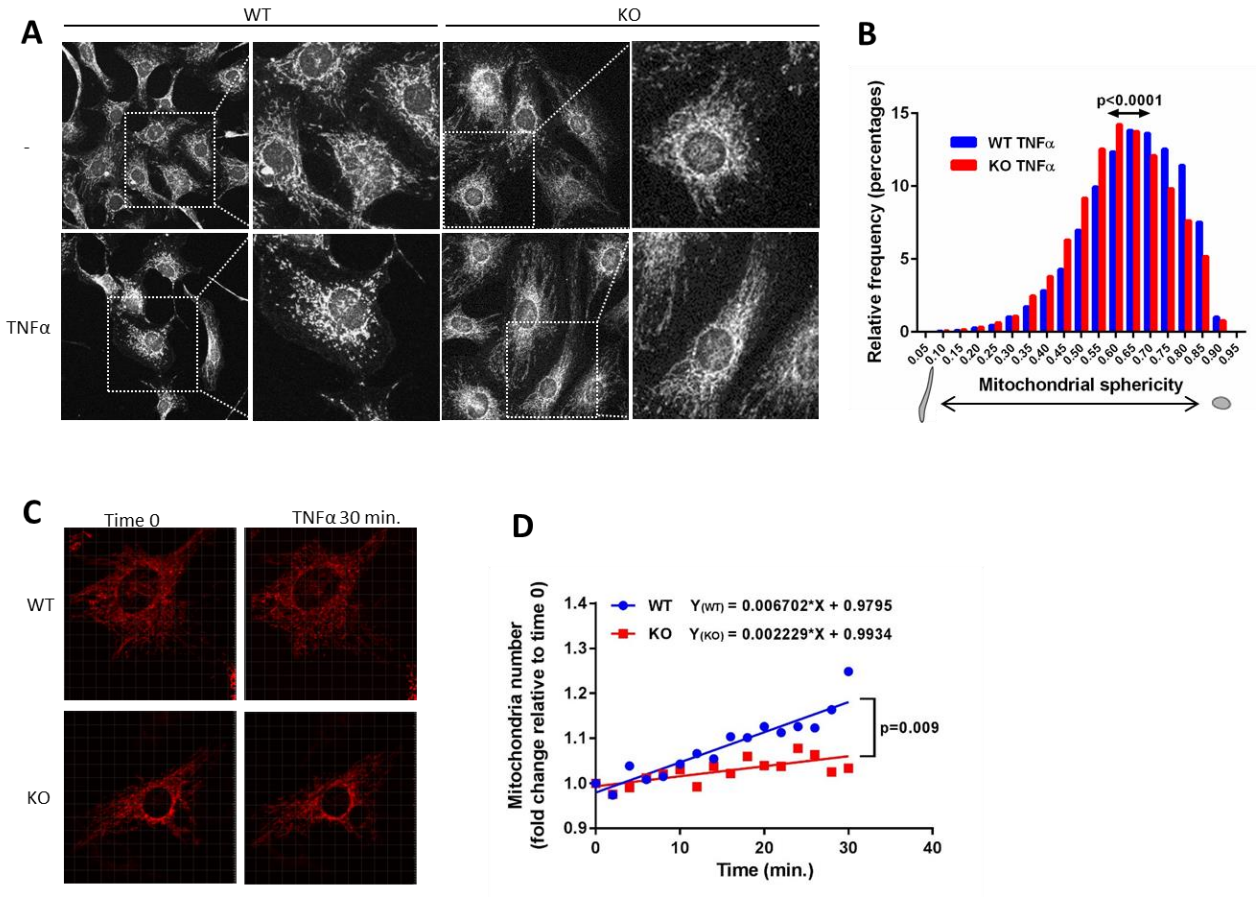

Figure 10: EBP50 promotes TNFα induced mitochondrial fragmentation in VSMC.

A, Primary mouse WT and EBP50$^{-/-}$ VSMC were seeded on coverslips and starved in 0.1% FBS DMEM overnight. Then 10 ng/mL TNFα was added for 5-6 hours to the cells. Following TNFα treatment cells were fixed in 4% paraformaldehyde (PFA) and stained with Tom20 antibody. Sphericity ratio was calculated with Imaris software according to Tom20 staining and plotted as frequency distribution. Histogram shows WT and EBP50$^{-/-}$ VSMC treated with TNFα (n=4). **B**, Primary mouse WT and EBP50$^{-/-}$ VSMC were transfected with mitoRFP. 24 hours post transfection TNFα (10 ng/mL) was added and cells were imaged with confocal microscope during 30 min (in 2 minutes intervals). Images represent time 0 and time 30 minutes, after TNFα treatment. Mitochondria number per each cell was quantified with Imaris and plotted on a graph, followed by linear regression analysis. (n=3, $p<0.05$).

2.3.4 EBP50 promotes TNFα induced extracellular acidification rate and VSMC proliferation

Dynamics alterations in mitochondria affect their function, cell proliferation and have been associated with various diseases [7, 8, 53, 76, 203, 212, 213]. Due to the differences in mitochondria morphology and fragmentation between WT and EBP50$^{-/-}$ VSMC, we wanted to examine the potential impact on mitochondrial function. To this end, we performed flux analysis in WT and EBP50$^{-/-}$ VSMC. While we did not detect significant differences in oxygen consumption rate (OCR) and mitochondrial ultrastructure between WT and EBP50$^{-/-}$ VSMC (Figure 11A-B), we detected significantly lower extracellular acidification rate (ECAR) in EBP50$^{-/-}$ VSMC both at basal condition and upon stimulation with TNFα (Figure 11C). ECAR is directly linked to the amount of lactate production (end product of glycolysis) in cells and can be considered a glycolysis readout. Despite of producing less molecules of ATP compared to oxidative phosphorylation, glycolysis provides biosynthetic intermediates for growth and is enhanced in cells that undergo active division [7, 214]. Therefore, we hypothesized that lower glycolysis rate in EBP50$^{-/-}$ VSMC will result in reduced proliferation. Indeed, we detected that in response to TNFα and EGF EBP50$^{-/-}$ VSMC proliferation was lower (Figure 11D). To determine whether different mitochondrial dynamics regulate these proliferation differences, we measured VSMC proliferation in the presence of the mitochondrial division inhibitor (Mdivi-1). Treatment with Mdivi-1 completely abolished TNFα and EGF proliferative effects in VSMC (Figure 11D), Suggesting, that the differences in mitochondrial dynamics observed in EBP50 depleted cells, contribute to VSMC metabolism and proliferation.

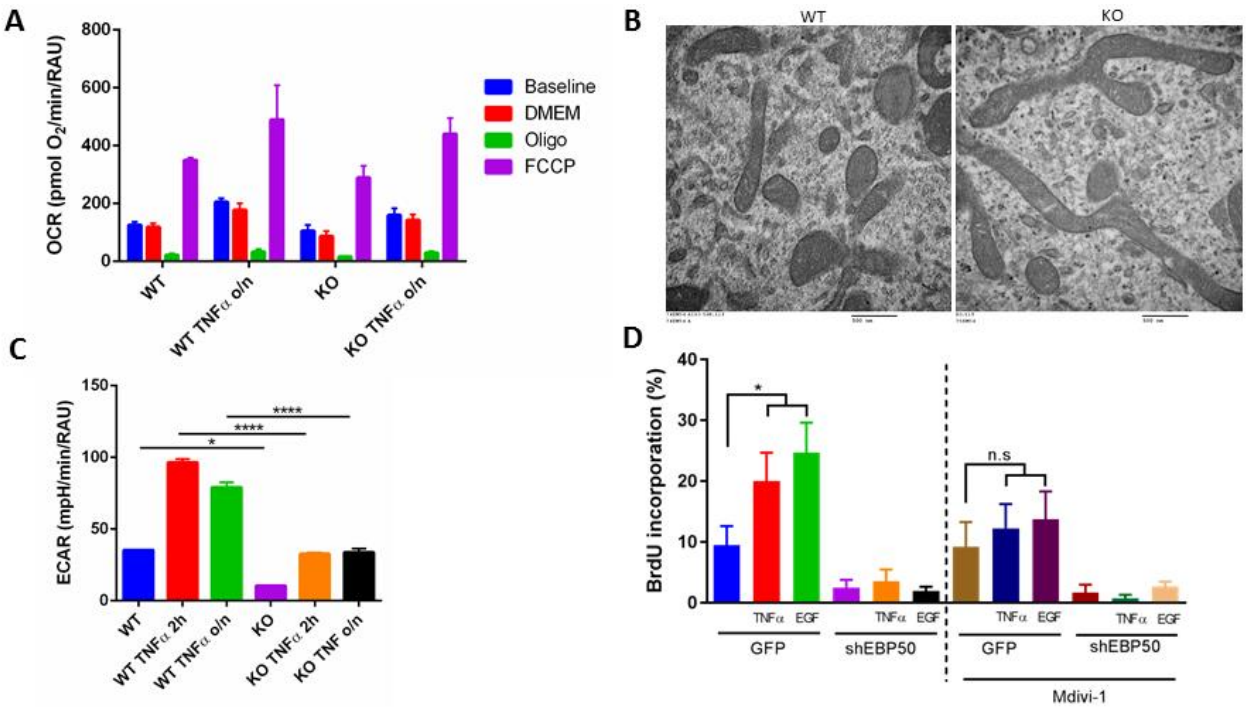

Figure 11: EBP50 promotes TNFα induced VSMC proliferation and extracellular acidification.

A, Primary mouse WT and EBP50$^{-/-}$ VSMC were subjected to seahorse measurement of oxygen consumption rate (OCR). 20,000 VSMC per well were seeded on a seahorse XF96 cell culture micro-plate 2 days prior to analysis. One day prior to analysis 10 ng/mL TNFα was added to the cells overnight. During bioenergetics analysis cells were treated with 1 μM Oligomycin to access ATP coupled respiration, 2.5 μM FCCP to access maximal respiratory capacity and 2 μM Rotenone to differentiate between mitochondrial and non-mitochondrial respiration. Results are normalized to total cell number according to crystal violet staining that was done at the end of the experiment. Graph represents mean +/-SEM of 3 independent experiments ($p<0.05$). **B**, Representative transmission electron microscopy images (TEM) of primary mouse WT and EBP50$^{-/-}$ VSMC mitochondria. Scale bar indicates 500nm. **C**, Extracellular acidification rate (ECAR) for WT and EBP50$^{-/-}$ VSMC was measured in parallel with OCR. Graph represents the average +/-SEM of 3 independent experiments ($p<0.05$).

D, Primary mouse WT VSMC were infected with lenti-virus expressing GFP or shEBP50. 7 days post infection cells were seeded on a glass coverslip and serum starved for 24 hours. Following that VSMC were treated with TNFα 100 ng/mL or EGF 10 ng/mL and Mdivi-1 10 μM for total 18h. BrdU 0.1 mM was added 6 hours after TNFα and EGF. Cells were fixed in 4% PFA and stained with anti-BrdU antibody. Graph represent means +/- SEM of 7 independent experiments ($p<0.05$).

2.4 DISCUSSION

In this paper we identified a new action of the scaffolding protein EBP50 that impacts mitochondrial dynamics and VSMC metabolism (Figure 12). EBP50 affects mitochondrial dynamics by regulating Mfn2 levels transcriptionally and by promoting cytokine-induced Drp1 activation. These observations add to the previously reported effects of EBP50 on VSMC migration, proliferation and inflammatory responses and reveal a complex regulatory network of EBP50 on vascular cell function.

Mitochondrial dynamics is crucial in maintaining proper vascular function. Alterations in mitochondrial dynamics are associated with various vascular pathologies that include pulmonary hypertension [94], hypertension [207] and arterial restenosis [76, 207]. Mfn2 is a critical inducer of mitochondrial fusion that is regulated transcriptionally. PGC-1α is a known regulator of mitochondrial biogenesis and Mfn2 expression [67]. The PGC-1α promoter contains a FoxO1 binding sequence and activation of PGC-1α/FoxO1 can up-regulate Mfn2 expression in kidney cells [69]. We found that EBP50$^{-/-}$ VSMC contain more stable and nuclear FoxO1. Therefore, we rationalized that in EBP50$^{-/-}$ VSMC FoxO1 may be more transcriptionally active and affect Mfn2 expression. Indeed, we found that EBP50$^{-/-}$ VSMC express higher Mfn2 mRNA and protein, and altering FoxO1 levels had corresponding effects on Mfn2 mRNA and protein levels. This indicates that FoxO1 transcriptionally regulates Mfn2 expression in VSMC. In addition to

FoxO1, we also measured the levels of PGC-1α, but found similar expression levels between WT and EBP50$^{-/-}$ VSMC. This suggests that, in our cell system, FoxO1 is primarily responsible for the differences in Mfn2.

To function properly, mitochondria need to maintain a balance between fusion and fission. Since Drp1 is a key protein that promotes fission, we measured the phosphorylated form (Ser616) of Drp1 which represents the active Drp1 state. In both basal and inflammatory conditions, EBP50 depleted VSMC had lower pDrp1 levels compared to WT VSMC. We identified PKCζ as the kinase that phosphorylates Drp1 in response to TNFα. Although this is the first time this has been reported, another PKC isoform, PKCδ, has been shown to induce Drp1 phosphorylation and subsequent mitochondrial fission in neuronal cells [87]. PKCζ mediates inflammatory and oxidative stress responses [215, 216] that are associated with mitochondrial fission. Therefore the ability of PKCζ to phosphorylate Drp1 is consistent with these observations. In VSMC expressing a kinase dead construct (KD-PKCζ), the reduction in pDrp1 levels was significant but not complete. This indicates that PKCζ is only one of several kinases that regulate Drp1 activation and the remaining phosphorylation might be attributed to other kinases such as CDK1/cyclin B, PKCδ or PKA. EBP50 has been shown to scaffolds PKA in proximity to its substrate in T cells [217], which raises possibility that EBP50 may regulate Drp1 activation also through PKA. The possibility of EBP50-PKA-Drp1 regulatory pathway remains to be determined in future studies.

The combination of increased Mfn2 levels together with reduced pDrp1 in EBP50$^{-/-}$ VSMC is predicted to result in more fused mitochondria and our analysis of unstimulated VSMC confirmed it. In addition, and consistent with the reduced Drp1 phosphorylation, TNFα induced less fission in EBP50$^{-/-}$ cells compared to WT. It has been reported that acute TNFα treatment in

primary neurons induces profound mitochondrial dysfunction by affecting membrane potential and leading to cytochrome C release followed by cell death [218]. In addition, chronic TNFα treatment for 4 days in adipocytes resulted in morphological changes in mitochondria that included swollen and smaller mitochondria with abnormal cristae structure and increased Drp1 levels [219]. However, TNFα impact on Drp1 phosphorylation and VSMC mitochondrial dynamics has not been reported. Here we show that TNFα promotes Drp1 phosphorylation in VSMC and that this phosphorylation event is regulated by PKCζ. These results contribute to a mechanistic understanding of mitochondrial fission that is observed under inflammatory conditions.

We observed interesting functional consequences in TNFα-stimulated VSMC. While TNFα induced modest effects on mitochondrial respiration in VSMC, it induced significant increase in glycolytic metabolism (represented by ECAR). Moreover, EBP50$^{-/-}$ VSMC had significantly lower ECAR in basal state and following TNFα treatment compared to WT VSMC. TNFα has been shown to induce glycolytic metabolism and proliferation in skeletal muscle cells and VSMC respectively [5, 220]. Glycolytic metabolism is enhanced during phenotypic switch of VSMC and is a characteristic of actively dividing cells. Consistent with this, we show that TNFα induces VSMC proliferation, and this effect was abrogated by the Drp1 inhibitor Mdivi-1. In addition, Mfn2 is also known for its inhibitory effect on VSMC proliferation [76, 221]. Consistent with all the previous observations, both basal and TNFα-induced proliferation is reduced in EBP50$^{-/-}$ VMSC compared to WT.

In conclusion, our study shows that EBP50 regulates mitochondrial dynamics and response to inflammation through its effect on the expression and activation of mitochondrial shaping proteins Mfn2 and Drp1. As a consequence, EBP50$^{-/-}$ VSMC have higher Mfn2 and

lower pDrp1 levels, which lead to reduced mitochondrial fission, glycolysis and proliferation in response to TNFα. These findings reveal a new function of EBP50 in VSMC, further indicating its promise as a therapeutic target for vascular proliferative diseases.

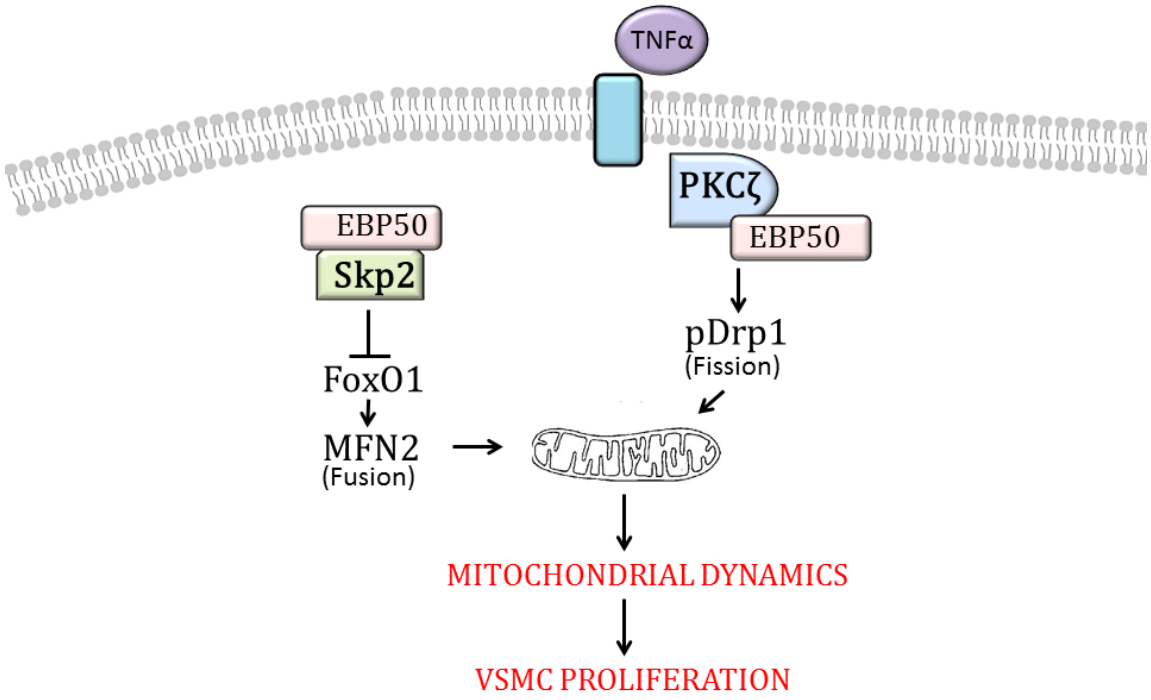

Figure 12: Proposed model for the mechanism by which EBP50 controls mitochondrial dynamics in VSMC.

The scaffolding protein EBP50 regulates mitochondrial dynamics through two arms. In basal conditions EBP50 promotes FoxO1 degradation and regulates Mfn2 translation. Under inflammatory conditions, EBP50 promotes TNFα signaling via PKCζ to phosphorylate Drp1 leading to mitochondrial fission. In the absence of EBP50, VSMC exhibit fused mitochondria and reduced TNFα-stimulated mitochondrial fragmentation. These differences in mitochondrial dynamics, lead to reduced glycolytic metabolism and proliferation in EBP50$^{-/-}$ VSMC in response to TNFα.

3.0 EBP50 REGULATES MNSOD, CATALASE AND MITOCHONDRIAL ROS LEVELS

Inflammation and oxidative stress play important roles in cardiovascular disease. Reactive oxygen- and NO-derived species affect proliferation and migration of VSMC, and amplify vascular inflammation. We reported that EBP50 promotes migration and proliferation of VSMC. In addition, EBP50 potentiates inflammatory responses (including iNOS expression) in both macrophages and vascular cells, and is critical for Nox1 mediated superoxide production. Mitochondria are major organelles that are responsible for ROS production in the cell, however their role in VSMC redox balance is not fully understood.

EBP50 is a scaffolding PDZ domain protein that stabilizes Skp2 – a substrate recruiting component of the E3 ubiquitin ligase that targets FoxO1 for degradation. FoxO1 is a transcription factor that controls the expression of two key antioxidant enzymes - MnSOD and catalase. Therefore, I hypothesized that EBP50 regulates mitochondrial ROS levels through the Skp2-FoxO1 axis. Consistent with observations that indicate more stable and nuclear FoxO1 in EBP50$^{-/-}$ VSMC, I found that the expression of MnSOD and catalase is higher in EBP50$^{-/-}$ VSMC than in WT VSMC. Furthermore, I found that mitochondrial superoxide levels in EBP50$^{-/-}$ VSMC following antimycin A (Ant A) and TNFα treatments are considerably lower compared to WT cells.

Mitochondrial ROS and MnSOD have been implicated in VSMC migration. Indeed, I found that EBP50 depleted VSMC migrate significantly less in response to TNFα and that downregulation of MnSOD with siRNA increases EBP50$^{-/-}$ VSMC migration. These results indicate that EBP50 regulates mitochondrial ROS levels through the anti-oxidant enzymes MnSOD and catalase. Moreover, MnSOD is an important regulator of VSMC migration that is increased in the absence of EBP50.

3.1 INTRODUCTION

Redox balance is required for normal cellular function. This balance is kept by antioxidant enzymes that are responsible for the clearance of reactive oxygen species. Multiple processes that are linked to CVD initiation and progression, such as endothelial dysfunction, VSMC migration and vascular inflammation, are regulated by ROS signaling. Therefore, ROS targeted therapeutics have been proposed as a potential strategy to treat and prevent CVD. Vascular redox state and inflammation co-exist in a positive feedback type of regulation. High levels of inflammation produce ROS in the vascular wall and local ROS induce inflammatory responses through activation of ROS sensitive transcription factors [222]. It has been recognized for several years that ROS have signaling properties and that they mediate vascular processes involved in CVD. The strong relations between ROS and vascular remodeling include effects on VSMC proliferation, differentiation and migration. One of the first studies addressing the importance of ROS in VSMC migration, showed that in cells treated with catalase, PDGF- induced migration was significantly reduced [223]. Later on, it was shown that migration stimulated by other factors was also blocked with anti-oxidant treatments [224, 225].

The anti-oxidant system is essential to maintain redox balance. Two major anti-oxidant enzymes are MnSOD and catalase. MnSOD is localized exclusively in mitochondria and is essential to maintain life of aerobic organisms [117, 226]. MnSOD reacts with superoxide radicals that are produced in mitochondria and converts them to hydrogen peroxide. Then, catalase eliminates hydrogen peroxide by converting it to water. Both MnSOD and catalase expression is regulated by the FoxO transcription factors family, in particular FoxO1. FoxO1 activity is mainly regulated through its subcellular localization and degradation. Phosphorylation by Akt causes relocalization of FoxO1 from the nucleus to the cytoplasm where it is targeted for degradation by ubiquitin protein ligase complex SCF (Skp1-cullin-F-box) in which Skp2 act as substrate recognition component.

EBP50 is an adaptor PDZ-containing phospho-protein that regulates multiple signaling processes in vascular cells. Our previous studies indicate that EBP50 promotes inflammatory responses, VSMC proliferation and migration [163, 191, 196]. EBP50 interacts with Skp2 in the cytoplasm, which leads to Skp2 stabilization and enhanced activity [167]. The effects of EBP50 on Skp2 led us to examine its role on FoxO1 levels and localization in VSMC. In my thesis work I showed that EBP50 promotes FoxO1 degradation by Skp2-containing E3 ligase and that EBP50 depleted VSMC express more nuclear and stable FoxO1 (Figure 7). Based on these findings, I hypothesized that by affecting FoxO1 stability and localization, EBP50 regulates MnSOD and catalase levels and subsequently mitochondrial ROS levels. Consequently, EBP50 will also regulate VSMC motility.

3.2 MATERIALS AND METHODS

3.2.1 Cell culture and transfections

Primary VSMC were isolated from mouse aortic explants and grown in DMEM containing 10% FBS in 5% CO_2 at 37^0 C as described previously [196].

Lentiviral shRNA vector specific to mouse EBP50 and GFP-expression control were prepared by the Lentiviral Facility at the University of Pittsburgh Cancer Institute. The target sequence of the EBP50 shRNA is GAGTTCTTCAAGAAGTGCAAA. WT VSMCs were infected at 4 MOI with 8 μg/mL polybrene in the media. Media was changed 24 hours post infection and the cells were used 7 days post infection.

Mouse MnSOD ON-TARGET plus siRNA - SMARTpool was purchased from Dharmacon and was introduced to VSMC by electroporation with AMAXA electroporator and the basic Nucleofector kit for primary vascular smooth muscle cells (Lonza) as described previously [196]. Cells were used 96 hours after transfection.

3.2.2 Western blot

For MnSOD and catalase detection cells were lysed in urea lysis buffer (4 M urea, 62.5 mM Tris, 2% SDS, 1 mM EDTA) containing protease and phosphatase inhibitors (Roche). Cell lysates were resolved by SDS-PAGE. Proteins were transferred onto nitrocellulose membrane and

incubated with primary antibodies 1:1000 dilution for MnSOD (Millipore) and catalase (Athenes Research and Technology), 1:500 dilution for EBP50 (Santa Cruz Biotechnology), 1:5000 dilution for β-actin (Sigma) and 1:2000 dilution for horseradish peroxidase-conjugated anti-rabbit and anti-mouse IgG antibody (Cell Signaling). Immunoreactivity was detected by incubation with WesternBright ECL HRP substrate (Advansta). Quantification of bands intensity was performed with ImageJ (National Institute of Health).

3.2.3 Immunofluorescence

Femoral arteries were fixed with 4% paraformaldehyde and embedded in OCT Tissue-Tek (Sakura Finetek). Sections (10 μm) were incubated in boiled Tris-EDTA buffer (10 mM Tris base, 8 μM EDTA, 0.05% Tween 20) for 10 min, blocked in 4% normal goat serum, 1% BSA, 0.5% Triton X-100 for 20 min at room temperature, and incubated with antibodies to MnSOD (Millipore, 1:100 dilution), and a secondary antibody, anti-rabbit Alexa Fluor 546- conjugated IgG (Invitrogen, 1:1000) was used before DAPI staining. Fluorescence intensities were measured with ImageJ software (National Institutes of Health). For MnSOD visualization in cells, WT and EBP50$^{-/-}$ VSMC were seeded on glass coverslips. MitoTracker® 100 nM (Molecular Probes) was added to cells for 30 minutes then the cells were fixed with 4% PFA and permeabelized in 0.1% SDS, 0.2% Triton X-100, 4% FBS in PBS for 30 minutes and incubated with MnSOD antibody (Millipore, 1:100) overnight at 4° C. As a secondary antibody anti-rabbit Alexa-Flour 488 (Invitrogen, 1:1000) was used for 1 hour at room temperature prior to DAPI staining. For imaging cells were visualized using Olympus Fluoview 1000 confocal laser scanning microscope with a 60X oil immersion objective. Fluorescence intensities were measured with ImageJ software (National Institutes of Health).

3.2.4 MitoSox assay

To detect mitochondrial superoxide levels in live cells MitoSox^{TM} Red mitochondrial superoxide detector for live cells imaging (Molecular Probes) was used. We used both HPLC and live imaging approaches to detect superoxide levels. For live imaging, WT and EBP50$^{-/-}$ VSMC were seeded on glass bottom 35mm^2 culture dishes (MatTeck). On the next day MitoTempo (10 μM) was added for 2 hours. Then MitoSox^{TM} (0.5 μM) was added to the cells for 10 minutes at 37°C. Then MitoSox^{TM} was washed three times with HBSS and warm media was added to the cells. Baseline fluorescence was measured using Nikon Eclipse Ti microscope with 60x/1.40 NA oil lens with 390 nm wave length. Then Antimycine A (1 μM) or TNFα (100 ng/mL) was added to the cells after baseline imaging and 10 stage positions were imaged every 2 minutes for 20 minutes total. Fluorescence was quantified with Elements software. For HPLC analysis 80,000 WT and EBP50$^{-/-}$ VSMC per well were seeded on a 6 well plate. On the next day 10 μM mitoTEMPO was added for two hours and then MitoSOX^{TM} probe was administered in the same manner as for the live cell imaging. TNFα (100 ng/mL) was added for 15 minutes. Then the cells were washed in PBS and scraped in 1 mL PBS into eppendorf tubes. Cells were pelleted, PBS aspirated and the pellet was stored in -80° C until HPLC analysis. At the time of analysis cell pellet was lysed in ice-cold lysis buffer containing PBS and 0.1% Triton X-100 and spinned down. Then the supernatant was transferred to a tube containing equal amount of 0.2 M $HClO_4$ in MeOH and vortexed to precipitate the protein. Protein pellet was precipitated by centrifugation and the supernatant was transferred to a tube containing equal amount of 1 M phosphate buffer pH 2.6 and vortexed. Excess of buffer and $KClO_4$ precipitate was pelleted by

centrifugation. Then 200 µL of supernatant was transferred to HPLC vial equipped with conical glass insert. For HPLC we used gradient elution method with two mobile phases: A-50 mM phosphate buffer (pH 2.6), 10% acetonitrile, 90% water; and B-50 mM phosphate buffer (pH 2.6), 60% acetonitrile, 40% water. Hydroethidine (HE), 2-hydroxyethidium (2-OH-E^+) and ethidium (E^+) were separated using a Phenomenex (Kinex, 2.6 µm pentafluorophenyl (PFP) column (part #: 00D-447-E0) 100 x 4.5 mm) and eluting with a gradient of A and B mobile phases changing from 3:2 to pure B phase over a period of 20 min using a flow rate of 1 mL min^{-1}. Hydroethidine, ethidium and 2-OH-E+ were detected electrochemically by pass through an ESA CoulArray electro chemical detector with the following potentials (0, 200, 280, 365, 400, 450, 500 and 600 mV). Stocks of hydroethidine, ethidium and 2-OH-E+ were prepared as described previously [227].

3.2.5 Migration assay

Cell migration was quantified using Boyden chamber 24 well inserts (BD BioCoat) with a pore size of 8 µm. The upper compartment was filled with 300 µL DMEM containing 0.1% FBS and $5x10^5$ cells. The lower chamber contained 500 µL of DMEM and 0.1% FBS and TNFα (100 ng/mL). Cell migrated for 5-6 hours. Then, cells were fixed in 4% paraformaldehyde and stained with 0.1% crystal violet. Images of 5 fields per treatment were acquired with Olympus IX71 microscope using 10x objective.

3.2.6 Statistical analysis

Data are presented as mean +/- SEM. Two groups were compared using student t-test and multiple groups were compared with One-way or Two-way Anova test. Statistical analyses were done using GraphPad Prism 7.03 and p value < 0.05 was considered significant.

3.3 RESULTS

3.3.1 EBP50 regulates MnSOD and catalase protein levels

FoxO1 is ubiquitinated and targeted for degradation by Skp2 [228]. EBP50 binds Skp2 and stabilizes it in the cytoplasm which prevents Skp2 degradation in the nucleus [167]. Therefore, EBP50$^{-/-}$ VMSC exhibit lower Skp2 levels and more stable and nuclear FoxO1 (Figure 7). FoxO1 transcriptionally regulates a large number of genes, including MnSOD and catalase. Therefore, I hypothesized that the increased FoxO1 levels in EBP50$^{-/-}$ VSMC leads to an increase in MnSOD and catalase transcription. Using immunoblot I determined MnSOD and catalase protein levels (Figure 13A-B). I found that both MnSOD and catalase protein levels are increased in EBP50$^{-/-}$ VMSC compared to WT VSMC (Figure 13A-B). Similarly, MnSOD expression in femoral arteries was greater in EBP50$^{-/-}$ mice than in WT mice (Figure 13C). In order to rule out an upregulation of MnSOD due to miss-localization of MnSOD in the cells, I determined the subcellular localization of MnSOD by confocal fluorescence microscopy. I found that MnSOD in EBP50$^{-/-}$ VSMC exhibit mitochondrial localization similar to WT VMSC (Figure 13D).

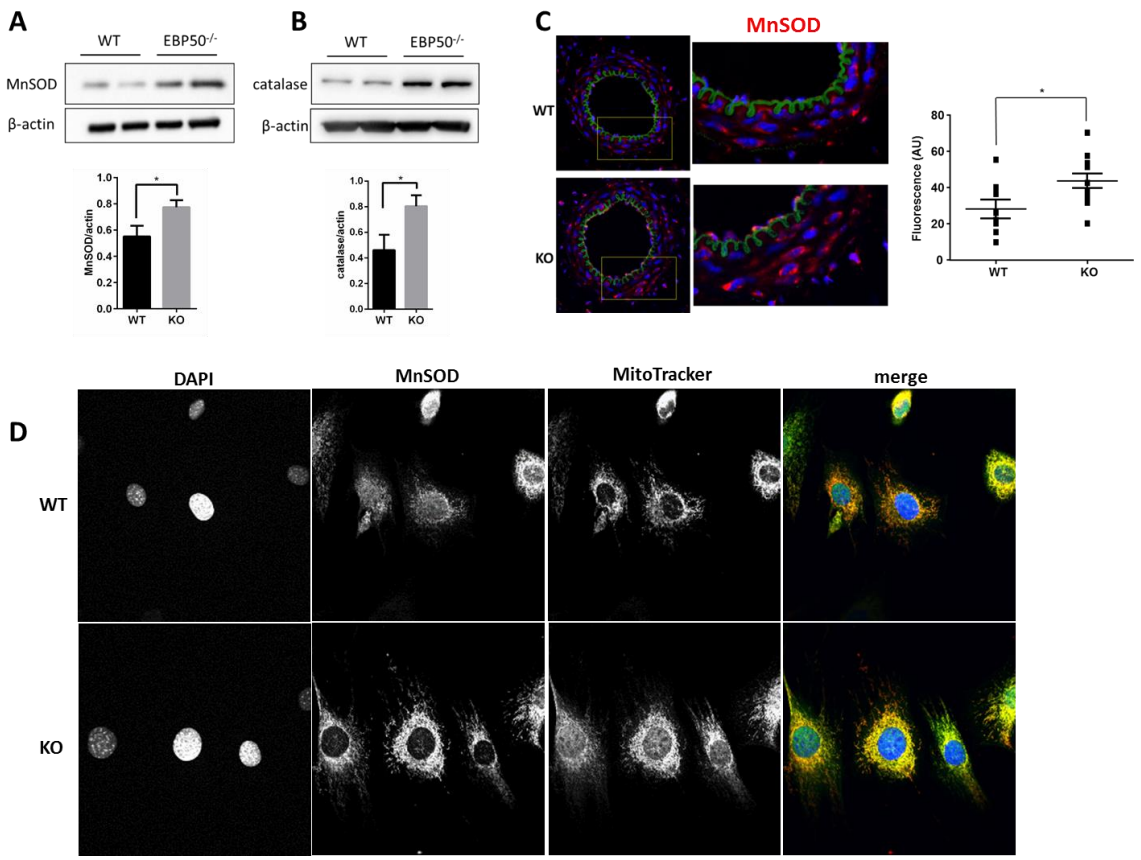

Figure 13: EBP50$^{-/-}$ VSMC express higher levels of MnSOD and catalase.

A-B, Primary WT and EBP50$^{-/-}$ VSMC were subjected to immunoblot to detect MnSOD and catalase levels in basal state. Graphs represent densitometry (calculated with Image J) means +/- SEM from three independent experiments ($p < 0.05$). **C**, Mouse femoral arteries were immunostained with MnSOD antibody and DAPI. Fluorescence intensity was quantified with Image J ($p < 0.05$). **D**, Representative images of primary mouse WT and EBP50$^{-/-}$ VSMC with MitoTracker and immune-stained with MnSOD. Cells were seeded on coverslips. On the next day 100 nM of MitoTracker red was added to the cells for 30 min. Then the cells were fixes in 4% PFA and MnSOD antibody was applied overnight. 3-5 images per condition were acquired with Olympus Fluoview 1000 confocal microscope equipped with 60X oil immersion objective.

3.3.2 EBP50$^{-/-}$ VSMC have lower superoxide levels than WT VSMC in response to TNFα

MnSOD is the first enzyme that reacts with superoxide in mitochondria and converts it to hydrogen peroxide which in turn is converted to water by catalase [136]. Since EBP50$^{-/-}$ VSMC express more MnSOD, I hypothesized that EBP50$^{-/-}$ VSMC will have less mitochondrial superoxide in response to inflammatory stimuli or a mitochondrial toxin – Antimycin A (Ant A) that induces superoxide production in mitochondria. In order to measure mitochondrial superoxide I used MitoSox, a probe that localizes to the mitochondria due to its positive charge (Figure 14A) and produces red fluorescence when oxidized by superoxide. In order to make sure that the signal is specific to mitochondrial superoxide I used MitoTempo. MitoTempo localizes in mitochondria and scavenges superoxide [229], creating a baseline for superoxide detection.

In basal state, there were no differences in mitochondrial superoxide levels between WT and EBP50$^{-/-}$ VSMC (Figure 14B). Then, I stimulated superoxide production by treating the cells with Ant A, that inhibits complex III in mitochondria and induces superoxide production [230]. Due to high sensitivity of MitoSox to light and oxidation, I used a kinetic quantification method to determine superoxide levels in live cells. Following Ant A treatment WT VSMC generated superoxide that was reflected by a gradual increase in fluorescence (Figure 14C). In contrast, EBP50$^{-/-}$ VSMC did not produce detectable levels of superoxide in response to Ant A and the fluorescence was similar to the cells pre-treated with MitoTempo (Figure 14C). TNFα is known to induce superoxide production from mitochondria [231, 232] and is a central cytokine that is expressed in multiple cardiovascular pathologies [233, 234]. Therefore, I examined TNFα ability to induce mitochondrial superoxide in EBP50$^{-/-}$ and WT VSMC. TNFα addition to the cells

resulted in superoxide production in WT VSMC, however, EBP50$^{-/-}$ VSMC produced minimal levels of superoxide that were similar to mitoTEMPO pre-treated cells (Figure 13D).

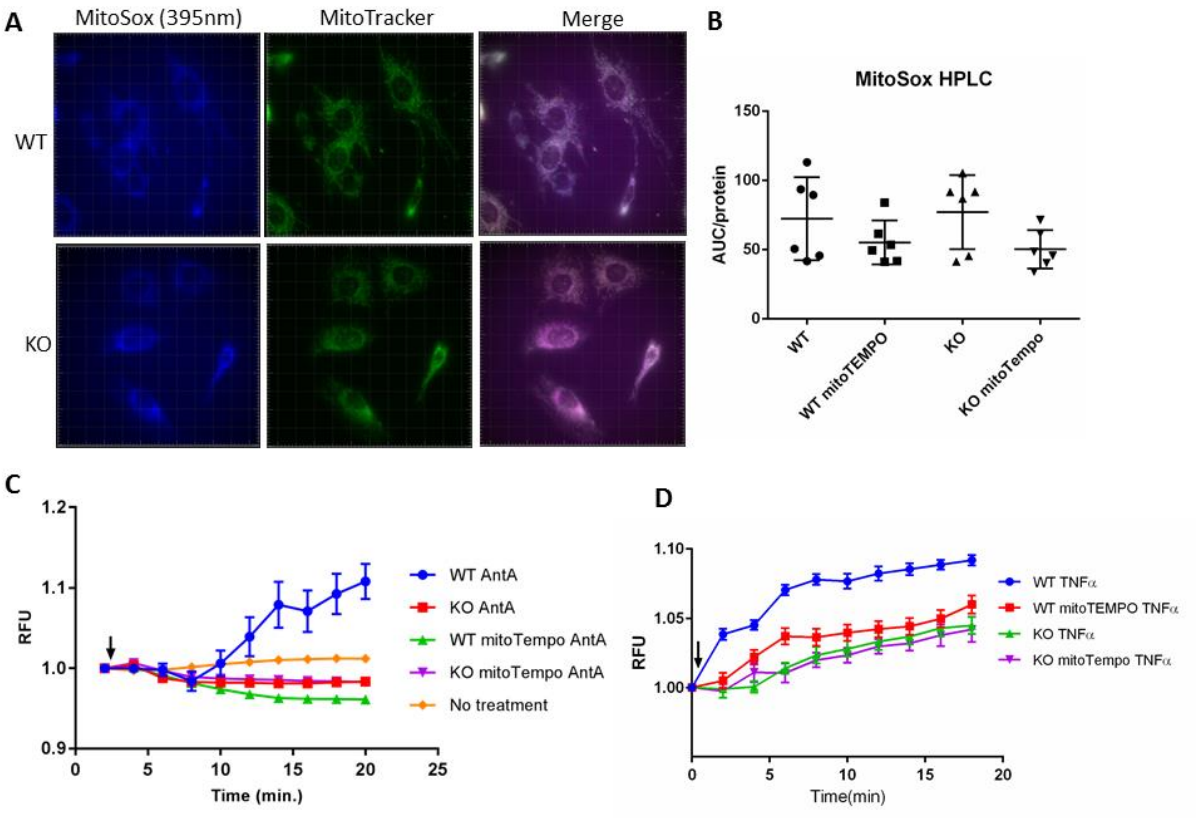

Figure 14: EBP50$^{-/-}$ VSMC produce less superoxide in response to TNF*α*.

A, Primary mouse WT and EBP50$^{-/-}$ VSMC were seeded on glass bottom 30mm^2 culture dishes (MatTek). MitoSox (0.5 μM) and MitoTracker (100 nM) were added to the cells to verify mitochondrial localization of MitoSox. **B**, Primary mouse WT and EBP50$^{-/-}$ VSMC were grown on a 6-well plate. MitoTempo (10 μM) was added two hours prior to MitoSox. MitoSox (1 μM) was added to the cells for 15 minutes and then the cells were collected in PBS. Hydroethidine (HE), 2-hydroxyethidium (2-OH-E$^+$) and ethidium (E$^+$) were separated using a Phenomenex column and were detected electrochemically by pass through an ESA CoulArray electro chemical detector. Graphs represent measurements from three independent experiments.

C, Primary mouse WT and EBP50$^{-/-}$ VSMC were seeded on glass bottom 30 mm^2 culture dishes (MatTek). MitoTempo (10 μM) was added at least 1 hour prior to MitoSox. MitoSox (0.5 μM) was added for 10 minutes. After MitoSox washout baseline images (395 nm) were collected from 10 fields. Then, antimycin A (Ant A) (1 μM) was added cells were imaged every two minutes for 20 minutes. Graphs represent means +/- SEM of each field that was imaged. No treatment represents MitoSox only (without Ant A or MitoTemo) to account for MitoSox basal signal. **D**, Primary mouse WT and EBP50$^{-/-}$ VSMC were seeded on glass bottom 30 mm^2 culture dishes (MatTek). MitoTempo (10 μM) was added at least 1 hour prior to MitoSox. MitoSox (0.5 μM) was added for 10 minutes. After MitoSox washout baseline images (395 nm) were collected from 10 fields. Then, TNFα (100 ng/mL) was added cells were imaged every two minutes for 20 minutes. Graphs represent means +/- SEM of each field that was imaged.

3.3.3 Mitochondrial superoxide promotes VSMC migration

Several studies have shown that ROS promote cell migration [211, 235, 236]. However, most of the studies in vascular cells focused on Nox derived ROS [237] and mitochondrial ROS are understudied in this aspect. Because of the differences in the anti-oxidant enzymes levels and mitochondrial superoxide production between EBP50$^{-/-}$ and WT VSMC, I wanted to examine whether these differences impact cell migration.

EBP50 has been shown to regulate EGF and serum induced VSMC migration, by scaffolding FAK and EGFR and increasing focal adhesions dynamics [196]. However, we have not examined the effects of TNFα on VSMC migration and whether EBP50 plays a role in this process. Both ROS and MnSOD are important for migration [237, 238] therefore, my next question was whether the different levels of MnSOD contribute to reduced migration of EBP50$^{-/-}$ VSMC. When I compared VSMC migration following 6 hours of TNFα treatment, I found that

EBP50 depleted cells migrated significantly less compared to control VSMC (Figure 15A). In order to single out the effect of MnSOD on the reduced migration of EBP50 depleted VSMC, I knocked down MnSOD in EBP50$^{-/-}$ VSMC and measured migration rate. MnSOD knock down in EBP50$^{-/-}$ VSMC led to an increase in migration (Figure 15B). These results indicate that MnSOD is a significant contributor to VSMC migration and suggest that mitochondrial superoxide contributes to VSMC migration.

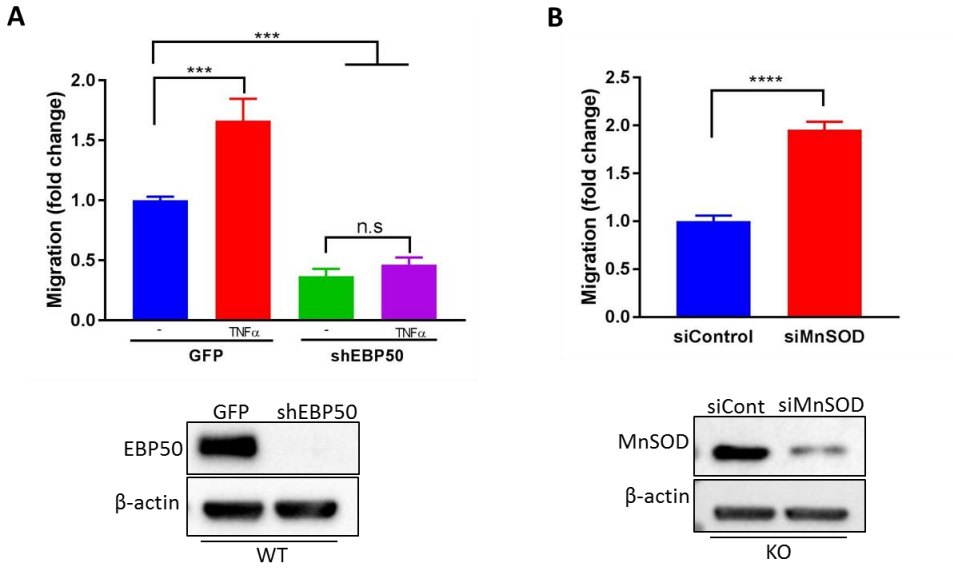

Figure 15: MnSOD inhibits VSMC migration.

A, Primary mouse WT VSMC were infected with GFP or shEBP50 constructs. 7 days post infection 50,000 cells were seeded on a upper transwell in 0.1% FBS DMEM and were let to attach overnight. TNFα (100 ng/mL) was added for 6 hours. Following that the cells were fixed in 4% PFA and stained with crystal violet. Five images were taken per condition and the number of cells was counted. Cell number is normalized to GFP. Graph represent results from three independent experiments ($p<0.05$). **B**, Primary mouse EBP50$^{-/-}$ VSMC were transfected with siControl and siMnSOD. 72 hours after transfection 50,000 cells were seeded on the upper insert of a transwell in 0.1% FBS DMEM and were let to attach overnight. Then media was changed to a fresh DMEM with 0.1% FBS and cells were left to migrate for 6 hours. Then cells were fixed in Methanol and stained with Diff Quick modified stain kit. Five images per condition were taken and number of cells per image was counted. Graphs represent normalized migration values to siControl from three independent experiments. ($p<0.05$).

3.4 DISCUSSION

EBP50 has been implicated before in the regulation of ROS in the vasculature through activation of Nox1 in response to AngII [200]. However, mitochondrial ROS have not been studied in the context of EBP50 regulation. In this study I showed that EBP50 regulates anti-oxidants enzymes expression and mitochondrial superoxide levels. The increased levels of MnSOD and catalase and the low superoxide in EBP50$^{-/-}$ VSMC contribute to the low migration of VSMC in response to TNFα. These finding describe an additional regulatory arm of EBP50 affecting mitochondrial redox balance in VSMC that has an impact on migration. Moreover, I found that MnSOD knock down in EBP50$^{-/-}$ VSMC restores migration. The direct connection between MnSOD levels and migration strongly suggest a role for mitochondrial ROS in VSMC migration.

VSMC migration is important during development and in pathological conditions such as neointima formation. Interestingly, migratory effects are abrogated by anti-oxidants including catalase [239] suggesting that these effects are at least in part mediated by ROS. TNFα is a potent migration inducer [240] and a central cytokine that is involved in vascular pathologies. Despite being a central mediator in vascular disease, TNFα effects on VSMC migration and ROS production in VSMC have not been extensively studied. My studies indicate that TNFα induces migration in VSMC and that MnSOD has crucial impact on this process.

The signaling mechanisms that lead to TNFα effects on VSMC migration are not completely understood. Among the signaling pathways that are involved in VSMC migration are

MAPK/ERK1-2 [241, 242] as well as phospholipase C activation [243] and increase of intracellular calcium and the activation of calcium/ calmodulin kinase II [244] pathways. Studies showed that activation of MAPK/ERK1-2 is critical for induction of migration by TNFα in VSMC [240]. In addition, it has been shown that TNFα promotes cells migration through activation of NFκB that is dependent on mitochondrial ROS [245]. Furthermore, inhibition of mitochondrial fission leads to decreased mitochondrial membrane potential, reduced ROS and uncoupled respiration. These effects in turn, caused decreased VMSC migration in response to mitogens [211]. Collectively, these observations are consistent with the effect of EBP50 described in this thesis. However, determining the exact mechanisms by which MnSOD affects VSMC migration requires additional studies.

In summary, I was able to show that EBP50 regulates two key anti-oxidant enzymes – MnSOD and catalase in VSMC. Increased levels of MnSOD and catalase resulted in minimal mitochondrial ROS in EBP50$^{-/-}$ VSMC and reduced TNFα induced migration. These effects may lead to protection of EBP50$^{-/-}$ vasculature from oxidative damage that occurs in CVD.

4.0 GENERAL DISCUSSION

CVD is the leading cause of death worldwide and the three major vascular diseases – atherosclerosis, restenosis and vein graft disease are interconnected and share a common feature which is proliferation of VSMC. Angina caused by obstructive coronary disease such as atherosclerosis most often lead to balloon angioplasty and stents or a bypass surgery. Lumen narrowing is a very common consequence of these interventions and the main cell type that contributes to intimal hyperplasia is VSMC. A critical process that occurs in VSMC under these conditions is activation of proliferation and migration. Even though VSMC proliferation is the major contributor to intimal hyperplasia, targeting single molecules that promote proliferation did not prove to be always effective in clinic. Therefore, a strategy of targeting multiple pathways that regulate phenotypic switching might be a more effective therapeutic approach.

In recent years an increasing amount of evidence point to mitochondria as master regulators of proliferation, metabolism and redox balance, particularly in vascular proliferative diseases. It was demonstrated that mitochondria have differential morphology in disease states which ultimately leads to alterations in cellular processes such as metabolism and proliferation. In fact, manipulations of mitochondrial morphology are effective in animal models to ameliorate intimal hyperplasia [76, 94, 203, 211].

EBP50 is a scaffolding protein that regulates multiple pathways in VSMC including proliferation, migration and inflammatory responses that are critical in vascular diseases.

EBP50 inhibits the anti-proliferative effects of PTH1R agonists by increasing PTH1R at the cell membrane and increasing calcium signaling [195]. Furthermore, EBP50 promotes proliferation through stabilization of Skp2 that ubiquitinates and degrades $p21^{CIP}$ and $p27^{KIP}$ cell cycle regulators [191]. In addition to proliferation, EBP50 promotes VSMC migration by scaffolding FAK and EGFR and facilitating FAK activation and focal adhesion turnover [196]. Even though the basal levels of EBP50 in VSMC under normal conditions are relatively low, it is significantly upregulated after vascular injury in a feed forward loop, through NFκB [163]. These regulatory effects lead to reduced neointimal hyperplasia in $EBP50^{-/-}$ mice. My thesis work expanded further the complex regulatory network of EBP50 in VSMC and showed that EBP50 is able to impact mitochondrial dynamics and regulate redox balance both basally and under inflammatory conditions. Therefore, inhibiting EBP50 during pathological conditions might serve as a useful approach to modulate multiple processes that lead to adverse effects in the vasculature.

4.1 SUMMARY AND FUTURE DIRECTIONS

4.1.1 EBP50 regulates mitochondrial dynamics

Increasing amount of evidence supports the important role of mitochondria in vascular diseases. Mitochondria regulate various processes in cells including metabolism, apoptosis, cell cycle and redox balance that contribute to the progression of vascular disease. Recent studies demonstrate that mitochondrial dynamics has an impact on cellular functions. Moreover, in multiple cardiovascular diseases mitochondria exhibit altered morphology that ultimately affects various cellular processes such as proliferation and migration.

VSMC play a dominant role in vascular diseases such as restenosis and atherosclerosis and contain large amount of mitochondria. Therefore, it is logical to assume that alterations in mitochondria properties will affect VSMC and ultimately the progression of CVD. Indeed it was noted that in humans and in mouse models of atherosclerosis there is accumulation of mitochondrial damage that could be either a result of the impact of various risk factors (such as smoking, oxidative stress and lipid accumulation) that can damage mitochondrial DNA, or due to dysregulated mitochondrial dynamics.

Mitochondria undergo constant fission and fusion processes that are essential for their proper function. Mitochondrial fusion allows mixing of mitochondrial content that dilutes the damaged genome and allows mitochondria to function properly. On the other hand, fission is required for mitophagy, a process that is responsible for the removal of dysfunctional mitochondria. In PAH there is a decrease in Mfn2 levels which is required for mitochondrial fusion. Reduction of Mfn2 levels contribute to the fragmented mitochondrial phenotype in PAH and to the increased proliferation of VSMC that is observed in this disease [67]. In addition, PAH exhibits an upregulation of Cyclin B1/CDK1 dependent phosphorylation of Drp1 on Ser616. Several pre-clinical studies restoring Mfn2 expression and inhibiting fission with Mdivi-1, showed partial regression of experimentally induced pulmonary hypertension and decreased VSMC proliferation [67, 94]. In addition, downregulation of Mfn2 is accompanied by a metabolic switch from glucose oxidation to fatty acid oxidation. This suggests that changes in mitochondrial morphology and bioenergetics may underline the effects on proliferation. Drp1 has also been shown to contribute to VSMC proliferation. Following AngII stimulation PKCδ phosphorylates and activates Drp1 and the MEK1-2/ERK1-2 signaling cascade [246]. Mdivi-1

abrogated the proliferative response to AngII which suggest that mitochondrial fission is required for proliferation [246].

EBP50 regulates the localization and activity of proteins that are involved in processes such as migration, proliferation and inflammatory responses in VSMC. In my thesis work I showed that EBP50 effects extend beyond that and it can impact mitochondrial dynamics. I showed that under basal conditions EBP50 regulates Mfn2 expression by promoting FoxO1 degradation. As a result, EBP50$^{-/-}$ VSMC exhibit increased Mfn2 levels and more fused mitochondria network. In addition, my work indicates that TNFα induces Drp1 phosphorylation on Ser616 through activation of PKCζ that ultimately leads to mitochondrial fission. There are several reports that indicate TNFα ability to induce mitochondrial fission [219, 247], however the mechanism behind that action in VSMC was not reported previously. The involvement of PKCζ in TNFα signaling in vascular cells was described before [248] and data from our lab indicate that EBP50 mediates the recruitment and activation of PKCζ at the membrane following TNFα stimulation [163]. My studies demonstrate that PKCζ mediates TNFα phosphorylation of Drp1. My findings provide a mechanistic explanation for TNFα-induced mitochondrial fragmentation in VSMC.

Mitochondrial morphology has an impact on communication of mitochondria with other organelles such as the endoplasmic reticulum (ER). It was shown that Mfn2 resides in the ER and is tethered to Mfn1 or Mfn2 on mitochondria, thus forming ER mitochondrial contacts [77]. These contacts impact mitochondrial calcium uptake and can influence calcium signaling during apoptosis. It will be interesting to explore whether higher Mfn2 protein levels in EBP50$^{-/-}$ VSMC have an impact on ER-mitochondria communication and calcium signaling.

Mitophagy is an important quality control mechanism to remove damaged or dysfunctional mitochondria. Mitophagy has been linked to mitochondrial dynamics, and in order to be engulfed, mitochondria need to be fragmented by Drp1. Moreover, during mitophagy, Mfn2 is ubiquitinated by Parkin and targeted for degradation. There are two interesting elements that impose future investigation. The first, is whether EBP50 affects mitophagy. The second, is whether the E3 ubiquitin ligase, Parkin, that contains a putative PDZ binding motif, binds and is regulated by EBP50. It will be interesting to explore if Parkin localization or function and consequently mitophagy are altered in EBP50$^{-/-}$ VSMC.

4.1.2 EBP50 regulates mitochondrial metabolism and VSMC proliferation

Mitochondrial dynamics may impact cellular bioenergetics and other cellular functions such as proliferation and migration. Therefore, differences in mitochondrial dynamics led us to explore VSMC bioenergetics in EBP50 depleted VSMC. I found that despite the fact that there is no significant differences in oxygen consumption rate (OCR), extracellular acidification rate (ECAR) that is a direct result of lactate production and glycolysis, of EBP50 depleted VSMC is significantly lower compared to WT VSMC. Moreover, TNFα-induced lactate production was significantly lower in EBP50$^{-/-}$ VSMC. ECAR is an indicator of glycolytic metabolism and actively proliferating cells tend to upregulate glycolytic metabolism [249-251]. Indeed, I found that EBP50 depleted VSMC proliferate less than WT cells, both in basal (serum starved) condition and after TNFα stimulation. Importantly, Mdivi-1 treatment suppressed TNFα-induced proliferation in WT VSMC and had no effect in EBP50 depleted cells. The impact of Mdivi-1 suggests that mitochondrial dynamics have a significant effect on TNFα-induced proliferation of VSMC.

Given the striking differences in ECAR between WT and EBP50 depleted cells it will be interesting to explore further the differences in the metabolic profile between WT and EBP50 depleted VSMC. Full metabolomics analysis of TCA cycle metabolites will provide a more complete understanding of the metabolic differences between WT and EBP50$^{-/-}$ VSMC. Lactate dehydrogenase A (LDHA), a key enzyme in glycolysis, is crucial for VSMC proliferation and migration [251]. In addition, HIF-1α was shown to mediate the metabolic shift following TNFα in skeletal muscle [220]. Therefore, exploring the expression of LDHA and HIF-1α and their target genes in WT versus EBP50$^{-/-}$ VSMC will expand the mechanistic understanding of the metabolic differences between EBP50$^{-/-}$ and WT VSMC.

Altered mitochondrial dynamics in EBP50$^{-/-}$ VSMC is a result of increased Mfn2 levels and reduced Drp1 activation. Both Mfn2 and Drp1 have been implicated in VSMC proliferation. Mfn2 was originally discovered as "Hyperplasia suppressor gene" (HSG) and its overexpression reduced neointimal hyperplasia [6, 76]. Mfn2 effects on proliferation were mainly attributed to its binding to Ras and inhibiting the MAPK/ERK1-2 pathway [76]. Drp1 was also implicated in cell cycle [92] by regulating cyclin E build up [252] and degradation [253]. It will be interesting to continue exploring mechanisms that connect mitochondrial shaping proteins to proliferation in VSMC.

4.1.3 EBP50 regulates MnSOD and catalase levels and mitochondria derived superoxide following TNFα treatment

MnSOD and catalase are two key antioxidant enzymes that regulate redox balance in cells [136]. Both MnSOD and catalase are transcriptionally regulated by FoxO1. My data indicate that EBP50 regulates FoxO1 degradation through Skp2 stabilization in the cytoplasm. Consistent

with this, EBP50$^{-/-}$ VSMC and femoral arteries express higher MnSOD and catalase protein levels. Despite the fact that EBP50$^{-/-}$ VSMC have more MnSOD, I did not detect differences in basal mitochondrial superoxide between WT and EBP50$^{-/-}$ VSMC. This is probably due to the low basal superoxide production in VSMC. However, when superoxide production is stimulated with Ant A or TNFα, EBP50$^{-/-}$ VSMC had markedly lower mitochondria derived superoxide compared to WT VSMC. Differences in superoxide levels may have an impact on the ability of EBP50$^{-/-}$ mitochondria to handle stress condition and create a protective effect from inflammatory and oxidative damage. To address that, it will be interesting to determine how WT and EBP50$^{-/-}$ VSMC respond to oxidative stress and to assess mitochondrial ultra-structure and the presence of oxidative modifications such as nitro-tyrosine (NY) on mitochondrial proteins. In addition, mitochondrial DNA is very susceptible to oxidative damage [254]. Examining whether the increased levels of MnSOD and catalase can prevent mtDNA damage in EBP50$^{-/-}$ VSMC can have interesting implications.

4.1.4 MnSOD regulates VMSC migration

TNFα is a potent cytokine that induces migration of VSMC [240]. ROS have been implicated in cell migration [110] through multiple mechanisms that include cysteine residues modification [255] that alter many proteins functions. Some of the proteins that bear these redox sensitive residues include PKC [256], Akt [257], ERK [258] and MAPK. In addition it was shown that H_2O_2 modifies specific subunits in intergrin α7β1 and facilitates the formation of membrane protrusions and migration [259]. Therefore I decided to determine whether the reduced levels of mitochondrial superoxide and increased MnSOD will have an effect on TNFα-induced migration of EBP50$^{-/-}$ VSMC. I found that these cells migrated significantly less compared to WT VSMC.

Remarkably, when I knocked down MnSOD in EBP50$^{-/-}$ VSMC, migration was significantly increased. These results indicate that in addition to the known effect on FAK activity, EBP50 regulates VSMC migration through MnSOD. This is consistent with previous reports showing that MnSOD regulates VSMC proliferation and migration [238]. I did not explore the mechanism that underlines the differences in migration attributed to differential MnSOD levels. One possibility is that MnSOD regulates Akt activity. It was shown that MnSOD overexpression decreases Akt phosphorylation, and MnSOD knockdown increases Akt phosphorylation [238]. Consistently, our data indicates that EBP50 promotes Akt activity [167]. It is possible that the effect of EBP50 on Akt occurs through MnSOD.

Given the multiple regulatory pathway through which EBP50 regulates vascular responses to inflammation and injury it will be very interesting to explore EBP50 effect on vascular proliferative diseases such as atherosclerosis and PAH *in vivo*. EBP50 absence might have a protective effect in animal models of these diseases due to the higher levels of anti-oxidant enzymes and the reduced VSMC proliferation and migration that will result in lower vascular remodeling and will slower disease progression. In addition to VSMC, endothelial cells are also important contributors to the initiation and progression of atherosclerosis and PAH. Endothelial cells dysfunction contributes to the vascular structural abnormalities that are observed in PAH [260] and is one of the earliest events in atherosclerosis. EBP50 is highly expressed in endothelial cells, however its effects on endothelial function, proliferation and migration were not extensively studied. Therefore, it will be interesting to investigate the effects of EBP50 on endothelial cell proliferation and migration, anti-oxidant enzymes levels, NO production and mitochondrial function that have important roles in atherosclerosis and PAH. Understanding EBP50 effects in endothelial cells and its impact on CVD progression *in vivo* is

an important piece of revealing EBP50 regulations in the vasculature and might have a great value in developing new therapeutic strategies.

BIBLIOGRAPHY

1. Wang, H.D., et al., *Global, regional, and national life expectancy, all-cause mortality, and cause-specific mortality for 249 causes of death, 1980-2015: a systematic analysis for the Global Burden of Disease Study 2015.* Lancet, 2016. **388**(10053): p. 1459-1544.
2. Schwartz, S.M., R.L. Heimark, and M.W. Majesky, *Developmental mechanisms underlying pathology of arteries.* Physiol Rev, 1990. **70**(4): p. 1177-209.
3. Marx, S.O., H. Totary-Jain, and A.R. Marks, *Vascular smooth muscle cell proliferation in restenosis.* Circ Cardiovasc Interv, 2011. **4**(1): p. 104-11.
4. Lutgens, E., et al., *Biphasic pattern of cell turnover characterizes the progression from fatty streaks to ruptured human atherosclerotic plaques.* Cardiovasc Res, 1999. **41**(2): p. 473-9.
5. Davis, R., et al., *TNF-alpha-mediated proliferation of vascular smooth muscle cells involves Raf-1-mediated inactivation of Rb and transcription of E2F1-regulated genes.* Cell Cycle, 2012. **11**(1): p. 109-18.
6. Guo, Y.H., et al., *Overexpression of Mitofusin 2 inhibited oxidized low-density lipoprotein induced vascular smooth muscle cell proliferation and reduced atherosclerotic lesion formation in rabbit.* Biochem Biophys Res Commun, 2007. **363**(2): p. 411-7.
7. Chiong, M., et al., *Mitochondrial metabolism and the control of vascular smooth muscle cell proliferation.* Front Cell Dev Biol, 2014. **2**: p. 72.
8. Salabei, J.K. and B.G. Hill, *Mitochondrial fission induced by platelet-derived growth factor regulates vascular smooth muscle cell bioenergetics and cell proliferation.* Redox Biology, 2013. **1**(1): p. 542-551.
9. Ahn, S.Y., et al., *Mitochondrial dysfunction enhances the migration of vascular smooth muscles cells via suppression of Akt phosphorylation.* Biochim Biophys Acta, 2010. **1800**(3): p. 275-81.
10. Peppel, K., et al., *Activation of vascular smooth muscle cells by TNF and PDGF: overlapping and complementary signal transduction mechanisms.* Cardiovasc Res, 2005. **65**(3): p. 674-82.
11. Hamid, H. and J. Coltart, *'Miracle stents'--a future without restenosis.* Mcgill J Med, 2007. **10**(2): p. 105-11.
12. Reul, R.M., *Will drug-eluting stents replace coronary artery bypass surgery?* Texas Heart Institute Journal, 2005. **32**(3): p. 323-330.
13. Grech, E.D., *ABC of interventional cardiology - Percutaneous coronary intervention. II: The procedure.* British Medical Journal, 2003. **326**(7399): p. 1137-1140.

14. Dangas, G. and F. Kuepper, *Restenosis: Repeat narrowing of a coronary artery - Prevention and treatment.* Circulation, 2002. **105**(22): p. 2586-2587.
15. Schoenhagen, P., et al., *Arterial remodeling and coronary artery disease: the concept of "dilated" versus "obstructive" coronary atherosclerosis.* J Am Coll Cardiol, 2001. **38**(2): p. 297-306.
16. Bennett, M.R., *In-stent stenosis: pathology and implications for the development of drug eluting stents.* Heart, 2003. **89**(2): p. 218-224.
17. Mitra, A.K. and D.K. Agrawal, *In stent restenosis: bane of the stent era.* J Clin Pathol, 2006. **59**(3): p. 232-9.
18. Faxon, D.P., T.A. Sanborn, and C.C. Haudenschild, *Mechanism of angioplasty and its relation to restenosis.* Am J Cardiol, 1987. **60**(3): p. 5B-9B.
19. Fischman, D.L., et al., *A randomized comparison of coronary-stent placement and balloon angioplasty in the treatment of coronary artery disease. Stent Restenosis Study Investigators.* N Engl J Med, 1994. **331**(8): p. 496-501.
20. Serruys, P.W., et al., *A comparison of balloon-expandable-stent implantation with balloon angioplasty in patients with coronary artery disease. Benestent Study Group.* N Engl J Med, 1994. **331**(8): p. 489-95.
21. Holmes, D.R., Jr., et al., *Analysis of 1-year clinical outcomes in the SIRIUS trial: a randomized trial of a sirolimus-eluting stent versus a standard stent in patients at high risk for coronary restenosis.* Circulation, 2004. **109**(5): p. 634-40.
22. Iijima, R., et al., *Impact of diabetes mellitus on long-term outcomes in the drug-eluting stent era.* Am Heart J, 2007. **154**(4): p. 688-93.
23. Spaulding, C., et al., *A pooled analysis of data comparing sirolimus-eluting stents with bare-metal stents.* N Engl J Med, 2007. **356**(10): p. 989-97.
24. Pandya, B., et al., *Biodegradable polymer stents vs second generation drug eluting stents: A meta-analysis and systematic review of randomized controlled trials.* World J Cardiol, 2016. **8**(2): p. 240-6.
25. Chistiakov, D.A., et al., *The role of monocytosis and neutrophilia in atherosclerosis.* J Cell Mol Med, 2018.
26. Ross, R. and L. Agius, *The process of atherogenesis--cellular and molecular interaction: from experimental animal models to humans.* Diabetologia, 1992. **35 Suppl 2**: p. S34-40.
27. Ross, R., *Atherosclerosis--an inflammatory disease.* N Engl J Med, 1999. **340**(2): p. 115-26.
28. Owens, G.K., *Regulation of differentiation of vascular smooth muscle cells.* Physiol Rev, 1995. **75**(3): p. 487-517.
29. Belo, V.A., D.A. Guimaraes, and M.M. Castro, *Matrix Metalloproteinase 2 as a Potential Mediator of Vascular Smooth Muscle Cell Migration and Chronic Vascular Remodeling in Hypertension.* J Vasc Res, 2015. **52**(4): p. 221-31.
30. Gurjar, M.V., et al., *Mechanism of inhibition of matrix metalloproteinase-9 induction by NO in vascular smooth muscle cells.* J Appl Physiol (1985), 2001. **91**(3): p. 1380-6.
31. Gurjar, M.V., et al., *Role of reactive oxygen species in IL-1 beta-stimulated sustained ERK activation and MMP-9 induction.* Am J Physiol Heart Circ Physiol, 2001. **281**(6): p. H2568-74.
32. Wagsater, D., et al., *MMP-2 and MMP-9 are prominent matrix metalloproteinases during atherosclerosis development in the Ldlr(-/-)Apob(100/100) mouse.* Int J Mol Med, 2011. **28**(2): p. 247-53.

33. Johnson, J.L., et al., *Divergent effects of matrix metalloproteinases 3, 7, 9, and 12 on atherosclerotic plaque stability in mouse brachiocephalic arteries.* Proc Natl Acad Sci U S A, 2005. **102**(43): p. 15575-80.
34. Koepp, D.M., J.W. Harper, and S.J. Elledge, *How the cyclin became a cyclin: Regulated proteolysis in the cell cycle.* Cell, 1999. **97**(4): p. 431-434.
35. Sherr, C.J., *Mammalian G1 cyclins and cell cycle progression.* Proc Assoc Am Physicians, 1995. **107**(2): p. 181-6.
36. Levine, A.J., *p53, the cellular gatekeeper for growth and division.* Cell, 1997. **88**(3): p. 323-331.
37. Smith, R.C., et al., *p21CIP1-mediated inhibition of cell proliferation by overexpression of the gax homeodomain gene.* Genes Dev, 1997. **11**(13): p. 1674-89.
38. Narita, N., et al., *The gene for transcription factor GATA-6 resides on mouse chromosome 18 and is expressed in myocardium and vascular smooth muscle.* Genomics, 1996. **36**(2): p. 345-8.
39. Perlman, H., et al., *GATA-6 induces p21(Cip1) expression and G1 cell cycle arrest.* J Biol Chem, 1998. **273**(22): p. 13713-8.
40. Chin, Y.E., et al., *Cell growth arrest and induction of cyclin-dependent kinase inhibitor p21 WAF1/CIP1 mediated by STAT1.* Science, 1996. **272**(5262): p. 719-22.
41. Qian, H., et al., *Nitric oxide synthase gene therapy rapidly reduces adhesion molecule expression and inflammatory cell infiltration in carotid arteries of cholesterol-fed rabbits.* Circulation, 1999. **99**(23): p. 2979-82.
42. Mann, M.J., et al., *Cell cycle inhibition preserves endothelial function in genetically engineered rabbit vein grafts.* J Clin Invest, 1997. **99**(6): p. 1295-301.
43. Perkins, N.D., et al., *Regulation of NF-kappaB by cyclin-dependent kinases associated with the p300 coactivator.* Science, 1997. **275**(5299): p. 523-7.
44. Kleemann, R., et al., *Intracellular action of the cytokine MIF to modulate AP-1 activity and the cell cycle through Jab1.* Nature, 2000. **408**(6809): p. 211-6.
45. Hudson, J.D., et al., *A proinflammatory cytokine inhibits p53 tumor suppressor activity.* J Exp Med, 1999. **190**(10): p. 1375-82.
46. Gilroy, D.W., et al., *Cell cycle-dependent expression of cyclooxygenase-2 in human fibroblasts.* FASEB J, 2001. **15**(2): p. 288-90.
47. Gershlick, A.H., *Treating atherosclerosis: local drug delivery from laboratory studies to clinical trials.* Atherosclerosis, 2002. **160**(2): p. 259-71.
48. Archer, S.L., E.K. Weir, and M.R. Wilkins, *Basic science of pulmonary arterial hypertension for clinicians: new concepts and experimental therapies.* Circulation, 2010. **121**(18): p. 2045-66.
49. Hagan, G. and J. Pepke-Zaba, *Pulmonary hypertension, nitric oxide and nitric oxide-releasing compounds.* Expert Rev Respir Med, 2011. **5**(2): p. 163-71.
50. Yu, A.Y., et al., *Impaired physiological responses to chronic hypoxia in mice partially deficient for hypoxia-inducible factor 1alpha.* J Clin Invest, 1999. **103**(5): p. 691-6.
51. McMurtry, M.S., et al., *Dichloroacetate prevents and reverses pulmonary hypertension by inducing pulmonary artery smooth muscle cell apoptosis.* Circ Res, 2004. **95**(8): p. 830-40.
52. Andersson, S.G., et al., *The genome sequence of Rickettsia prowazekii and the origin of mitochondria.* Nature, 1998. **396**(6707): p. 133-40.

53. Yu, E., J. Mercer, and M. Bennett, *Mitochondria in vascular disease.* Cardiovasc Res, 2012. **95**(2): p. 173-82.
54. Birben, E., et al., *Oxidative stress and antioxidant defense.* World Allergy Organ J, 2012. **5**(1): p. 9-19.
55. Miller, D.M., G.R. Buettner, and S.D. Aust, *Transition-Metals as Catalysts of Autoxidation Reactions.* Free Radical Biology and Medicine, 1990. **8**(1): p. 95-108.
56. Murphy, M.P., *How mitochondria produce reactive oxygen species.* Biochemical Journal, 2009. **417**: p. 1-13.
57. Sena, L.A. and N.S. Chandel, *Physiological roles of mitochondrial reactive oxygen species.* Mol Cell, 2012. **48**(2): p. 158-67.
58. Majander, A., M. Finel, and M. Wikstrom, *Diphenyleneiodonium inhibits reduction of iron-sulfur clusters in the mitochondrial NADH-ubiquinone oxidoreductase (Complex I).* J Biol Chem, 1994. **269**(33): p. 21037-42.
59. Schieber, M. and N.S. Chandel, *ROS Function in Redox Signaling and Oxidative Stress.* Current Biology, 2014. **24**(10): p. R453-R462.
60. Lewis, M.R. and W.H. Lewis, *Mitochondria in Tissue Culture.* Science, 1914. **39**(1000): p. 330-3.
61. Alward, W.L.M., *Optic neuropathy - The OPA1 gene and optic neuropathy.* British Journal of Ophthalmology, 2003. **87**(1): p. 2-3.
62. Delettre, C., et al., *Nuclear gene OPA1, encoding a mitochondrial dynamin-related protein, is mutated in dominant optic atrophy.* Nat Genet, 2000. **26**(2): p. 207-10.
63. Alexander, C., et al., *OPA1, encoding a dynamin-related GTPase, is mutated in autosomal dominant optic atrophy linked to chromosome 3q28.* Nat Genet, 2000. **26**(2): p. 211-5.
64. Reilly, M.M., S.M. Murphy, and M. Laura, *Charcot-Marie-Tooth disease.* J Peripher Nerv Syst, 2011. **16**(1): p. 1-14.
65. Zhang, J., et al., *G-protein beta2 subunit interacts with mitofusin 1 to regulate mitochondrial fusion.* Nat Commun, 2010. **1**: p. 101.
66. Liesa, M., et al., *Mitochondrial fusion is increased by the nuclear coactivator PGC-1beta.* PLoS One, 2008. **3**(10): p. e3613.
67. Ryan, J.J., et al., *PGC1alpha-mediated mitofusin-2 deficiency in female rats and humans with pulmonary arterial hypertension.* Am J Respir Crit Care Med, 2013. **187**(8): p. 865-78.
68. Puigserver, P., et al., *Insulin-regulated hepatic gluconeogenesis through FOXO1-PGC-1alpha interaction.* Nature, 2003. **423**(6939): p. 550-5.
69. Wu, L., et al., *Activation of FoxO1/ PGC-1alpha prevents mitochondrial dysfunction and ameliorates mesangial cell injury in diabetic rats.* Mol Cell Endocrinol, 2015. **413**: p. 1-12.
70. Tanaka, A., et al., *Proteasome and p97 mediate mitophagy and degradation of mitofusins induced by Parkin.* J Cell Biol, 2010. **191**(7): p. 1367-80.
71. Gegg, M.E., et al., *Mitofusin 1 and mitofusin 2 are ubiquitinated in a PINK1/parkin-dependent manner upon induction of mitophagy.* Human Molecular Genetics, 2010. **19**(24): p. 4861-4870.
72. Ehses, S., et al., *Regulation of OPA1 processing and mitochondrial fusion by m-AAA protease isoenzymes and OMA1.* J Cell Biol, 2009. **187**(7): p. 1023-36.

73. Frezza, C., et al., *OPA1 controls apoptotic cristae remodeling independently from mitochondrial fusion.* Cell, 2006. **126**(1): p. 177-89.
74. Cipolat, S., et al., *Mitochondrial rhomboid PARL regulates cytochrome c release during apoptosis via OPA1-dependent cristae remodeling.* Cell, 2006. **126**(1): p. 163-75.
75. Chen, K.H., et al., *Role of mitofusin 2 (Mfn2) in controlling cellular proliferation.* FASEB J, 2014. **28**(1): p. 382-94.
76. Chen, K.H., et al., *Dysregulation of HSG triggers vascular proliferative disorders.* Nat Cell Biol, 2004. **6**(9): p. 872-83.
77. de Brito, O.M. and L. Scorrano, *Mitofusin 2 tethers endoplasmic reticulum to mitochondria.* Nature, 2008. **456**(7222): p. 605-10.
78. Chen, L., et al., *OPA1 mutation and late-onset cardiomyopathy: mitochondrial dysfunction and mtDNA instability.* J Am Heart Assoc, 2012. **1**(5): p. e003012.
79. Ong, S.B., et al., *Mitochondrial fusion and fission proteins as novel therapeutic targets for treating cardiovascular disease.* Eur J Pharmacol, 2015. **763**(Pt A): p. 104-14.
80. Cogliati, S., et al., *Mitochondrial cristae shape determines respiratory chain supercomplexes assembly and respiratory efficiency.* Cell, 2013. **155**(1): p. 160-71.
81. Cribbs, J.T. and S. Strack, *Reversible phosphorylation of Drp1 by cyclic AMP-dependent protein kinase and calcineurin regulates mitochondrial fission and cell death.* EMBO Rep, 2007. **8**(10): p. 939-44.
82. Figueroa-Romero, C., et al., *SUMOylation of the mitochondrial fission protein Drp1 occurs at multiple nonconsensus sites within the B domain and is linked to its activity cycle.* FASEB J, 2009. **23**(11): p. 3917-27.
83. Nakamura, N., et al., *MARCH-V is a novel mitofusin 2- and Drp1-binding protein able to change mitochondrial morphology.* EMBO Rep, 2006. **7**(10): p. 1019-22.
84. Zaja, I., et al., *Cdk1, PKCdelta and calcineurin-mediated Drp1 pathway contributes to mitochondrial fission-induced cardiomyocyte death.* Biochem Biophys Res Commun, 2014. **453**(4): p. 710-21.
85. Taguchi, N., et al., *Mitotic phosphorylation of dynamin-related GTPase Drp1 participates in mitochondrial fission.* J Biol Chem, 2007. **282**(15): p. 11521-9.
86. Han, X.J., et al., *CaM kinase I alpha-induced phosphorylation of Drp1 regulates mitochondrial morphology.* J Cell Biol, 2008. **182**(3): p. 573-85.
87. Qi, X., et al., *Aberrant mitochondrial fission in neurons induced by protein kinase C{delta} under oxidative stress conditions in vivo.* Mol Biol Cell, 2011. **22**(2): p. 256-65.
88. Dickey, A.S. and S. Strack, *PKA/AKAP1 and PP2A/Bbeta2 regulate neuronal morphogenesis via Drp1 phosphorylation and mitochondrial bioenergetics.* J Neurosci, 2011. **31**(44): p. 15716-26.
89. Cereghetti, G.M., et al., *Dephosphorylation by calcineurin regulates translocation of Drp1 to mitochondria.* Proc Natl Acad Sci U S A, 2008. **105**(41): p. 15803-8.
90. Zhao, Y., et al., *PDGF-induced vascular smooth muscle cell proliferation is associated with dysregulation of insulin receptor substrates.* Am J Physiol Cell Physiol, 2011. **300**(6): p. C1375-85.
91. Hsieh, H.L., et al., *Thrombin induces EGF receptor expression and cell proliferation via a PKC(delta)/c-Src-dependent pathway in vascular smooth muscle cells.* Arterioscler Thromb Vasc Biol, 2009. **29**(10): p. 1594-601.

92. Marsboom, G., et al., *Dynamin-related protein 1-mediated mitochondrial mitotic fission permits hyperproliferation of vascular smooth muscle cells and offers a novel therapeutic target in pulmonary hypertension.* Circ Res, 2012. **110**(11): p. 1484-97.
93. Boucherat, O., et al., *The cancer theory of pulmonary arterial hypertension.* Pulm Circ, 2017. **7**(2): p. 285-299.
94. Marsboom, G., et al., *Dynamin-Related Protein 1-Mediated Mitochondrial Mitotic Fission Permits Hyperproliferation of Vascular Smooth Muscle Cells and Offers a Novel Therapeutic Target in Pulmonary Hypertension.* Circulation Research, 2012. **110**(11): p. 1484-+.
95. Yu, E.P.K., et al., *Mitochondrial Respiration Is Reduced in Atherosclerosis, Promoting Necrotic Core Formation and Reducing Relative Fibrous Cap Thickness.* Arterioscler Thromb Vasc Biol, 2017. **37**(12): p. 2322-2332.
96. Yang, X., et al., *Oxidative Stress-Mediated Atherosclerosis: Mechanisms and Therapies.* Front Physiol, 2017. **8**: p. 600.
97. Krishnan, K.J., et al., *What causes mitochondrial DNA deletions in human cells?* Nat Genet, 2008. **40**(3): p. 275-9.
98. Ballinger, S.W., et al., *Hydrogen peroxide- and peroxynitrite-induced mitochondrial DNA damage and dysfunction in vascular endothelial and smooth muscle cells.* Circ Res, 2000. **86**(9): p. 960-6.
99. Harrison, C.M., et al., *Mitochondrial oxidative stress significantly influences atherogenic risk and cytokine-induced oxidant production.* Environ Health Perspect, 2011. **119**(5): p. 676-81.
100. Bernal-Mizrachi, C., et al., *Vascular respiratory uncoupling increases blood pressure and atherosclerosis.* Nature, 2005. **435**(7041): p. 502-6.
101. Leanderson, P. and C. Tagesson, *Cigarette smoke-induced DNA damage in cultured human lung cells: role of hydroxyl radicals and endonuclease activation.* Chem Biol Interact, 1992. **81**(1-2): p. 197-208.
102. Simone, S., et al., *Mechanism of oxidative DNA damage in diabetes: tuberin inactivation and downregulation of DNA repair enzyme 8-oxo-7,8-dihydro-2'-deoxyguanosine-DNA glycosylase.* Diabetes, 2008. **57**(10): p. 2626-36.
103. Cathcart, M.K., *Regulation of superoxide anion production by NADPH oxidase in monocytes/macrophages: contributions to atherosclerosis.* Arterioscler Thromb Vasc Biol, 2004. **24**(1): p. 23-8.
104. Verhaar, M.C., et al., *Free radical production by dysfunctional eNOS.* Heart, 2004. **90**(5): p. 494-5.
105. McCubrey, J.A., M.M. Lahair, and R.A. Franklin, *Reactive oxygen species-induced activation of the MAP kinase signaling pathways.* Antioxid Redox Signal, 2006. **8**(9-10): p. 1775-89.
106. Morgan, M.J. and Z.G. Liu, *Crosstalk of reactive oxygen species and NF-kappaB signaling.* Cell Res, 2011. **21**(1): p. 103-15.
107. Aharoni-Simon, M., R. Reifen, and O. Tirosh, *ROS-production-mediated activation of AP-1 but not NFkappaB inhibits glutamate-induced HT4 neuronal cell death.* Antioxid Redox Signal, 2006. **8**(7-8): p. 1339-49.
108. Jing, L., et al., *Protective Effect of Tempol Against Hypoxia-Induced Oxidative Stress and Apoptosis in H9c2 Cells.* Med Sci Monit Basic Res, 2017. **23**: p. 159-165.

109. Hamanaka, R.B. and N.S. Chandel, *Mitochondrial reactive oxygen species regulate hypoxic signaling.* Curr Opin Cell Biol, 2009. **21**(6): p. 894-9.
110. Finkel, T., *Redox-dependent signal transduction.* Febs Letters, 2000. **476**(1-2): p. 52-54.
111. Douglas, G., et al., *Endothelial-specific Nox2 overexpression increases vascular superoxide and macrophage recruitment in ApoE(-)/(-) mice.* Cardiovasc Res, 2012. **94**(1): p. 20-9.
112. Vendrov, A.E., et al., *NOX4 NADPH Oxidase-Dependent Mitochondrial Oxidative Stress in Aging-Associated Cardiovascular Disease.* Antioxid Redox Signal, 2015. **23**(18): p. 1389-409.
113. Kuroda, J., et al., *NADPH oxidase 4 (Nox4) is a major source of oxidative stress in the failing heart.* Proc Natl Acad Sci U S A, 2010. **107**(35): p. 15565-70.
114. Zhang, M., et al., *NADPH oxidase-4 mediates protection against chronic load-induced stress in mouse hearts by enhancing angiogenesis.* Proc Natl Acad Sci U S A, 2010. **107**(42): p. 18121-6.
115. Carlioz, A. and D. Touati, *Isolation of superoxide dismutase mutants in Escherichia coli: is superoxide dismutase necessary for aerobic life?* EMBO J, 1986. **5**(3): p. 623-30.
116. Li, Y., et al., *Dilated cardiomyopathy and neonatal lethality in mutant mice lacking manganese superoxide dismutase.* Nat Genet, 1995. **11**(4): p. 376-81.
117. Lebovitz, R.M., et al., *Neurodegeneration, myocardial injury, and perinatal death in mitochondrial superoxide dismutase-deficient mice.* Proc Natl Acad Sci U S A, 1996. **93**(18): p. 9782-7.
118. Nakanishi, S., et al., *Manganese superoxide dismutase Ala16Val polymorphism is associated with the development of type 2 diabetes in Japanese-Americans.* Diabetes Res Clin Pract, 2008. **81**(3): p. 381-5.
119. Hirooka, Y., *Role of reactive oxygen species in brainstem in neural mechanisms of hypertension.* Auton Neurosci, 2008. **142**(1-2): p. 20-4.
120. Arsova-Sarafinovska, Z., et al., *Manganese superoxide dismutase (MnSOD) genetic polymorphism is associated with risk of early-onset prostate cancer.* Cell Biochem Funct, 2008. **26**(7): p. 771-7.
121. Rosenblum, J.S., N.B. Gilula, and R.A. Lerner, *On signal sequence polymorphisms and diseases of distribution.* Proc Natl Acad Sci U S A, 1996. **93**(9): p. 4471-3.
122. Guo, G., et al., *Manganese superoxide dismutase-mediated gene expression in radiation-induced adaptive responses.* Mol Cell Biol, 2003. **23**(7): p. 2362-78.
123. Darville, M.I., Y.S. Ho, and D.L. Eizirik, *NF-kappaB is required for cytokine-induced manganese superoxide dismutase expression in insulin-producing cells.* Endocrinology, 2000. **141**(1): p. 153-62.
124. Eastgate, J., et al., *A role for manganese superoxide dismutase in radioprotection of hematopoietic stem cells by interleukin-1.* Blood, 1993. **81**(3): p. 639-46.
125. Xu, Y., et al., *An intronic NF-kappaB element is essential for induction of the human manganese superoxide dismutase gene by tumor necrosis factor-alpha and interleukin-1beta.* DNA Cell Biol, 1999. **18**(9): p. 709-22.
126. Dhar, S.K., et al., *Manganese superoxide dismutase is a p53-regulated gene that switches cancers between early and advanced stages.* Cancer Res, 2011. **71**(21): p. 6684-95.
127. Drane, P., et al., *Reciprocal down-regulation of p53 and SOD2 gene expression-implication in p53 mediated apoptosis.* Oncogene, 2001. **20**(4): p. 430-9.

128. Kops, G.J., et al., *Forkhead transcription factor FOXO3a protects quiescent cells from oxidative stress.* Nature, 2002. **419**(6904): p. 316-21.
129. Dhar, S.K., et al., *Specificity protein 1-dependent p53-mediated suppression of human manganese superoxide dismutase gene expression.* J Biol Chem, 2006. **281**(31): p. 21698-709.
130. MacMillan-Crow, L.A., J.P. Crow, and J.A. Thompson, *Peroxynitrite-mediated inactivation of manganese superoxide dismutase involves nitration and oxidation of critical tyrosine residues.* Biochemistry, 1998. **37**(6): p. 1613-22.
131. Qiu, X., et al., *Calorie restriction reduces oxidative stress by SIRT3-mediated SOD2 activation.* Cell Metab, 2010. **12**(6): p. 662-7.
132. Ozden, O., et al., *Acetylation of MnSOD directs enzymatic activity responding to cellular nutrient status or oxidative stress.* Aging (Albany NY), 2011. **3**(2): p. 102-7.
133. Goth, L., P. Rass, and A. Pay, *Catalase enzyme mutations and their association with diseases.* Mol Diagn, 2004. **8**(3): p. 141-9.
134. Goth, L. and T. Nagy, *Acatalasemia and diabetes mellitus.* Arch Biochem Biophys, 2012. **525**(2): p. 195-200.
135. Ho, Y.S., et al., *Mice lacking catalase develop normally but show differential sensitivity to oxidant tissue injury.* J Biol Chem, 2004. **279**(31): p. 32804-12.
136. Schriner, S.E., et al., *Extension of murine life span by overexpression of catalase targeted to mitochondria.* Science, 2005. **308**(5730): p. 1909-11.
137. Parastatidis, I., et al., *Overexpression of catalase in vascular smooth muscle cells prevents the formation of abdominal aortic aneurysms.* Arterioscler Thromb Vasc Biol, 2013. **33**(10): p. 2389-96.
138. Yang, H., et al., *Retardation of atherosclerosis by overexpression of catalase or both Cu/Zn-superoxide dismutase and catalase in mice lacking apolipoprotein E.* Circulation Research, 2004. **95**(11): p. 1075-1081.
139. Yano, S., N. Arroyo, and N. Yano, *Catalase binds Grb2 in tumor cells when stimulated with serum or ligands for integrin receptors.* Free Radic Biol Med, 2004. **36**(12): p. 1542-54.
140. Yano, S., N. Arroyo, and N. Yano, *SHP2 binds catalase and acquires a hydrogen peroxide-resistant phosphatase activity via integrin-signaling.* FEBS Lett, 2004. **577**(3): p. 327-32.
141. Nenoi, M., et al., *Regulation of the catalase gene promoter by Sp1, CCAAT-recognizing factors, and a WT1/Egr-related factor in hydrogen peroxide-resistant HP100 cells.* Cancer Res, 2001. **61**(15): p. 5885-94.
142. Luo, D. and T.A. Rando, *The regulation of catalase gene expression in mouse muscle cells is dependent on the CCAAT-binding factor NF-Y.* Biochem Biophys Res Commun, 2003. **303**(2): p. 609-18.
143. Awad, H., et al., *AMPK and FoxO1 regulate catalase expression in hypoxic pulmonary arterial smooth muscle.* Pediatr Pulmonol, 2014. **49**(9): p. 885-97.
144. Taniguchi, M., et al., *CCAAT/enhancer binding protein-beta (C/EBP-beta), a pivotal regulator of the TATA-less promoter in the rat catalase gene.* FEBS Lett, 2005. **579**(25): p. 5785-90.
145. Yakunin, E., et al., *The regulation of catalase activity by PPAR gamma is affected by alpha-synuclein.* Ann Clin Transl Neurol, 2014. **1**(3): p. 145-59.

146. Farr, R.L., et al., *Peroxisome biogenesis in mammalian cells: The impact of genes and environment.* Biochim Biophys Acta, 2016. **1863**(5): p. 1049-60.
147. Calnan, D.R. and A. Brunet, *The FoxO code.* Oncogene, 2008. **27**(16): p. 2276-88.
148. Brunet, A., et al., *Akt promotes cell survival by phosphorylating and inhibiting a Forkhead transcription factor.* Cell, 1999. **96**(6): p. 857-68.
149. Nemoto, S. and T. Finkel, *Redox regulation of forkhead proteins through a p66shc-dependent signaling pathway.* Science, 2002. **295**(5564): p. 2450-2.
150. Akasaki, Y., et al., *FoxO transcription factors support oxidative stress resistance in human chondrocytes.* Arthritis Rheumatol, 2014. **66**(12): p. 3349-58.
151. Halasi, M., et al., *Combination of oxidative stress and FOXM1 inhibitors induces apoptosis in cancer cells and inhibits xenograft tumor growth.* Am J Pathol, 2013. **183**(1): p. 257-65.
152. Xiong, S., et al., *PGC-1 alpha serine 570 phosphorylation and GCN5-mediated acetylation by angiotensin II drive catalase down-regulation and vascular hypertrophy.* J Biol Chem, 2010. **285**(4): p. 2474-87.
153. Qin, G., et al., *Overexpression of the FoxO1 Ameliorates Mesangial Cell Dysfunction in Male Diabetic Rats.* Mol Endocrinol, 2015. **29**(7): p. 1080-91.
154. Sheng, R., et al., *Cholesterol modulates cell signaling and protein networking by specifically interacting with PDZ domain-containing scaffold proteins.* Nat Commun, 2012. **3**: p. 1249.
155. Reczek, D., M. Berryman, and A. Bretscher, *Identification of EBP50: A PDZ-containing phosphoprotein that associates with members of the ezrin-radixin-moesin family.* J Cell Biol, 1997. **139**(1): p. 169-79.
156. Hanono, A., et al., *EPI64 regulates microvillar subdomains and structure.* J Cell Biol, 2006. **175**(5): p. 803-13.
157. Morales, F.C., et al., *Ezrin-radixin-moesin (ERM)-binding phosphoprotein 50 organizes ERM proteins at the apical membrane of polarized epithelia.* Proc Natl Acad Sci U S A, 2004. **101**(51): p. 17705-10.
158. Broere, N., et al., *Defective jejunal and colonic salt absorption and alteredNa(+)/H (+) exchanger 3 (NHE3) activity in NHE regulatory factor 1 (NHERF1) adaptor protein-deficient mice.* Pflugers Arch, 2009. **457**(5): p. 1079-91.
159. Georgescu, M.M., M. Gagea, and G. Cote, *NHERF1/EBP50 Suppresses Wnt-beta-Catenin Pathway-Driven Intestinal Neoplasia.* Neoplasia, 2016. **18**(8): p. 512-23.
160. Hayashi, Y., et al., *NHERF1/EBP50 is a new marker in colorectal cancer.* Neoplasia, 2010. **12**(12): p. 1013-22.
161. Ediger, T.R., S.E. Park, and B.S. Katzenellenbogen, *Estrogen receptor inducibility of the human Na+/H+ exchanger regulatory factor/ezrin-radixin-moesin binding protein 50 (NHE-RF/EBP50) gene involving multiple half-estrogen response elements.* Mol Endocrinol, 2002. **16**(8): p. 1828-39.
162. Cardone, R.A., et al., *The NHERF1 PDZ2 domain regulates PKA-RhoA-p38-mediated NHE1 activation and invasion in breast tumor cells.* Mol Biol Cell, 2007. **18**(5): p. 1768-80.
163. Leslie, K.L., et al., *Ezrin-radixin-moesin-binding phosphoprotein 50 (EBP50) and nuclear factor-kappaB (NF-kappaB): a feed-forward loop for systemic and vascular inflammation.* J Biol Chem, 2013. **288**(51): p. 36426-36.

164. Fouassier, L., et al., *Protein kinase C regulates the phosphorylation and oligomerization of ERM binding phosphoprotein 50.* Exp Cell Res, 2005. **306**(1): p. 264-73.
165. He, J., et al., *Phosphorylation and cell cycle-dependent regulation of Na+/H+ exchanger regulatory factor-1 by Cdc2 kinase.* J Biol Chem, 2001. **276**(45): p. 41559-65.
166. Hall, R.A., et al., *G protein-coupled receptor kinase 6A phosphorylates the Na(+)/H(+) exchanger regulatory factor via a PDZ domain-mediated interaction.* J Biol Chem, 1999. **274**(34): p. 24328-34.
167. Song, G.J., et al., *Phosphorylation of ezrin-radixin-moesin-binding phosphoprotein 50 (EBP50) by Akt promotes stability and mitogenic function of S-phase kinase-associated protein-2 (Skp2).* J Biol Chem, 2015. **290**(5): p. 2879-87.
168. Lim, H.C. and T.S. Jou, *Ras-activated RSK1 phosphorylates EBP50 to regulate its nuclear localization and promote cell proliferation.* Oncotarget, 2016. **7**(9): p. 10283-96.
169. Li, J., et al., *Protein kinase C phosphorylation disrupts Na+/H+ exchanger regulatory factor 1 autoinhibition and promotes cystic fibrosis transmembrane conductance regulator macromolecular assembly.* J Biol Chem, 2007. **282**(37): p. 27086-99.
170. Chen, J.Y., Y.Y. Lin, and T.S. Jou, *Phosphorylation of EBP50 negatively regulates beta-PIX-dependent Rac1 activity in anoikis.* Cell Death Differ, 2012. **19**(6): p. 1027-37.
171. Shenolikar, S., et al., *Targeted disruption of the mouse NHERF-1 gene promotes internalization of proximal tubule sodium-phosphate cotransporter type IIa and renal phosphate wasting.* Proc Natl Acad Sci U S A, 2002. **99**(17): p. 11470-5.
172. Biber, J., et al., *Phosphate transport in established renal epithelial cell lines.* Methods Enzymol, 1990. **191**: p. 494-505.
173. Karim, Z., et al., *NHERF1 mutations and responsiveness of renal parathyroid hormone.* N Engl J Med, 2008. **359**(11): p. 1128-35.
174. Liu, L., et al., *Na+/H+ exchanger regulatory factor 1 (NHERF1) directly regulates osteogenesis.* J Biol Chem, 2012. **287**(52): p. 43312-21.
175. Dai, J.L., et al., *NHERF (Na+/H+ exchanger regulatory factor) gene mutations in human breast cancer.* Oncogene, 2004. **23**(53): p. 8681-7.
176. Kreimann, E.L., et al., *Cortical stabilization of beta-catenin contributes to NHERF1/EBP50 tumor suppressor function.* Oncogene, 2007. **26**(36): p. 5290-9.
177. Zheng, J.F., et al., *EBP50 exerts tumor suppressor activity by promoting cell apoptosis and retarding extracellular signal-regulated kinase activity.* Amino Acids, 2010. **38**(4): p. 1261-8.
178. Song, J., et al., *Expression and clinicopathological significance of oestrogen-responsive ezrin-radixin-moesin-binding phosphoprotein 50 in breast cancer.* Histopathology, 2007. **51**(1): p. 40-53.
179. Mangia, A., et al., *Biological role of NHERF1 protein expression in breast cancer.* Histopathology, 2009. **55**(5): p. 600-8.
180. Stemmer-Rachamimov, A.O., et al., *NHE-RF, a merlin-interacting protein, is primarily expressed in luminal epithelia, proliferative endometrium, and estrogen receptor-positive breast carcinomas.* Am J Pathol, 2001. **158**(1): p. 57-62.
181. Radford, D.M., et al., *Allelotyping of ductal carcinoma in situ of the breast: deletion of loci on 8p, 13q, 16q, 17p and 17q.* Cancer Res, 1995. **55**(15): p. 3399-405.
182. Presneau, N., et al., *Loss of heterozygosity and transcriptome analyses of a 1.2 Mb candidate ovarian cancer tumor suppressor locus region at 17q25.1-q25.2.* Mol Carcinog, 2005. **43**(3): p. 141-54.

183. Georgescu, M.M., et al., *Roles of NHERF1/EBP50 in cancer.* Curr Mol Med, 2008. **8**(6): p. 459-68.
184. Karn, T., et al., *Gene expression profiling of luminal B breast cancers reveals NHERF1 as a new marker of endocrine resistance.* Breast Cancer Res Treat, 2011. **130**(2): p. 409-20.
185. Malfettone, A., et al., *Peritumoral vascular invasion and NHERF1 expression define an immunophenotype of grade 2 invasive breast cancer associated with poor prognosis.* BMC Cancer, 2012. **12**: p. 106.
186. Wheeler, D.S., et al., *Direct interaction between NHERF1 and Frizzled regulates beta-catenin signaling.* Oncogene, 2011. **30**(1): p. 32-42.
187. Molina, J.R., et al., *Loss of PTEN binding adapter protein NHERF1 from plasma membrane in glioblastoma contributes to PTEN inactivation.* Cancer Res, 2010. **70**(17): p. 6697-703.
188. Barreiro, O., et al., *Dynamic interaction of VCAM-1 and ICAM-1 with moesin and ezrin in a novel endothelial docking structure for adherent leukocytes.* J Cell Biol, 2002. **157**(7): p. 1233-45.
189. Li, M., et al., *Na+/H+ exchanger regulatory factor 1 knockout mice have an attenuated hepatic inflammatory response and are protected from cholestatic liver injury.* Hepatology, 2015. **62**(4): p. 1227-1236.
190. Wu, Y., et al., *A chemokine receptor CXCR2 macromolecular complex regulates neutrophil functions in inflammatory diseases.* J Biol Chem, 2012. **287**(8): p. 5744-55.
191. Song, G.J., et al., *The scaffolding protein EBP50 promotes vascular smooth muscle cell proliferation and neointima formation by regulating Skp2 and p21(cip1).* Arterioscler Thromb Vasc Biol, 2012. **32**(1): p. 33-41.
192. Lin, H.K., et al., *Phosphorylation-dependent regulation of cytosolic localization and oncogenic function of Skp2 by Akt/PKB.* Nat Cell Biol, 2009. **11**(4): p. 420-32.
193. Ozeki, S., et al., *Evidence that implicates the parathyroid hormone-related peptide in vascular stenosis - Increased gene expression in the intima of injured rat carotid arteries and human restenotic coronary lesions.* Arteriosclerosis Thrombosis and Vascular Biology, 1996. **16**(4): p. 565-575.
194. Song, G.J., N. Fiaschi-Taesch, and A. Bisello, *Endogenous parathyroid hormone-related protein regulates the expression of PTH type 1 receptor and proliferation of vascular smooth muscle cells.* Mol Endocrinol, 2009. **23**(10): p. 1681-90.
195. Song, G.J., et al., *EBP50 inhibits the anti-mitogenic action of the parathyroid hormone type 1 receptor in vascular smooth muscle cells.* J Mol Cell Cardiol, 2010. **49**(6): p. 1012-21.
196. Song, G.J., et al., *EBP50 promotes focal adhesion turnover and vascular smooth muscle cells migration.* J Mol Cell Cardiol, 2012. **53**(6): p. 809-19.
197. Baeyens, N., et al., *EBP50 Is Involved in the Regulation of Vascular Smooth Muscle Cell Migration and Cytokinesis.* Journal of Cellular Biochemistry, 2011. **112**(9): p. 2574-2584.
198. Boratko, A., P. Gergely, and C. Csortos, *Cell cycle dependent association of EBP50 with protein phosphatase 2A in endothelial cells.* PLoS One, 2012. **7**(4): p. e35595.
199. Boratko, A., M. Peter, and C. Csortos, *Regulation of merlin by protein phosphatase 1-TIMAP and EBP50 in endothelial cells.* Int J Biochem Cell Biol, 2017. **82**: p. 10-17.

200. Al Ghouleh, I., et al., *Binding of EBP50 to Nox organizing subunit p47(phox) is pivotal to cellular reactive species generation and altered vascular phenotype.* Proceedings of the National Academy of Sciences of the United States of America, 2016. **113**(36): p. E5308-E5317.
201. Chalmers, S., et al., *Mitochondrial motility and vascular smooth muscle proliferation.* Arterioscler Thromb Vasc Biol, 2012. **32**(12): p. 3000-11.
202. Zhao, T., et al., *Central role of mitofusin 2 in autophagosome-lysosome fusion in cardiomyocytes.* J Biol Chem, 2012. **287**(28): p. 23615-25.
203. Hall, A.R., et al., *Mitochondrial fusion and fission proteins: novel therapeutic targets for combating cardiovascular disease.* Br J Pharmacol, 2014. **171**(8): p. 1890-906.
204. Escobar-Henriques, M., *Mitofusins: ubiquitylation promotes fusion.* Cell Res, 2014. **24**(4): p. 387-8.
205. Wiedemann, N., S.B. Stiller, and N. Pfanner, *Activation and degradation of mitofusins: two pathways regulate mitochondrial fusion by reversible ubiquitylation.* Mol Cell, 2013. **49**(3): p. 423-5.
206. Otera, H., N. Ishihara, and K. Mihara, *New insights into the function and regulation of mitochondrial fission.* Biochim Biophys Acta, 2013. **1833**(5): p. 1256-68.
207. Archer, S.L., *Mitochondrial dynamics--mitochondrial fission and fusion in human diseases.* N Engl J Med, 2013. **369**(23): p. 2236-51.
208. Kitamura, Y.I., et al., *FoxO1 protects against pancreatic beta cell failure through NeuroD and MafA induction.* Cell Metabolism, 2005. **2**(3): p. 153-163.
209. Gross, D.N., A.P. van den Heuvel, and M.J. Birnbaum, *The role of FoxO in the regulation of metabolism.* Oncogene, 2008. **27**(16): p. 2320-36.
210. Bach, D., et al., *Mitofusin-2 determines mitochondrial network architecture and mitochondrial metabolism. A novel regulatory mechanism altered in obesity.* J Biol Chem, 2003. **278**(19): p. 17190-7.
211. Wang, L., et al., *Decreasing mitochondrial fission diminishes vascular smooth muscle cell migration and ameliorates intimal hyperplasia.* Cardiovasc Res, 2015. **106**(2): p. 272-83.
212. Pich, S., et al., *The Charcot-Marie-Tooth type 2A gene product, Mfn2, up-regulates fuel oxidation through expression of OXPHOS system.* Hum Mol Genet, 2005. **14**(11): p. 1405-15.
213. Suen, D.F., K.L. Norris, and R.J. Youle, *Mitochondrial dynamics and apoptosis.* Genes Dev, 2008. **22**(12): p. 1577-90.
214. TeSlaa, T. and M.A. Teitell, *Techniques to monitor glycolysis.* Methods Enzymol, 2014. **542**: p. 91-114.
215. Hirai, T., *Protein Kinase Czeta (PKCzeta): Activation Mechanisms and Cellular Functions.* Journal of Biochemistry, 2003. **133**(1): p. 1-7.
216. Kwan, J., et al., *In high glucose protein kinase C-zeta activation is required for mesangial cell generation of reactive oxygen species.* Kidney Int, 2005. **68**(6): p. 2526-41.
217. Stokka, A.J., et al., *The adaptor protein EBP50 is important for localization of the protein kinase A-Ezrin complex in T-cells and the immunomodulating effect of cAMP.* Biochem J, 2009. **425**(2): p. 381-8.
218. Doll, D.N., et al., *Rapid mitochondrial dysfunction mediates TNF-alpha-induced neurotoxicity.* J Neurochem, 2015. **132**(4): p. 443-51.

219. Chen, X.H., et al., *TNF-alpha induces mitochondrial dysfunction in 3T3-L1 adipocytes.* Mol Cell Endocrinol, 2010. **328**(1-2): p. 63-9.
220. Remels, A.H., et al., *TNF-alpha-induced NF-kappaB activation stimulates skeletal muscle glycolytic metabolism through activation of HIF-1alpha.* Endocrinology, 2015. **156**(5): p. 1770-81.
221. de Brito, O.M. and L. Scorrano, *Mitofusin 2: a mitochondria-shaping protein with signaling roles beyond fusion.* Antioxid Redox Signal, 2008. **10**(3): p. 621-33.
222. Hulsmans, M. and P. Holvoet, *The vicious circle between oxidative stress and inflammation in atherosclerosis.* Journal of Cellular and Molecular Medicine, 2010. **14**(1-2): p. 70-78.
223. Sundaresan, M., et al., *Requirement for Generation of H2o2 for Platelet-Derived Growth-Factor Signal-Transduction.* Science, 1995. **270**(5234): p. 296-299.
224. Nishio, E. and Y. Watanabe, *The involvement of reactive oxygen species and arachidonic acid in alpha(1)-adrenoceptor-induced smooth muscle cell proliferation and migration.* British Journal of Pharmacology, 1997. **121**(4): p. 665-670.
225. Wang, Z., M.R. Castresana, and W.H. Newman, *Reactive oxygen and NF-kappaB in VEGF-induced migration of human vascular smooth muscle cells.* Biochem Biophys Res Commun, 2001. **285**(3): p. 669-74.
226. Oh, S.S., et al., *Neurodegeneration and early lethality in superoxide dismutase 2-deficient mice: a comprehensive analysis of the central and peripheral nervous systems.* Neuroscience, 2012. **212**: p. 201-13.
227. Zielonka, J., J. Vasquez-Vivar, and B. Kalyanaraman, *Detection of 2-hydroxyethidium in cellular systems: a unique marker product of superoxide and hydroethidine.* Nat Protoc, 2008. **3**(1): p. 8-21.
228. Huang, H., et al., *Skp2 inhibits FOXO1 in tumor suppression through ubiquitin-mediated degradation.* Proc Natl Acad Sci U S A, 2005. **102**(5): p. 1649-54.
229. Murphy, M.P. and R.A. Smith, *Targeting antioxidants to mitochondria by conjugation to lipophilic cations.* Annu Rev Pharmacol Toxicol, 2007. **47**: p. 629-56.
230. Quinlan, C.L., et al., *The mechanism of superoxide production by the antimycin-inhibited mitochondrial Q-cycle.* J Biol Chem, 2011. **286**(36): p. 31361-72.
231. Mariappan, N., et al., *TNF-alpha-induced mitochondrial oxidative stress and cardiac dysfunction: restoration by superoxide dismutase mimetic Tempol.* Am J Physiol Heart Circ Physiol, 2007. **293**(5): p. H2726-37.
232. Wong, G.H., et al., *Manganous superoxide dismutase is essential for cellular resistance to cytotoxicity of tumor necrosis factor.* Cell, 1989. **58**(5): p. 923-31.
233. Blaser, H., et al., *TNF and ROS Crosstalk in Inflammation.* Trends Cell Biol, 2016. **26**(4): p. 249-261.
234. Ferrari, R., *The role of TNF in cardiovascular disease.* Pharmacol Res, 1999. **40**(2): p. 97-105.
235. Qu, A.J., et al., *PGC-1 alpha attenuates neointimal formation via inhibition of vascular smooth muscle cell migration in the injured rat carotid artery.* American Journal of Physiology-Cell Physiology, 2009. **297**(3): p. C645-C653.
236. Jiang, F.R., et al., *Genipin Inhibits TNF-alpha-Induced Vascular Smooth Muscle Cell Proliferation and Migration via Induction of HO-1.* Plos One, 2013. **8**(8).
237. San Martin, A. and K.K. Griendling, *Redox control of vascular smooth muscle migration.* Antioxid Redox Signal, 2010. **12**(5): p. 625-40.

238. Wang, J.N., N. Shi, and S.Y. Chen, *Manganese superoxide dismutase inhibits neointima formation through attenuation of migration and proliferation of vascular smooth muscle cells.* Free Radic Biol Med, 2012. **52**(1): p. 173-81.
239. Weber, D.S., et al., *Phosphoinositide-dependent kinase 1 and p21-activated protein kinase mediate reactive oxygen species-dependent regulation of platelet-derived growth factor-induced smooth muscle cell migration.* Circ Res, 2004. **94**(9): p. 1219-26.
240. Goetze, S., et al., *TNF-alpha-induced migration of vascular smooth muscle cells is MAPK dependent.* Hypertension, 1999. **33**(1 Pt 2): p. 183-9.
241. Graf, K., et al., *Mitogen-activated protein kinase activation is involved in platelet-derived growth factor-directed migration by vascular smooth muscle cells.* Hypertension, 1997. **29**(1): p. 334-339.
242. Law, R.E., et al., *Troglitazone inhibits vascular smooth muscle cell growth and intimal hyperplasia.* Journal of Clinical Investigation, 1996. **98**(8): p. 1897-1905.
243. Bornfeldt, K.E., et al., *Insulin-Like Growth-Factor-I and Platelet-Derived Growth Factor-Bb Induce Directed Migration of Human Arterial Smooth-Muscle Cells Via Signaling Pathways That Are Distinct from Those of Proliferation.* Journal of Clinical Investigation, 1994. **93**(3): p. 1266-1274.
244. Bilato, C., et al., *Inhibition of vascular smooth muscle cell migration by peptide and antibody antagonists of the alpha(v)beta(3) integrin complex is reversed by activated calcium/calmodulin-dependent protein kinase II.* Journal of Clinical Investigation, 1997. **100**(3): p. 693-704.
245. Kastl, L., et al., *TNF-alpha mediates mitochondrial uncoupling and enhances ROS-dependent cell migration via NF-kappa B activation in liver cells.* Febs Letters, 2014. **588**(1): p. 175-183.
246. Lim, S., et al., *Regulation of mitochondrial morphology by positive feedback interaction between PKCdelta and Drp1 in vascular smooth muscle cell.* J Cell Biochem, 2015. **116**(4): p. 648-60.
247. Motori, E., et al., *Inflammation-induced alteration of astrocyte mitochondrial dynamics requires autophagy for mitochondrial network maintenance.* Cell Metab, 2013. **18**(6): p. 844-59.
248. Aveleira, C.A., et al., *TNF-alpha signals through PKCzeta/NF-kappaB to alter the tight junction complex and increase retinal endothelial cell permeability.* Diabetes, 2010. **59**(11): p. 2872-82.
249. Perez, J., et al., *Role of cellular bioenergetics in smooth muscle cell proliferation induced by platelet-derived growth factor.* Biochem J, 2010. **428**(2): p. 255-67.
250. Heiss, E.H., et al., *Increased aerobic glycolysis is important for the motility of activated VSMC and inhibited by indirubin-3 '-monoxime.* Vascular Pharmacology, 2016. **83**: p. 47-56.
251. Kim, J.H., et al., *Lactate dehydrogenase-A is indispensable for vascular smooth muscle cell proliferation and migration.* Biochemical and Biophysical Research Communications, 2017. **492**(1): p. 41-47.
252. Mitra, K., et al., *A hyperfused mitochondrial state achieved at G(1)-S regulates cyclin E buildup and entry into S phase.* Proceedings of the National Academy of Sciences of the United States of America, 2009. **106**(29): p. 11960-11965.
253. Parker, D.J., et al., *A new mitochondrial pool of cyclin E, regulated by Drp1, is linked to cell-density-dependent cell proliferation.* J Cell Sci, 2015. **128**(22): p. 4171-82.

254. Furda, A.M., et al., *Oxidants and not alkylating agents induce rapid mtDNA loss and mitochondrial dysfunction.* DNA Repair (Amst), 2012. **11**(8): p. 684-92.
255. Veal, E.A., A.M. Day, and B.A. Morgan, *Hydrogen peroxide sensing and signaling.* Mol Cell, 2007. **26**(1): p. 1-14.
256. Chaplin, N.L. and G.C. Amberg, *Stimulation of arterial smooth muscle L-type calcium channels by hydrogen peroxide requires protein kinase C.* Channels, 2012. **6**(5): p. 385-389.
257. Byon, C.H., et al., *Oxidative stress induces vascular calcification through modulation of the osteogenic transcription factor Runx2 by AKT signaling.* Journal of Biological Chemistry, 2008. **283**(22): p. 15319-15327.
258. Song, H.J., et al., *Hydrogen peroxide-induced extracellular signal-regulated kinase activation in cultured feline ileal smooth muscle cells.* Journal of Pharmacology and Experimental Therapeutics, 2005. **312**(1): p. 391-398.
259. de Rezende, F.F., et al., *Integrin alpha7beta1 is a redox-regulated target of hydrogen peroxide in vascular smooth muscle cell adhesion.* Free Radic Biol Med, 2012. **53**(3): p. 521-31.
260. Tuder, R.M., et al., *Exuberant endothelial cell growth and elements of inflammation are present in plexiform lesions of pulmonary hypertension.* Am J Pathol, 1994. **144**(2): p. 275-85.